UNIVERSITY OF AMSTERDAM

UvA-DARE (Digital Academic Repository)

Search for charged-lepton-flavor violating μτqt interactions in top-quark production and decay in pp collisions at √s = 13 TeV with the ATLAS detector at the LHC

Aad, G.; ATLAS Collaboration

DOI
10.1103/PhysRevD.110.012014

Publication date
2024

Document Version
Final published version

Published in
Physical Review D

License
CC BY

Link to publication

Citation for published version (APA):
Aad, G., & ATLAS Collaboration (2024). Search for charged-lepton-flavor violating *μτqt* interactions in top-quark production and decay in *pp* collisions at √s = 13 TeV with the ATLAS detector at the LHC. *Physical Review D*, *110*(1), Article 112014. https://doi.org/10.1103/PhysRevD.110.012014

General rights
It is not permitted to download or to forward/distribute the text or part of it without the consent of the author(s) and/or copyright holder(s), other than for strictly personal, individual use, unless the work is under an open content license (like Creative Commons).

Disclaimer/Complaints regulations
If you believe that digital publication of certain material infringes any of your rights or (privacy) interests, please let the Library know, stating your reasons. In case of a legitimate complaint, the Library will make the material inaccessible and/or remove it from the website. Please Ask the Library: https://uba.uva.nl/en/contact, or a letter to: Library of the University of Amsterdam, Secretariat, P.O. Box 19185, 1000 GD Amsterdam, The Netherlands. You will be contacted as soon as possible.

UvA-DARE is a service provided by the library of the University of Amsterdam (https://dare.uva.nl)

Download date:07 Sept 2026

Search for charged-lepton-flavor violating $\mu\tau qt$ interactions in top-quark production and decay in pp collisions at $\sqrt{s} = 13$ TeV with the ATLAS detector at the LHC

G. Aad *et al.*[*]
(ATLAS Collaboration)

(Received 12 March 2024; accepted 16 May 2024; published 25 July 2024)

A search for charged-lepton-flavor violating $\mu\tau qt$ ($q = u, c$) interactions is presented, considering both top-quark production and decay. The data analyzed correspond to 140 fb^{-1} of proton-proton collisions at a center-of-mass energy of $\sqrt{s} = 13$ TeV recorded with the ATLAS detector at the Large Hadron Collider. The analysis targets events containing two muons with the same electric charge, a hadronically decaying τ-lepton and at least one jet, with exactly one b-tagged jet, produced by a $\mu\tau qt$ interaction. Agreement with the Standard Model expectation within 1.6 standard deviations is observed, and limits are set at the 95% confidence level (CL) on the charged-lepton-flavor violation branching ratio of $\mathcal{B}(t \to \mu\tau q) < 8.7 \times 10^{-7}$. An effective field theory interpretation is performed yielding 95% CL limits on Wilson coefficients, dependent on the flavor of the associated light quark and the Lorentz structure of the coupling. These range from $|c_{\mathrm{lequ}}^{3(2313)}|/\Lambda^2 < 0.10$ TeV^{-2} for $\mu\tau ut$ to $|c_{\mathrm{lequ}}^{1(2323)}|/\Lambda^2 < 1.8$ TeV^{-2} for $\mu\tau ct$. An additional interpretation is performed for scalar leptoquark production inducing charged-lepton-flavor violation, with fixed intergenerational couplings. Upper limits on leptoquark coupling strengths are set at the 95% CL, ranging from $\lambda^{\mathrm{LQ}} = 1.3$ to $\lambda^{\mathrm{LQ}} = 3.7$ for leptoquark masses between 0.5 and 2.0 TeV.

DOI: 10.1103/PhysRevD.110.012014

I. INTRODUCTION

Prior to the prediction and subsequent observation of neutrino oscillations [1–5], the flavor of both charged and neutral leptons was assumed to be conserved within the Standard Model (SM). Extensions to the SM that can accommodate neutrino mass and mixing may also allow for the local nonconservation of charged-lepton flavor. Charged-lepton-flavor violation (cLFV) may therefore occur at rates significantly lower than the current experimental sensitivity (for example, $\mu \to e\gamma$ due to a neutrino oscillation in a W-boson loop has a predicted branching ratio of 10^{-55} [6]). Any observation of cLFV would hence provide strong evidence for new physics. Beyond-the-SM theories, such as those that predict leptoquarks (LQ), entail cLFV [6,7] with a rate as high as $\mathcal{B}(t \to \ell\ell' c) \approx 10^{-6}$ [8], where $\ell, \ell' = \{e, \mu, \tau\}$ and $\ell \neq \ell'$. Examples include the unification of leptons and quarks into representations of the SU(5) [9], SO(10) [10,11], or SU(5) $\otimes$ U(1) [12–15] groups, supersymmetric scenarios [16–20], and technicolor models [21–23]. In addition, some deviations from SM predictions were observed in the comparisons of hadron decays involving τ-leptons and other leptons that might hint at the presence of new phenomena, such as measurements of $R(D)$ and $R(D^*)$ [24–33].

Assuming that the energy scale probed experimentally is significantly lower than the scale of new physics, it is convenient to consider a model-independent approach with an effective field theory (EFT). Constraints on the operators describing two-quark two-lepton (2Q2L) contact interactions were compiled [34], and top-quark 2Q2L operators related to electrons and muons were probed by the CMS Collaboration at the Large Hadron Collider (LHC) [35]. Top-quark 2Q2L operators involving muons and τ-leptons however remain highly unconstrained [34], such that some cLFV top-quark interactions could be within the current sensitivity of the LHC [36].

This analysis searches for the production of a single top quark via $gq_k \to t\ell^{\pm}\ell'^{\mp}$ and the charge-conjugate process, where $q_k = \{u, c\}$ for $k = \{1, 2\}$ and $\ell\ell' = \{\mu\tau, \tau\mu\}$. The final state is chosen such that the top quark decays into a b-quark and a W boson, and the W boson subsequently decays leptonically into a muon and a neutrino. The τ-lepton is required to decay hadronically. A cLFV top-quark decay in $t\bar{t}$ events is also targeted, $t \to \ell^{\pm}\ell'^{\mp}q_k$ and the charge-conjugate process, where the other top quark of the pair decays into a muon according to the SM. These

[*]Full author list given at the end of the article.

Published by the American Physical Society under the terms of the Creative Commons Attribution 4.0 International license. Further distribution of this work must maintain attribution to the author(s) and the published article's title, journal citation, and DOI. Funded by SCOAP[3].

 © 2024 CERN, for the ATLAS Collaboration

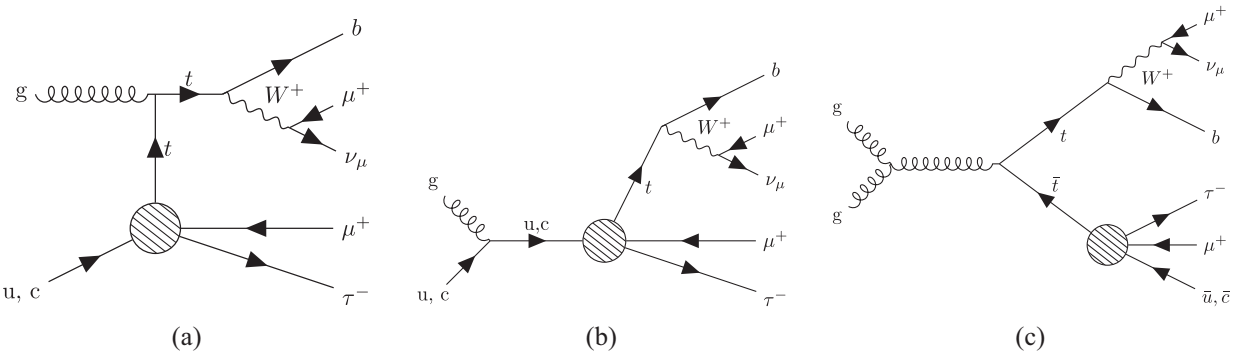

FIG. 1. Example Feynman diagrams of the process under study, where the hatched circle represents the cLFV vertex: (a) single-top-quark production with a cLFV process in the t-channel; (b) single-top-quark production with a cLFV process in the s-channel; (c) top-quark pair production with a cLFV top-quark decay process. The charge conjugate of each process is also considered.

processes are shown in Figs. 1(a) and 1(b) for single-top-quark production and Fig. 1(c) for top-quark pair production with a cLFV top-quark decay process, each enabled through an EFT vertex. The search presented is performed using the full Run 2 data sample of proton-proton (pp) collision data collected with the ATLAS detector in 2015–2018 at $\sqrt{s} = 13$ TeV, corresponding to an integrated luminosity of 140 fb^{-1}. The observed data are interpreted within the EFT framework, and also to test a leptoquark hypothesis [37].

In the EFT framework, the $gq_k \to t\ell^{\pm}\ell'^{\mp}$ production and $t \to \ell^{\pm}\ell'^{\mp}q_k$ decay processes are described by the $\mathrm{SU(3)_C} \otimes \mathrm{SU(2)_L} \otimes \mathrm{U(1)_Y}$ dimension-six EFT operators listed in Table I. The list includes all the relevant 2Q2L operators that contribute, and consists of a subset of the Warsaw basis operators [38]. Wilson coefficients (c) may be assigned to each of the operators ($\mathcal{O}$) in Table I. The Wilson coefficients weight the contributions of the EFT operators in an effective Lagrangian, which assumes a mass scale of new physics, Λ, which is much larger than the energy scale directly accessible at the LHC:

$$\mathcal{L} = \mathcal{L}_{\mathrm{SM}} + \mathcal{L}_{\mathrm{eff}} = \mathcal{L}_{\mathrm{SM}} + \sum_{\mathrm{x}} \frac{c_{\mathrm{x}}}{\Lambda^2}\mathcal{O}_{\mathrm{x}} + \cdots. \quad (1)$$

The cLFV single-top-quark production cross section grows quadratically with the values of the Wilson coefficients. Nonzero Wilson coefficients would lead to a large cLFV single-top-quark production cross section and this process therefore dominates the search sensitivity. However, it is also instructive to relate the Wilson coefficients concisely through the top-quark decay width Γ in terms of 6 degrees of freedom as follows [34]:

$$\begin{aligned}\Gamma(t \to \ell_i^+\ell_j^-q_k) &= \frac{m_t}{6144\pi^3}\left(\frac{m_t}{\Lambda}\right)^4\{4|c_{\mathsf{lq}}^{-(ijk3)}|^2 + 4|c_{\mathsf{eq}}^{(ijk3)}|^2 + 4|c_{\mathsf{lu}}^{(ijk3)}|^2 \\ &\quad + 4|c_{\mathsf{eu}}^{(ijk3)}|^2 + 2|c_{\mathsf{lequ}}^{1(ijk3)}|^2 + 96|c_{\mathsf{lequ}}^{3(ijk3)}|^2\}, \end{aligned} \quad (2)$$

where $c_{\mathsf{lq}}^{-(ijk3)} \equiv c_{\mathsf{lq}}^{1(ijk3)} - c_{\mathsf{lq}}^{3(ijk3)}$ is a combination used to contain the interactions of two up-type quarks with two charged leptons (the alternative sum $c_{\mathsf{lq}}^{+(ijk3)} \equiv c_{\mathsf{lq}}^{1(ijk3)} + c_{\mathsf{lq}}^{3(ijk3)}$ contains the interations of two up-type quarks and two neutrinos) [39] and m_t is the mass of the top quark. Real values of the Wilson coefficients are assumed, which implies invariance with respect to the ordering of the leptons and quarks: $c^{(jilk)} = c^{(ijkl)}$.

The current constraints on the Wilson coefficients come from a reinterpretation [34] of a previous ATLAS flavor-changing neutral current (FCNC) search in the tZq channel [40], based on a subset of 36 fb^{-1} of the data sample used in this analysis. These Wilson coefficient limits range from $|c_{\mathsf{lequ}}^{3(2313)}|/\Lambda^2 < 3.4$ TeV^{-2} for $\mu\tau ut$ to $|c_{\mathsf{lequ}}^{1(2323)}|/\Lambda^2 < 29$ TeV^{-2} for $\mu\tau ct$, and are dependent on

TABLE I. EFT operator basis and degrees of freedom. In the convention used, l and q are the left-handed lepton and quark doublets, respectively, while u and e are the right-handed up-type quark and charged-lepton singlets, respectively. The indices $i, j = \{1, 2, 3\}$ represent the lepton flavor generations and $k, l = \{1, 2, 3\}$ represent the quark flavor generations, respectively. The Pauli matrices are denoted by σ^I, $\varepsilon = i\sigma^2$ is the antisymmetric $SU(2)$ tensor and $\sigma^{\mu\nu} = \frac{i}{2}[\gamma^\mu, \gamma^\nu]$ and γ^μ are the Dirac matrices.

Operator	Interaction	Lorentz structure
$\mathcal{O}_{\mathsf{lq}}^{1(ijkl)}$	$(\bar{\mathsf{l}}_i\gamma^\mu\mathsf{l}_j)(\bar{\mathsf{q}}_k\gamma_\mu\mathsf{q}_l)$	Vector
$\mathcal{O}_{\mathsf{lq}}^{3(ijkl)}$	$(\bar{\mathsf{l}}_i\gamma^\mu\sigma^I\mathsf{l}_j)(\bar{\mathsf{q}}_k\gamma_\mu\sigma_I\mathsf{q}_l)$	Vector
$\mathcal{O}_{\mathsf{eq}}^{(ijkl)}$	$(\bar{\mathsf{e}}_i\gamma^\mu\mathsf{e}_j)(\bar{\mathsf{q}}_k\gamma_\mu\mathsf{q}_l)$	Vector
$\mathcal{O}_{\mathsf{lu}}^{(ijkl)}$	$(\bar{\mathsf{l}}_i\gamma^\mu\mathsf{l}_j)(\bar{\mathsf{u}}_k\gamma_\mu\mathsf{u}_l)$	Vector
$\mathcal{O}_{\mathsf{eu}}^{(ijkl)}$	$(\bar{\mathsf{e}}_i\gamma^\mu\mathsf{e}_j)(\bar{\mathsf{u}}_k\gamma_\mu\mathsf{u}_l)$	Vector
$\mathcal{O}_{\mathsf{lequ}}^{1(ijkl)}$	$(\bar{\mathsf{l}}_i\mathsf{e}_j)\varepsilon(\bar{\mathsf{q}}_k\mathsf{u}_l)$	Scalar
$\mathcal{O}_{\mathsf{lequ}}^{3(ijkl)}$	$(\bar{\mathsf{l}}_i\sigma^{\mu\nu}\mathsf{e}_j)\varepsilon(\bar{\mathsf{q}}_k\sigma_{\mu\nu}\mathsf{u}_l)$	Tensor

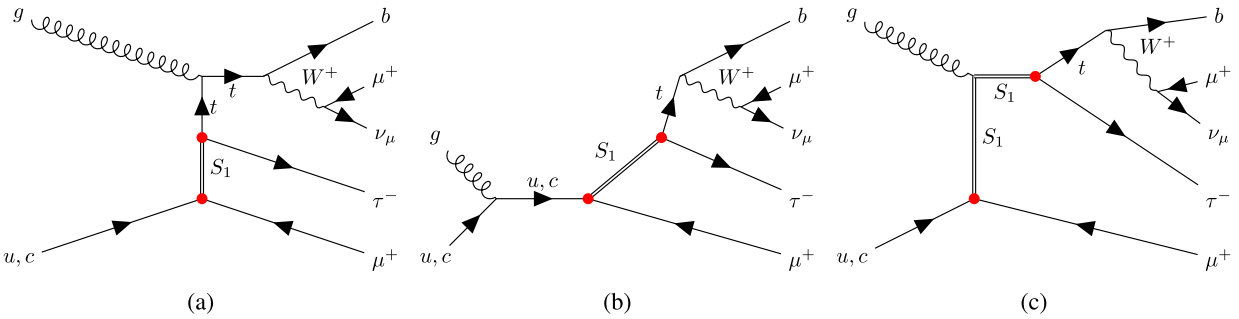

FIG. 2. Example Feynman diagrams of the scalar leptoquark S_1 model under study, producing a single top quark via (a) a nonresonant leptoquark, (b) a resonant leptoquark, and (c) a resonant leptoquark with an off-shell leptoquark exchange. The leptoquark S_1 carries electric charge $Q = -\frac{1}{3}$, spin $S = 1$, lepton number $L = 1$, and baryon number $B = \frac{1}{3}$. In each case, initial states using up or charm quarks are assumed, and a final state consisting of two same-sign muons and one τ-lepton is produced. The charge conjugate of each process is also considered. The dots represent vertices with a leptoquark-to-fermion coupling strength, λ_{ki}, for the appropriate quark generation (k) and lepton generation (i).

the flavor of the associated light quark and the Lorentz structure of the coupling. The range of Wilson coefficient limits set by this reinterpretation corresponds to minimal and maximal branching-ratio limits of approximately $\mathcal{B}(t \to \mu\tau u) < 3.5 \times 10^{-5}$ and $\mathcal{B}(t \to \mu\tau c) < 3.0 \times 10^{-4}$ for the respective operators.

Leptoquarks, which arise in beyond-the-SM theories, are also a natural candidate for introducing cLFV interactions. The couplings between leptons and quarks may be intergenerational. In this interpretation, a scalar leptoquark (S_1) model is assumed that introduces couplings between all up-type quarks and all charged leptons, leading to the single leptoquark production processes presented in Fig. 2 with the relevant final states.

This model, in which the leptoquark may couple to multiple generations of leptons and quarks, contains many degrees of freedom. The search for multigenerational single scalar leptoquarks is an extension to previous studies by ATLAS [41] and CMS [42] that search for single leptoquark production coupling to a single lepton and single quark generation only. The investigation of a fully general and complex scenario is beyond the scope of this measurement and for that reason, assumptions are made to simplify the multigenerational hypothesis. The couplings of S_1 to each generation of quarks k and leptons i, λ_{ki}, are fixed relative to one another such that the coupling of the leptoquark to the SM may be described by a single parameter λ^{LQ}:

$$\lambda_{ki} \in \begin{pmatrix} \lambda_{t\tau} & \lambda_{c\tau} & \lambda_{u\tau} \\ \lambda_{t\mu} & \lambda_{c\mu} & \lambda_{u\mu} \\ \lambda_{te} & \lambda_{ce} & \lambda_{ue} \end{pmatrix} \equiv \lambda^{\mathrm{LQ}} \begin{pmatrix} 10 & 1 & 0.1 \\ 1 & 0.1 & 0.01 \\ 0.1 & 0.01 & 0.001 \end{pmatrix}, \quad (3)$$

where the largest value is the S_1-t-τ vertex and the smallest is the S_1-u-e vertex. A flavor hierarchy in the coupling strengths is a common assumption in multigenerational leptoquark models. However, the magnitude of the hierarchies in the quark generations $(\lambda_{(k-1)i}/\lambda_{ki})$ and in the lepton generations $(\lambda_{k(i-1)}/\lambda_{ki})$ are not yet a matter of consensus, as different models span ratios ranging from $\sqrt{2}$ to $\frac{1}{16}$ for each [43–47]. In this search, a constant ratio in both the quark and lepton generations is assumed, $R = \lambda_{(k-1)i}/\lambda_{ki} = \lambda_{k(i-1)}/\lambda_{ki}$. An order of magnitude reduction ($R = 0.1$) is chosen for each generational step-down in either the quark or lepton flavor as a representative scenario, where $\lambda_{t\tau}$ is the strongest coupling. As R affects the relative sizes of the λ_{ki} couplings, this modifies the width of the leptoquark and the resulting kinematic properties of the decay. It is not straightforward to scale to alternative hierarchy assumptions and such a study is beyond the scope of this interpretation. However, this interpretation represents a robust first search for single scalar leptoquark production with large intergenerational couplings using the top quark. The search for the production of a single scalar leptoquark S_1 is performed using the same analysis strategy as is optimized for the EFT interpretation. Limits on the cross section of the S_1 model are expected to be slightly weaker than in the EFT interpretation due to this choice of optimization.

II. ATLAS DETECTOR

The ATLAS detector [48] at the LHC covers nearly the entire solid angle around the collision point.[1] It consists of an inner tracking detector surrounded by a thin superconducting solenoid, electromagnetic and hadronic

[1]ATLAS uses a right-handed coordinate system with its origin at the nominal interaction point (IP) in the center of the detector and the z-axis along the beam pipe. The x-axis points from the IP to the center of the LHC ring, and the y-axis points upward. Polar coordinates (r, ϕ) are used in the transverse plane, ϕ being the azimuthal angle around the z-axis. The pseudorapidity is defined in terms of the polar angle θ as $\eta = -\ln\tan(\theta/2)$ and is equal to the rapidity $y = \frac{1}{2}\ln(\frac{E+p_z c}{E-p_z c})$ in the relativistic limit. Angular distance is measured in units of $\Delta R \equiv \sqrt{(\Delta y)^2 + (\Delta\phi)^2}$.

calorimeters, and a muon spectrometer incorporating three large superconducting air-core toroidal magnets.

The inner-detector system (ID) is immersed in a 2 T axial magnetic field and provides charged-particle tracking in the range $|\eta| < 2.5$. The high-granularity silicon pixel detector covers the vertex region and typically provides four measurements per track, the first hit generally being in the insertable B-layer installed before Run 2 [49,50]. It is followed by the semiconductor tracker, which usually provides eight measurements per track. These silicon detectors are complemented by the transition radiation tracker (TRT), which enables radially extended track reconstruction up to $|\eta| = 2.0$. The TRT also provides electron identification information based on the fraction of hits (typically 30 in total) above a higher energy-deposit threshold corresponding to transition radiation.

The calorimeter system covers the pseudorapidity range $|\eta| < 4.9$. Within the region $|\eta| < 3.2$, electromagnetic calorimetry is provided by barrel and end cap high-granularity lead/liquid-argon (LAr) calorimeters, with an additional thin LAr presampler covering $|\eta| < 1.8$ to correct for energy loss in material upstream of the calorimeters. Hadronic calorimetry is provided by the steel/scintillator-tile calorimeter segmented into three barrel structures within $|\eta| < 1.7$, and two copper/LAr hadronic end cap calorimeters. The solid angle coverage is completed with forward copper/LAr and tungsten/LAr calorimeter modules optimized for electromagnetic and hadronic energy measurements respectively.

The muon spectrometer comprises separate trigger and high-precision tracking chambers measuring the deflection of muons in a magnetic field generated by the superconducting air-core toroidal magnets. The field integral of the toroids ranges between 2.0 and 6.0 T m across most of the detector. Three layers of precision chambers, each consisting of layers of monitored drift tubes, cover the region $|\eta| < 2.7$, complemented by cathode-strip chambers in the forward region, where the background is highest. The muon trigger system covers the range $|\eta| < 2.4$ with resistive-plate chambers in the barrel, and thin-gap chambers in the end cap regions.

The luminosity is measured mainly by the LUCID–2 [51] detector that records Cherenkov light produced in the quartz windows of photomultipliers located close to the beampipe.

Events are selected by the first-level trigger system implemented in custom hardware, followed by selections made by algorithms implemented in software in the high-level trigger [52]. The first-level trigger accepts events from the 40 MHz bunch crossings at a rate below 100 kHz, which the high-level trigger further reduces in order to record complete events to disk at about 1 kHz.

A software suite [53] is used in data simulation, in the reconstruction and analysis of real and simulated data, in detector operations, and in the trigger and data acquisition systems of the experiment.

III. ANALYSIS STRATEGY

An overview of the analysis strategy is provided here, before each step is described in detail throughout the following sections.

A signal-enriched region (SR) is defined to target the signal cLFV processes and selects events that contain two muons, one hadronically decaying τ-lepton and at least one jet. Exactly one jet is required to be identified as containing b-hadrons (b-tagged). The two muons are required to have the same electric charge [referred to as same sign (SS)], to avoid large background contributions of opposite-sign (OS) $\mu^+\mu^-$ pairs from Z-boson decays.

In addition, control regions (CRs) are defined that are enriched in backgrounds from fake or nonprompt (NP) muons or fake τ-lepton candidates, and are depleted of signal events. The main backgrounds stem from $t\bar{t}$ events with NP muons from heavy-flavor hadron decays inside jets, associated top-quark production processes ($t\bar{t}Z, t\bar{t}W, t\bar{t}H$) with prompt leptons, diboson events (WZ, ZZ) with prompt leptons, and events with jets that are misidentified as hadronically decaying τ-leptons (referred to as fake τ-lepton events). The prompt-lepton backgrounds are modeled by Monte Carlo (MC) simulations. The yield of the NP muon background is determined through a template fit in a dedicated CR denoted CR$t\bar{t}\mu$. This CR contains dilepton $t\bar{t}$ events with one electron and one muon, and an additional NP muon passing looser identification and isolation requirements, mainly originating from the decay of a B-meson in a hadronic jet. The contribution of the fake τ-lepton background is determined through a data-driven scale factor method in a dedicated CR denoted CRτ. This CR targets two OS muons and one hadronically decaying τ-lepton and is designed to be enriched in events with a jet misidentified as a τ-lepton. The fake τ-lepton scale factors are determined in CRτ as the first step of the analysis and propagated to the SR.

The signal contribution in the SR is then estimated with a binned profile-likelihood fit to the distribution of H_{T} (the scalar sum of the lepton and jet transverse momenta), with systematic uncertainties modeled as nuisance parameters. The region CR$t\bar{t}\mu$ is included in the fit, to simultaneously determine the normalization of the NP muon background. For each EFT coupling contributing to the signal process, MC samples are generated separately for single-top-quark production and top-quark decay. Two inclusive samples are also generated with all couplings activated simultaneously. These inclusive samples are used together to determine an upper limit on the inclusive branching-ratio [$\mathcal{B}(t \to \mu\tau q)$] limit, and the separate EFT samples are used to determine limits on each operator individually (as specified in Table I). Finally, dedicated

TABLE II. Theoretical cross sections for single-top-quark production and top-quark decays through cLFV interactions involving vector, scalar, and tensor EFT Wilson coefficients. The column titled $c_{\text{vector}}^{(ijk3)}$ represents the individual cross-section contributions from each of $c_{\text{lq}}^{-(ijk3)}$, $c_{\text{eq}}^{(ijk3)}$, $c_{\text{lu}}^{(ijk3)}$, and $c_{\text{eu}}^{(ijk3)}$. The coefficient indices represent the lepton flavor generations ($i, j = 1, 2, 3$ where $i \neq j$) and light quark flavor generations ($k = 1, 2$). The single-top-quark production cross sections are quoted for u- and c-quark couplings separately, while they are combined for the $t\bar{t}$ decay process ($q_k = u, c$). The scale and PDF uncertainties are given. The value of each Wilson coefficient is set to 1.0 for the calculation of the cross section, with an energy scale of $\Lambda = 1$ TeV.

	Cross-section $\sigma_{-\text{scale}}^{+\text{scale}} \pm \text{PDF}$ (fb)		
	$c_{\text{vector}}^{(ijk3)}$	$c_{\text{lequ}}^{1(ijk3)}$	$c_{\text{lequ}}^{3(ijk3)}$
Production $\ell\ell' ut$	$118^{+24}_{-19} \pm 1$	$101^{+21}_{-16} \pm 1$	$2150^{+410}_{-320} \pm 20$
Production $\ell\ell' ct$	$7.9^{+1.2}_{-1.0} \pm 1.6$	$6.1^{+1.0}_{-0.8} \pm 1.5$	$153^{+21}_{-18} \pm 29$
Decay $\ell\ell' q_k t$	$6.9^{+1.8}_{-1.3} \pm 0.1$	$3.46^{+0.90}_{-0.66} \pm 0.03$	$166^{+43}_{-32} \pm 2$

samples are generated for the leptoquark model and the fit is repeated to set limits on this hypothesis.

IV. DATA AND SIMULATED EVENT SAMPLES

The pp collision data analyzed for this search were recorded with the ATLAS detector from 2015 to 2018 at a center-of-mass energy of $\sqrt{s} = 13$ TeV. Events were selected using single-muon and single-electron triggers [54,55] and are required to have a reconstructed primary vertex that has at least two associated tracks with transverse momentum (p_{T}) greater than 500 MeV, where the primary vertex is defined as that for which the associated tracks have the highest sum of p_{T}^2. After the application of data-quality requirements [56], the data sample corresponds to an integrated luminosity of 140 fb^{-1}, as determined using the LUCID-2 detector [51,57] for the primary luminosity measurements.

To optimize the event selection and to predict contributions from various SM processes, MC simulated event samples are used. The effect of multiple interactions in the same and neighboring bunch crossings (pileup) was modeled by overlaying the simulated hard-scattering event with inelastic pp events generated by PYTHIA8.186 [58] using the NNPDF2.3LO set of parton distribution functions (PDFs) [59] and parameter values set according to the A3 tune [60]. After the event generation, the ATLAS detector response was simulated [61] with the GEANT4 toolkit [62] with either the full simulation of the ATLAS detector or a fast-simulation package that relies on a parametrization of the calorimeter response [63]. In all processes, the top-quark mass was set to 172.5 GeV. All samples of simulated events, except those produced with the SHERPA [64] generator, use EVTGEN [65] to model the decays of bottom and charm hadrons. SHERPA uses built-in decay tables from measurements.

Signal and background contributions to the search for cLFV are estimated by using MC event generators. Both cLFV single-top-quark production and top-quark pair production with a cLFV top-quark decay are treated as signal, while all other processes are treated as backgrounds. These backgrounds include SM top-quark pair and single-top-quark production, the associated production of top quarks with W, Z, γ, or Higgs bosons, and the production of diboson, triboson, and W/Z + jets. Possible contributions of the aforementioned EFT operators to the associated top-quark production backgrounds are assumed to be negligible and thus disregarded.

The EFT signal processes are simulated as $gq_k \to t\ell\ell'$ and $t\bar{t} \to (\ell\ell' q_k)((W \to \ell\nu)b)$ for the production and decay diagrams respectively, with $\ell, \ell' = \{e, \mu, \tau\}$ and $q_k = \{u, c\}$. For this purpose a universal FeynRules output (UFO) model [66] containing the EFT operators listed in Table I was created with FeynRules 2.0 [67] using the DIM6TOP model [68]. Events were generated at leading order (LO) in QCD with MadGraph 2.9.5 [69] for the hard process, in combination with PYTHIA8.306 [70] for showering and hadronization. All the decay channels of the τ-lepton are included. The five-flavor scheme is used, in which all the quark masses are set to zero except for the top quark. The renormalization and factorization scales (μ_{r}, μ_{f}) are dynamic and correspond to the center-of-mass energy of the incoming partons in the case of the top-quark decay process and half the sum of the transverse masses of all final state particles and partons for the single-top-quark production process. The NNPDF3.1NLO [71] PDF was chosen; PYTHIA8 was configured according to the A14 tune [72]. Theoretical cross sections for single-top-quark production and top-quark decays through cLFV interactions are shown in Table II. The cross sections for the cLFV $t\bar{t}$ decay samples are evaluated through

$$\sigma_{\text{CLFV}} = 2 \cdot \sigma_{t\bar{t}} \cdot \mathcal{B}(t \to W(\to \ell\nu)b) \cdot \frac{\Gamma(t \to \ell_i^+ \ell_j^- q_k)}{\Gamma_t}, \qquad (4)$$

where $\sigma_{t\bar{t}}$ is the $t\bar{t}$ production cross-section prediction at next-to-next-to-leading-order (NNLO) in QCD including the resummation of next-to-next-to-leading logarithmic

(NNLL) soft-gluon terms calculated using TOP++ 2.0 [73]. The relative scale and PDF uncertainties from the LO generation are maintained. The single-top-quark production cross sections are determined using MadGraph 2.9.5 with DIM6TOP and these values and related kinematic distributions were checked against the SMEFTsim 3.0 [74,75] UFO model and were found to be compatible. The cross sections in Table II are the sum over all lepton flavor generations (i, $j = 1, 2, 3$ where $i \neq j$) and assume a top-quark mass of 172.5 GeV, an LO top-quark decay width Γ_t of 1.51 GeV, a new physics scale of $\Lambda = 1$ TeV, and a value of 1.0 for each Wilson coefficient. The column labeled $c_{\text{vector}}^{(ijk3)}$ represents the individual cross-section contributions from each of $c_{\text{lq}}^{-(ijk3)}$, $c_{\text{eq}}^{(ijk3)}$, $c_{\text{lu}}^{(ijk3)}$, and $c_{\text{eu}}^{(ijk3)}$. While each vector coupling contributes comparably to the enhancement of the top-quark width, as shown in Eq. (2), they may result in different kinematic distributions. The production cross sections are quoted for up- and charm-quark couplings separately ($k = 1, 2$) and differ due to the proton PDFs. The $t\bar{t}$ cross sections involving $\ell\ell' q_k$ decays are quoted for up and charm quarks together as these are not distinguished in the analysis.

To consider an uncertainty due to the parton-shower generator, a second set of MC samples for the EFT signals are generated using the HERWIG7.1.6 [76,77] prediction with the HERWIG7.1 default tune instead of the PYTHIA8.306 generator.

Alternative signal samples for a scalar leptoquark production, $gq_k \to S_1\ell$ ($q_k = u, c$; $\ell = \mu, \tau$), and for $gq_k \to t\ell\ell'$ with the S_1 exchanged as a virtual particle, were generated at LO in QCD with MadGraph 2.9.5 for the hard process in combination with PYTHIA8.306 for showering and hadronization and the NNPDF3.0NLO PDF set [78]. The scales μ_r and μ_f correspond to the invariant mass of the leptoquark, m_{S_1}. A dedicated UFO model [37,79] was utilized for this purpose, defining S_1 to carry electric charge $Q = -\frac{1}{3}$, spin $S = 1$, lepton number $L = 1$, and baryon number $B = \frac{1}{3}$. Samples were generated assuming a charm quark in the initial state as the predominant production mechanism according to the flavor hierarchy described in Eq. (3). Diagrams with an initial-state up quark contribute an additional 10% to the cross sections and were considered by reweighting the charm-quark samples, accounting for small differences in the kinematics and acceptance. When following the leptoquark decay $S_1 \to t\ell'$ ($\ell' = \tau, \mu$), the total cross section scales with $(\lambda^{\text{LQ}})^4$ as an effective contact interaction. The contribution to the expected sensitivity from initial-state up quarks is less than 3%. The samples contain trilepton $\mu\mu\tau$ and $\tau\tau\mu$ final states only and cover a mass range of $0.5 < m_{S_1} < 2.5$ TeV and a coupling range of $0.5 < \lambda^{\text{LQ}} < 3.5$. These samples are only used in Sec. VIII B of the paper, for the interpretation of the search in the leptoquark S_1 model. Processes involving a leptoquark in a top-quark decay ($t \to q_k\ell\ell'$, mediated by S_1) are not considered as the contribution is expected to be negligible.

For the background processes, the production of $t\bar{t}$ events was modeled using the POWHEG BOX v2 [80–83] generator at next-to-leading-order (NLO) with the NNPDF3.0NLO PDF set and the h_{damp} parameter[2] set to 1.5 times the top-quark mass [84]. The events were interfaced to PYTHIA8.230 [85] to model the parton shower (PS), hadronization, and underlying event, with parameters set according to the A14 tune and using the NNPDF2.3LO set of PDFs. The functional form of the renormalization and factorization scales was set to the default scale $m_T(t) = \sqrt{m_t^2 + p_T^2}$, where $m_T(t)$ and p_T were the transverse mass and transverse momentum of the top quark in each event. The $t\bar{t}$ sample is normalized to the cross-section prediction at NNLO in QCD including the resummation of NNLL soft-gluon terms calculated using TOP++ 2.0.

The single-top-quark samples are split into the three processes: s-channel, t-channel, and tW associated production. These samples were modeled using the POWHEG BOX v2 generator at NLO in QCD using the four-flavor (five-flavor) scheme for the t-channel (s-channel and tW) [86,87] and the corresponding NNPDF3.0NLO set of PDFs. In the case of tW production, the diagram-removal scheme [88] was used to address the interference with $t\bar{t}$ production [84]. The events were interfaced with PYTHIA8.230, which used the A14 set of tuned parameters and the NNPDF2.3LO set of PDFs.

The associated production of a $t\bar{t}$ pair with a leptonically decaying Z boson is modeled using the MadGraph5_aMC@NLO 2.8.1 generator, which provides matrix elements (ME) at NLO in QCD with the NNPDF3.0NLO PDF set. The functional form of μ_r and μ_f is set to the default scale $0.5 \times \sum_i \sqrt{m_i^2 + p_{T,i}^2}$, where the sum runs over all the particles generated from the ME calculation. Top-quark decays are simulated at LO using MadSpin [89,90] to preserve all spin correlations. The events are interfaced with PYTHIA8.244 for the parton shower and hadronization, using the A14 set of tuned parameters and the NNPDF2.3LO PDF set.

The production of $t\bar{t}W$ events was simulated at NLO precision in QCD with SHERPA2.2.10 and the NNPDF3.0NNLO PDF set [78]. In this setup, multiple MEs were matched and merged with the SHERPA PS model based on the Catani-Seymour dipole factorization scheme [91,92]. The virtual QCD corrections (in the strong coupling constant α_s) for MEs at NLO accuracy were provided by the OpenLoops library [93–95]. Up to one additional parton was included

[2]The h_{damp} parameter is a resummation damping factor and one of the parameters that controls the matching of POWHEG matrix elements to the parton shower and thus effectively regulates the high-p_T radiation against which the $t\bar{t}$ system recoils.

in the NLO ME, and up to two additional partons were included at LO in QCD using Comix [91]. The merging scale parameter (μ_q), which sets a threshold to determine what part of the phase space is filled by the PS or the ME generator, was set to an energy of 30 GeV. In addition to the nominal prediction at NLO in QCD, higher-order corrections related to electroweak (EWK) $t\bar{t}W$ contributions (in the coupling α) were also added as part of the signal definition. The α^3 and $\alpha^2\alpha_s{}^2$ corrections were added through MC event weights derived using the virtual additive corrections in the formalism described in Ref. [96]. Second, subleading EWK corrections at order $\alpha^3\alpha_s$ [97] were partially accounted for (only the real emission contribution) via the addition of an independent SHERPA2.2.10 sample produced at LO in QCD for this final state. The combination of contributions of NLO QCD and NLO EWK effects taken from the SHERPA configuration outlined above closely follows the strategy outlined in Ref. [98]. This results in a total cross section of $\sigma(t\bar{t}W) = 722$ fb, which was used for the normalization of the simulation.

The production of $t\bar{t}H$ events was modeled using the POWHEG BOX v2 generator, which provided matrix elements at NLO [99] in QCD in the five-flavor scheme with the NNPDF3.0NLO PDF set. The functional forms of μ_r and μ_f were set to $\sqrt[3]{m_T(t) \cdot m_T(\bar{t}) \cdot m_T(H)}$. The events were interfaced to PYTHIA8.230 using the A14 tune and the NNPDF2.3LO PDF set. The sample is normalized to the cross section calculated at NLO QCD and NLO EWK accuracy [100].

The production of tWZ events was modeled using the MadGraph5_aMC@NLO 2.3.3 generator at NLO in QCD with the NNPDF3.0NLO PDF set. The events were interfaced with PYTHIA8.212 using the A14 tune and the NNPDF2.3LO PDF set. The top quark and the Z-boson decays were simulated at LO using MadSpin to preserve spin correlations.

Samples of diboson final states (VV) were simulated with the SHERPA2.2.1 ($WZ \to qqll, ZZ \to qqll$) or SHERPA2.2.2 (all other final states) generators, including off-shell effects and Higgs boson contributions, where appropriate. Fully leptonic final states and semileptonic final states, where one boson decays leptonically and the other hadronically, were simulated using matrix elements at NLO accuracy in QCD for up to one additional parton and at LO accuracy for up to three additional parton emissions. Samples were generated using the NNPDF3.0NNLO PDF set, along with the dedicated set of tuned parton-shower parameters developed by the SHERPA authors.

The production of V + jets was simulated with the SHERPA2.2.1 generator. In this setup, NLO matrix elements for up to two partons, and LO matrix elements for up to four partons were calculated with the Comix and OpenLoops libraries, and merged with the SHERPA parton shower using the MEPS@NLO prescription [101] based on Catani-Seymour dipole factorization and the cluster hadronization model [102]. They employed the dedicated set of tuned parameters developed by the SHERPA authors and the NNPDF3.0NNLO PDF set.

The production of triboson (VVV) events was simulated with the SHERPA2.2.2 generator using factorized gauge-boson decays. Matrix elements, accurate to NLO for the inclusive process and to LO for up to two additional parton emissions, were matched and merged with the SHERPA parton shower based on Catani-Seymour dipole factorization using the MEPS@NLO prescription [101,103–105]. The virtual QCD corrections for matrix elements at NLO accuracy were provided by the OpenLoops library. Samples were generated using the NNPDF3.0NNLO PDF set, along with the dedicated set of tuned parton-shower parameters developed by the SHERPA authors.

Other processes make only minor contributions and are also modeled by MC simulation: $t\bar{t}t\bar{t}$ is simulated with MadGraph5_aMC@NLO; $t\bar{t}t$ and $t\bar{t}WW$ with MadGraph 2.2.2; $t\bar{t}\gamma$ with MadGraph 2.3.3; WH/ZH with POWHEG BOX, and $Z\gamma$ with SHERPA2.2.4. All samples are interfaced to PYTHIA8 except for the $Z\gamma$ sample. An overlap removal procedure is applied to remove events in the $t\bar{t}$ and Z + jets samples that have a photon in the matrix element to prevent double counting with the $t\bar{t}\gamma$ and $Z\gamma$ samples. The small contributions from $t\bar{t}\gamma$ and $Z\gamma$, along with other processes that enter the event selection with a fake or nonprompt electron, are grouped and labeled "fake electron."

V. OBJECT AND EVENT SELECTION

The events used in the analysis are selected with high efficiency using single-lepton triggers based on electron and muon signatures. The lowest p_T thresholds were 20 GeV for muons and 24 GeV for electrons in 2015, and 26 GeV for both lepton types in 2016–2018. They were supplemented by additional triggers with higher p_T thresholds. Events must contain at least one reconstructed lepton candidate corresponding to a lepton selected by the trigger ("trigger matched"), where the lepton p_T exceeds the trigger p_T threshold by 1 GeV for electrons [54] or 5% for muons [55].

Electron candidates are reconstructed from energy clusters ("clu") in the electromagnetic calorimeter that are associated with charged-particle tracks reconstructed in the inner detector [106]. Only candidates with $p_T > 10$ GeV and $|\eta_{clu}| < 2.47$ are considered. Candidates in the transition region between different electromagnetic calorimeter components, $1.37 < |\eta_{clu}| < 1.52$, are rejected. A multivariate likelihood discriminant combining shower-shape and track information is used to distinguish real electrons from hadronic showers. Isolation criteria, exploiting both calorimeter and tracking variables, and impact parameter requirements are used to reduce the background from nonprompt electrons produced in hadronic decays. Electron candidates are required to meet tight identification criteria based on the multivariate likelihood discriminant

mentioned above [106]. The requirements for electrons on the transverse impact parameter significance and on the longitudinal impact parameter are $|d_0|/\sigma_{d_0} < 5$ and $|z_0 \sin(\theta)| < 0.5$ mm, respectively.

Muon candidates are reconstructed by combining inner detector tracks with track segments or full tracks in the muon spectrometer. Candidates are required to satisfy $p_{\mathrm{T}} > 10$ GeV and $|\eta| < 2.5$ and are required to satisfy a medium [107] identification criterion.

Leptons from heavy-flavor hadron decays, misidentified jets, or photon conversions (collectively referred to as "nonprompt leptons") are further suppressed using a boosted decision tree (BDT) discriminant referred to as the nonprompt lepton BDT [107]. This BDT uses isolation and lifetime information associated with a track jet that matches the electron or muon candidate, and both tight and loose working points are defined. Muon candidates populating the SR and CRτ must satisfy the nonprompt-lepton BDT tight isolation requirement, with impact parameter selections of $|d_0|/\sigma_{d_0} < 3$ and $|z_0 \sin(\theta)| < 0.5$ mm; these are "Tight" muon candidates. In CR$t\bar{t}\mu$, muons must satisfy the same longitudinal requirement of $|z_0 \sin(\theta)| < 0.5$ mm but an inverted transverse impact parameter significance requirement of $|d_0|/\sigma_{d_0} \geq 3$ is applied, together with loose isolation requirements for the nonprompt-lepton BDT. These muon candidates are labeled "Loose."

The constituents for jet reconstruction are identified by combining measurements from both the ID and the calorimeter using a particle flow algorithm [108]. Jet candidates are reconstructed from these particle flow objects using the anti-k_t algorithm [109,110] with a radius parameter of $R = 0.4$. They are calibrated using simulation with corrections obtained from data using *in situ* techniques [111]. Only jet candidates with $p_{\mathrm{T}} > 25$ GeV and $|\eta| < 2.5$ are selected. To reduce the effect of pileup, each jet with $p_{\mathrm{T}} < 60$ GeV and $|\eta| < 2.4$ is required to satisfy the tight working point of the jet vertex tagger (JVT) [112] criteria used to identify the jets as originating from the selected primary vertex. A set of quality criteria are also applied to reject events containing at least one jet arising from noncollision sources or detector noise [113].

Jets containing b-hadrons are identified (b-tagged) using the neural network "DL1r" algorithm [114]. The algorithm combines inputs from the impact parameters of displaced vertices and topological properties of secondary and tertiary vertices within a jet, and passes them to a neural network that outputs three values representing the probability of the jet being a "light-flavor" (initiated by u-, d-, or s-quarks or gluons), c- or b-jet, which is then combined into a single discriminant. The analysis uses a 77% efficiency working point calibrated using $t\bar{t}$ events at $\sqrt{s} = 13$ TeV, with rejection factors of 5.6 and 192 for c-jets and light-flavor jets, respectively [114].

Hadronically decaying τ-leptons, τ_{had}, produce visible decay products along with a neutrino that escapes the detector undetected. The τ_{had} candidates are seeded by jets reconstructed using the anti-k_t algorithm with a radius parameter $R = 0.4$ using topological energy clusters [115] with a local hadronic calibration [116]. Jets used to seed τ_{had} reconstruction are required to have $p_{\mathrm{T}} > 10$ GeV and $|\eta| < 2.5$. All τ_{had} candidates are required to have $p_{\mathrm{T}} > 20$ GeV and $|\eta| < 2.5$. As with electron candidates, τ_{had} candidates in the transition region, $1.37 < |\eta| < 1.52$, are rejected. The τ_{had} production vertex is identified and a set of BDTs determines which of the reconstructed tracks are likely to originate from the hadronically decaying τ-lepton [117]. The τ_{had} candidates are required to have one or three associated tracks, referred to as one-prong or three-prong τ_{had}, and these tracks must have measured charges summing to ± 1. A description of the p_T calibration applied to τ_{had} can be found in Ref. [118]. To suppress τ_{had} candidates originating from jets initiated by quarks or gluons, a recurrent neural network (RNN), described in Ref. [119], is used to apply identification criteria. This makes use of information from individual tracks and calorimeter clusters associated with the candidate along with high-level variables. An additional boosted decision tree discriminant, the eBDT, is used to reject τ_{had} candidates originating from electrons. The τ_{had} candidates are required to satisfy the "medium" identification working point of the RNN [119], corresponding to an efficiency of 75% (60%) for true one-prong (three-prong) τ_{had}.

To avoid double counting of detector signatures, objects are removed in the following order[3]: electrons sharing a track with a muon; jets within $\Delta R = 0.2$ of an electron; electrons within $\Delta R = 0.4$ of a jet; jets within $\Delta R = 0.4$ of a muon if they have at most two associated tracks; muons within $\Delta R = 0.4$ of a jet; τ_{had} within $\Delta R = 0.2$ of an electron; τ_{had} within $\Delta R = 0.2$ of a muon; any jet within $\Delta R = 0.2$ of the remaining τ_{had}.

Scale factors (SFs) are used to correct the efficiencies in simulation to match the efficiencies measured in data for the electron [106,120] and muon [107,121] trigger, reconstruction, identification, and isolation criteria, as well as for the τ_{had} reconstruction, identification, and electron-rejection criteria [118,119]. Additional SFs are also applied for the JVT requirement [112] for pileup and for the b-tagging efficiencies for jets that originate from the hadronization of b-quarks [122], c-quarks [123], and u-, d-, s-quarks or gluons [124].

Multiple selections are defined to create analysis regions that either focus on the cLFV signal processes, or constrain the normalization of fake-lepton backgrounds. All analysis regions are subject to the same lepton preselection requirements shown in Table III.

The SR requires two SS muons and a τ_{had} candidate, at least one jet, and exactly one b-tagged jet. The SS muon

[3]For the overlap removal, ΔR is defined as $\Delta R \equiv \sqrt{(\Delta y)^2 + (\Delta \phi)^2}$, where y is the rapidity of the object.

TABLE III. Common lepton selection requirements applied to all regions used in the analysis.

Preselection:	
Number of leptons	$N_\ell = 3, p_T > 10\,\text{GeV}, \lvert\eta\rvert < 2.5$
Leading muon/electron p_T	$p_T > 27$ GeV
Trigger matching	≥1 trigger-matched muon/electron
Sum of lepton charges	$\sum q_i = \pm 1$

requirement eliminates the large background from processes producing $\mu^+\mu^-$ pairs while the jet selection matches that of the signal process. The CRτ region requires instead two OS muons and a τ_{had} candidate, two or more jets, and exactly one b-tagged jet. This region targets events with two prompt muons from $t\bar{t}$ or $Z+$jets, in which a jet is misidentified as a τ_{had} (denoted "fake τ-lepton"). A requirement on the OS dimuon invariant mass in CRτ around the Z-boson mass is used to increase the proportion of light-flavor jets counted as fake τ-leptons (and decrease the contribution from heavy-flavor jets), consistent with the fraction observed in the SR.

The CR$t\bar{t}\mu$ region requires two muons and one electron of opposite charge to the highest p_T muon, at least one jet, and at most two b-tagged jets. Requiring that the two leptons with the highest p_T are an electron and a muon enhances the $t\bar{t}$ purity, as does the use of a veto on events with an OS dimuon invariant mass in the Z-boson mass window. It also requires the lowest p_T lepton to be a Loose muon to preferentially select events with NP muons. A selection on OS dilepton invariant masses and the leading muon p_T is used to reject signal events in CR$t\bar{t}\mu$ while retaining sufficient background statistics. This requirement was derived in simulation and rejects signal events in which the τ-lepton decays leptonically.

The full requirements for the analysis regions are reported in Table IV. NP muons tend to have lower p_T than those produced in the hard-scatter interaction. The SR and CRτ regions therefore require both the muons to have $p_T > 15$ GeV to suppress this background while CR$t\bar{t}\mu$ retains low p_T muons.

For the single-top-production ($t\bar{t}$ decay) EFT process, 4.6% (2.3%) of generated MC events are reconstructed and satisfy the signal region event selection. Depending on the LQ mass and coupling strength, between 6.9% and 8.1% of generated MC events are reconstructed and satisfy the signal region event selection. These efficiencies are calculated relative to the number of generated events with $\mu\mu\tau$ final states.

VI. NONPROMPT AND FAKE-LEPTON ESTIMATIONS

A. Fake-τ-lepton estimation

As τ_{had} candidates are reconstructed from jets, some jets that did not originate from a τ-lepton decay may be misidentified as a τ_{had}. These fake τ-leptons are suppressed by the τ_{had} identification algorithm but still form a non-negligible background in the SR. To estimate the background from fake τ-leptons, a SF method is used. The SF method involves applying multiplicative factors to the MC simulation to correct for mismodeling of the fake-τ-lepton background. The SFs are derived in CRτ, for which the fake background in data is found by subtracting the nonfake background in MC simulation from the data, and are determined separately for one-prong and three-prong τ_{had} candidates. These SFs are binned in the width[4] of the jet from which the τ_{had} is seeded, and are derived from the data in CRτ as follows:

$$SF_i = \frac{N^{\text{CR}\tau}_{\text{Data},i} - N^{\text{CR}\tau}_{\text{MC,nonfake},i}}{N^{\text{CR}\tau}_{\text{MC,fake},i}}. \tag{5}$$

The index i denotes a particular bin in the jet width distribution. A parametrization in the jet width is motivated as the SFs capture any mismodeling of the relative fractions of jets produced by quarks and gluons (quark-gluon fractions) for jets faking τ-leptons, and any differences in the quark-gluon fractions between CRτ and the SR. The estimated yield in the SR is then found by applying the SFs to the fake τ-leptons in the MC simulation:

$$N^{\text{SR}}_{\text{fakes},i} = N^{\text{SR}}_{\text{MC,fake},i} \times SF_i. \tag{6}$$

Sources of uncertainty relating to the prompt-lepton background subtraction are accounted for by propagating all

TABLE IV. Requirements for each analysis region. The symbol ℓ_3 denotes the lowest p_T lepton. In CR$t\bar{t}\mu$ an additional requirement is placed on the leading muon p_T ($p_T^{\mu_1}$) and dilepton invariant masses in order to reject signal events.

	SR	CRτ	CR$t\bar{t}\mu$
Lepton flavor	$2\mu 1\tau_{\text{had}}$		$2\mu 1e$ ($\ell_3 = \mu$)
N_{jets}	≥1	≥2	≥1
$N_{b-\text{tags}}$	1	1	≤2
τ_{had} p_T	>20 GeV	>20 GeV	…
Muon p_T	>15 GeV	>15 GeV	>10 GeV
Higher p_T muon	Tight	Tight	Tight
Lower p_T muon	Tight	Tight	Loose
Muon charges	SS	OS	…
$m^{\text{OS}}_{\mu\mu}$	…	…	>15 GeV
$\lvert m^{\text{OS}}_{\mu\mu} - M_Z\rvert$	…	<10 GeV	>10 GeV
$3p_T^{\mu_1} + \sum m^{\text{OS}}_{\ell\ell}$	…	…	<400 GeV

[4]The jet width w is defined as the p_T-weighted radial distance between objects associated with the jet and the jet axis: $w = \Sigma_j \Delta R^j p_T^j / \Sigma_j p_T^j$, where j denotes a jet constituent and ΔR^j is its radial distance from the center of the jet.

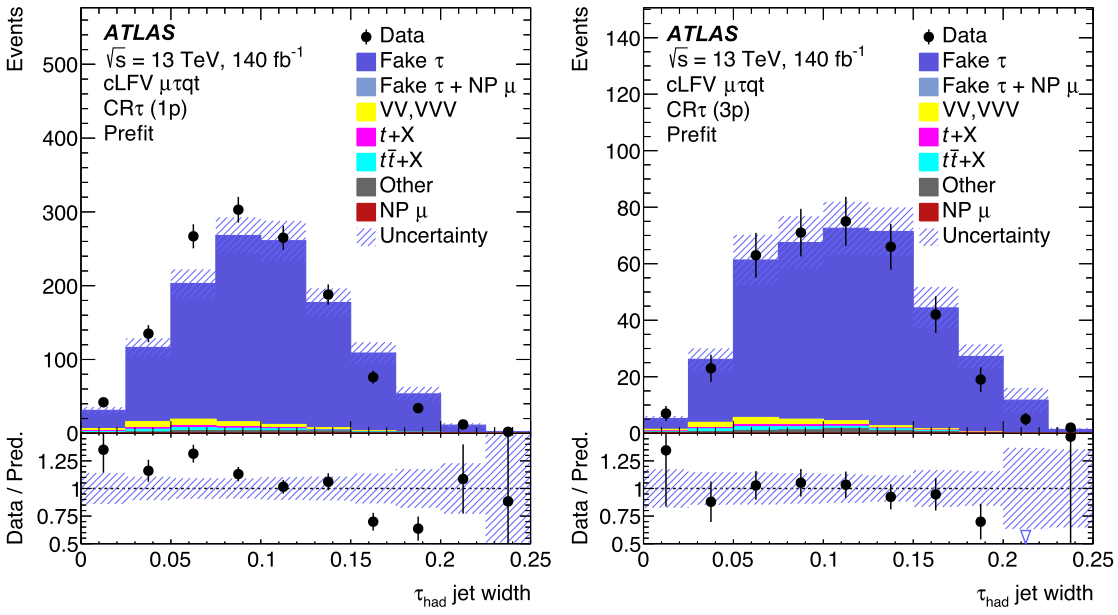

FIG. 3. Observed distribution of the τ_{had} jet width in CRτ compared with prefit expectations from Monte Carlo simulations, separated by (a) one-prong (1p) and (b) three-prong (3p) τ_{had} track multiplicity. This region is used to derive scale factors for the data-driven fake-τ-lepton estimation. The legend entry of $t\bar{t}+X$ is the sum of $t\bar{t}W$, $t\bar{t}Z$, and $t\bar{t}H$. The lower panels show the ratio of the data ("Data") to the background prediction ("Pred."). The uncertainty bands include the statistical and systematic uncertainties in the background prediction. An arrow on the lower panel indicates a point outside of the axis range. The last bin includes overflow events.

systematic uncertainties described in Sec. VII to the SF estimations, as well as uncertainties from limited MC statistics. Comparative SFs were also derived with alternative parametrizations, binned in jet p_{T}, jet η, missing transverse energy $E_{\text{T}}^{\text{miss}}$, total transverse energy H_{T}, and in the separation of the τ_{had} and muon, $\Delta R(\mu, \tau_{\text{had}})$. In all cases, the fake-τ-lepton estimations in the SR were compatible.

Observed event yields in CRτ compared with prefit expectations from MC simulations are shown in Fig. 3 for one-prong and three-prong τ_{had} candidates, as a function of the jet width, prior to the calculation of the fake-τ-lepton SFs. The data and MC event yields in this region are given in Table V.

B. Nonprompt muon estimation

The dominant background in the SR is due to $t\bar{t}$ events reconstructed with three leptons due to a NP muon from a heavy-flavor hadron decay inside a jet, typically a b-jet. A tight muon isolation working point is chosen to suppress this background but this process still constitutes a significant fraction of events that satisfy the event selection. A data-driven template fit is performed using CR$t\bar{t}\mu$ to fit the normalization of the NP muon background. This method allows the data in the CR to correct the rate at which events with NP muons enter the fit. This background is therefore determined simultaneously with the limits set on the signal strength of the process under consideration.

Events with both a NP muon and a fake τ-lepton are corrected using the SFs described in Sec. VI A before being included in the NP muon estimation.

TABLE V. Observed and predicted event yields for CRτ from Monte Carlo simulations with all systematic uncertainties, prior to the calculation of the fake-τ-lepton scale factors separated by one-prong (1p) or three-prong (3p) τ_{had} track multiplicity.

Process	CRτ (1p)	CRτ (3p)
Fake τ	1150 ± 80	364 ± 28
Fake τ+ NP μ	1.6 ± 1.2	0.3 ± 0.5
WZ	22 ± 7	6.5 ± 2.0
ZZ	11 ± 4	3.1 ± 1.0
t + X	12.0 ± 0.9	3.41 ± 0.28
$t\bar{t}Z$	16 ± 7	4.8 ± 2.3
$t\bar{t}W$	0.65 ± 0.34	0.25 ± 0.15
$t\bar{t}H$	0.84 ± 0.12	0.26 ± 0.04
VVV	0.12 ± 0.06	0.027 ± 0.014
$t\bar{t}$ + NP μ	1.0 ± 0.8	0.16 ± 0.24
Z + NP μ	0.022 ± 0.009	⋯
Other	17 ± 9	6.1 ± 3.1
Total	1230 ± 90	389 ± 30
Data	1324	373

VII. SYSTEMATIC UNCERTAINTIES

Systematic effects may change the expected numbers of events from the signal and background processes and the shape of the fitted distributions in the SR and the CRs. These effects are evaluated by varying each source of systematic uncertainty by $\pm 1\sigma$ and considering the resulting deviation from the nominal expectation as the uncertainty.

Uncertainties due to the modeling of both the EFT and leptoquark signals are estimated by considering independent variations of the renormalization and factorization scales by factors of 2 and 0.5, but normalizing the signal to the nominal cross section. The uncertainties due to the PDF are calculated using the NNPDF3.1NLO MC replica set. The standard deviation of this set is used to define a symmetrized uncertainty on the signal sample. The uncertainty arising from the modeling of initial-state radiation (ISR) is evaluated by varying α_s in the initial-state shower, while that arising from final-state radiation (FSR) modeling is evaluated using variations of μ_R for QCD emissions in the final-state shower.

Additionally, an uncertainty due to the choice of parton-shower generator is estimated for the EFT signal by considering the change when using an alternative MC sample that uses the HERWIG7.1.6 prediction instead of the PYTHIA8.306 generator. For $gq_k \to t\ell^{\pm}\ell'^{\mp}$ signal samples, HERWIG is found to predict inaccurate branching fractions for τ-lepton decays. The branching fractions in these HERWIG samples are subsequently corrected to match those predicted by PYTHIA, before the evaluation of the parton-shower uncertainty. The parton-shower uncertainty is increased by applying a conservative uncertainty to the branching ratio corrections, based on the statistical uncertainty of the samples from which the corrections are derived.

Cross-section uncertainties in SM predictions are applied to each background process. A cross-section uncertainty of 6.1% is used for the MC prediction of $t\bar{t}$ production [73]. The primary contribution of this process after the event selections is through NP muons, which may not be well modeled by the MC simulation, and the overall normalization is therefore determined in the fit. For the single-top process, a cross-section uncertainty of 5.3% is included [125,126]. Cross-section uncertainties of 12% and 10%, respectively, are applied to the $t\bar{t}Z$ and $t\bar{t}H$ processes, based on calculations reported in Ref. [100]. Some processes show discrepancies between data and MC simulations in previous measurements; in these cases more conservative uncertainties are applied to cover the difference. These include an uncertainty of 50% for $t\bar{t}W$ production [127–129] and 30% for diboson production [130–132]. For processes with very minor contributions to the signal regions, conservative uncertainties are applied of 40% for $W+$ jets and $Z+$ jets production [130], 50% for triboson production [133], and 50% for all other processes. The measurement is not sensitive to these minor contributions.

For the background processes, uncertainties due to the renormalization and factorization scales are estimated separately for each process, following the same procedure as for the signal.

The uncertainties due to the PDF for the $t\bar{t}$, single-top-quark, $t\bar{t}W$, and $t\bar{t}H$ processes are calculated using the PDF4LHC15 prescription [134] using the Hessian sets consisting of 30 eigenvectors. Each of the 30 eigenvectors is assigned a nuisance parameter that is profiled in the fit. For the $t\bar{t}Z$, $Z+$ jets, $W+$ jets, and diboson background processes the uncertainties due to the PDF are estimated following the same procedure as for the signal, separately for each sample. For the $t\bar{t}$ process, an additional uncertainty arising from the value of $\alpha_s(M_Z) = 0.118$, used to evaluate the PDF, is estimated by using the nominal PDF set evaluated with $\alpha_s(M_Z) = 0.117$ and $\alpha_s(M_Z) = 0.119$. This uncertainty has a negligible impact and is thus neglected for the subdominant background processes.

For the $t\bar{t}$ process, the uncertainty in the matrix-element matching is assessed as the full observed difference between simulated samples generated with the POWHEG BOX and MadGraph5_aMC@NLO programs. Both of the samples are showered with HERWIG7.1.3 [76,77], using the HERWIG7.1 default set of tuned parameters [77,135] and the MMHT2014LO PDF set [136].

To cover the choice of parton-shower and hadronization model, samples are produced with the POWHEG BOX program and then showered with either PYTHIA8.230 using the A14 tune and the NNPDF2.3LO PDF set, or HERWIG7.1.3 using the HERWIG7.1 default set of tuned parameters and the MMHT2014LO PDF set. The difference is taken as a systematic uncertainty. The uncertainties due to the choice of parton-shower generator for the $t\bar{t}H$ and $t\bar{t}Z$ backgrounds are also estimated by comparing the nominal predictions with an alternative set using HERWIG7.0.4 [76,77] showering, with the H7UE set of tuned parameters [77] and the MMHT2014LO PDF set.

The $t\bar{t}W$ background has an uncertainty to cover the choice of generator. This is evaluated for the QCD component as the difference between a sample generated with SHERPA2.2.10 and an alternative sample using MadGraph5_aMC@NLO+PYTHIA8.245 with an FxFx merging scheme [104,137,138]. To evaluate the generator uncertainty on the "subleading" EWK component, the SHERPA2.2.10 EWK sample is compared with a LO MadGraph2.6.2+PYTHIA8 sample that also models these EWK effects.

For the $t\bar{t}$, single-top-quark, $t\bar{t}Z$, and $t\bar{t}H$ processes, the uncertainty arising from the modeling of ISR is evaluated using an independent variation of the A14 tune to its Var3cUp and Var3cDown variants [72] corresponding to variations of α_s in the initial-state shower. For the $t\bar{t}$, single-top-quark, and $t\bar{t}H$ processes the modeling of FSR is

evaluated from an independent variation of the renormalization scale for emissions from the parton shower by factors of 2.0 and 0.5. For the $t\bar{t}$ process, the uncertainty arising from the choice of the h_{damp} parameter within POWHEG is evaluated using an alternative POWHEG+PYTHIA8 $t\bar{t}$ sample in which $h_{\text{damp}} = 3.0 m_{\text{top}}$ (the default setting is $h_{\text{damp}} = 1.5 m_{\text{top}}$).

For the tW single-top-quark process, an uncertainty arising from the removal of the overlap with the $t\bar{t}$ process is estimated by replacing the diagram-removal scheme with the diagram-subtraction scheme [88].

The uncertainty in the combined 2015–2018 integrated luminosity is 0.83% [57] obtained using the LUCID-2 detector [51] for the primary luminosity measurements, complemented by measurements employing the inner detector and calorimeters. The MC samples were reweighted to reproduce the pileup distributions in the data separately for the three periods 2015–2016, 2017, and 2018. The uncertainty due to pileup is evaluated by varying the correction factors used to perform the reweighting within their uncertainties.

The jet energy scale uncertainty is derived by combining information from test-beam data, LHC collision data and simulation, and the jet energy resolution uncertainty is obtained by combining dijet p_{T}-balance measurements and simulation [111]. Additional considerations related to jet flavor, pileup corrections, η intercalibration, and high-p_{T} jets are included. A total of 31 independent contributions are considered for the jet energy scale uncertainty, and 13 for the jet energy resolution uncertainty. There is an additional uncertainty in the efficiency of the JVT algorithm to identify and remove jets from pileup, which is measured with $Z \to \mu^+\mu^-$ events in data using techniques similar to those used in Ref. [112].

The efficiency to correctly tag b-jets is measured using dileptonic $t\bar{t}$ events [122]. The mistag rate for c-jets is measured using semileptonic $t\bar{t}$ events, exploiting the c-jets from the hadronic W-boson decays using techniques similar to those in Ref. [123]. The mistag rate for light jets is measured using a negative-tag method, similar to that in Ref. [124], applied to Z + jets events. Uncertainties on this efficiency and these mistag rates are due to reconstructed object calibrations and to the modeling of the different processes, and are decomposed into sets of uncorrelated sources of uncertainty: 9, 4, and 4 components for b-, c-, and light jets, respectively.

Uncertainties associated with electrons and muons arise from the trigger, reconstruction, identification, and isolation efficiencies, as well as the momentum scale and resolution. These are measured using $Z \to \ell^+\ell^-$ and $J/\psi \to \ell^+\ell^-$ events ($\ell = e, \mu$) [106,107]. Uncertainties associated with τ_{had} candidates cover reconstruction, identification, and electron-rejection efficiencies, as well as the momentum correction, and were estimated by using $Z \to \tau^+\tau^-$, $Z \to e^+e^-$, and dijet events [118,119,139].

The uncertainty originating from the limited number of simulated MC events is implemented via the Barlow-Beeston approach [140]. Three uncertainties for each bin of the fitted distributions are considered: one for the uncertainty originating from the SM backgrounds and one for each of the cLFV signals (single-top-quark production and top-quark pair production with a cLFV top-quark decay process).

The NP muon estimation is performed simultaneously with the limit-setting procedure so sources of uncertainty are accounted for in the same manner as the prompt backgrounds. For the fake-τ-lepton estimation, each source of uncertainty is propagated through the scale factor method to provide systematic variations for the fake-τ-lepton component of the SR. The uncertainty arising from the limited data and MC statistics used to derive the SFs in CRτ is also considered.

VIII. RESULTS

A. Effective field theory interpretation

The normalization factors of the EFT signal and the NP muon contributions are obtained from a simultaneous profile-likelihood fit to the SR and CR$t\bar{t}\mu$ with systematic uncertainties included as nuisance parameters. In both of the regions, the distribution of the scalar sum of the lepton and jet transverse momenta, H_{T}, is used. This distribution separates the EFT signal from the SM backgrounds, as the cLFV single-top-quark production diagrams (Fig. 1) produce high-p_{T} leptons. The likelihood function is constructed as a product of Poisson probability terms over all bins considered in the search. This function depends on a signal strength parameter, μ_{cLFV}, which is defined as a multiplicative factor applied to the predicted yield for the two signal cLFV processes, the normalization of the nonprompt muon contribution $k(\text{NP}\mu)$, and a set of nuisance parameters, θ, that encode the effect of systematic uncertainties on the signal and background expectations. The expected total number of events in a given bin depends on μ_{cLFV}, $k(\text{NP}\mu)$, and θ. All nuisance parameters are subject to Gaussian distribution constraints in the likelihood. For a given value of μ_{cLFV}, the nuisance parameters θ allow variations of the expectations for signal and background according to the corresponding systematic uncertainties, and their fitted values result in the deviations from the nominal expectations that globally provide the best fit to the data. This procedure allows a reduction of the impact of systematic uncertainties on the search sensitivity. Statistical uncertainties in each bin are taken into account by dedicated parameters in the fit. The best fit is obtained by performing a profile-likelihood fit to the data under the signal-plus-background hypothesis, maximizing the likelihood function over μ_{cLFV}, $k(\text{NP}\mu)$, and θ. The fit is evaluated with the RooFit package [141,142].

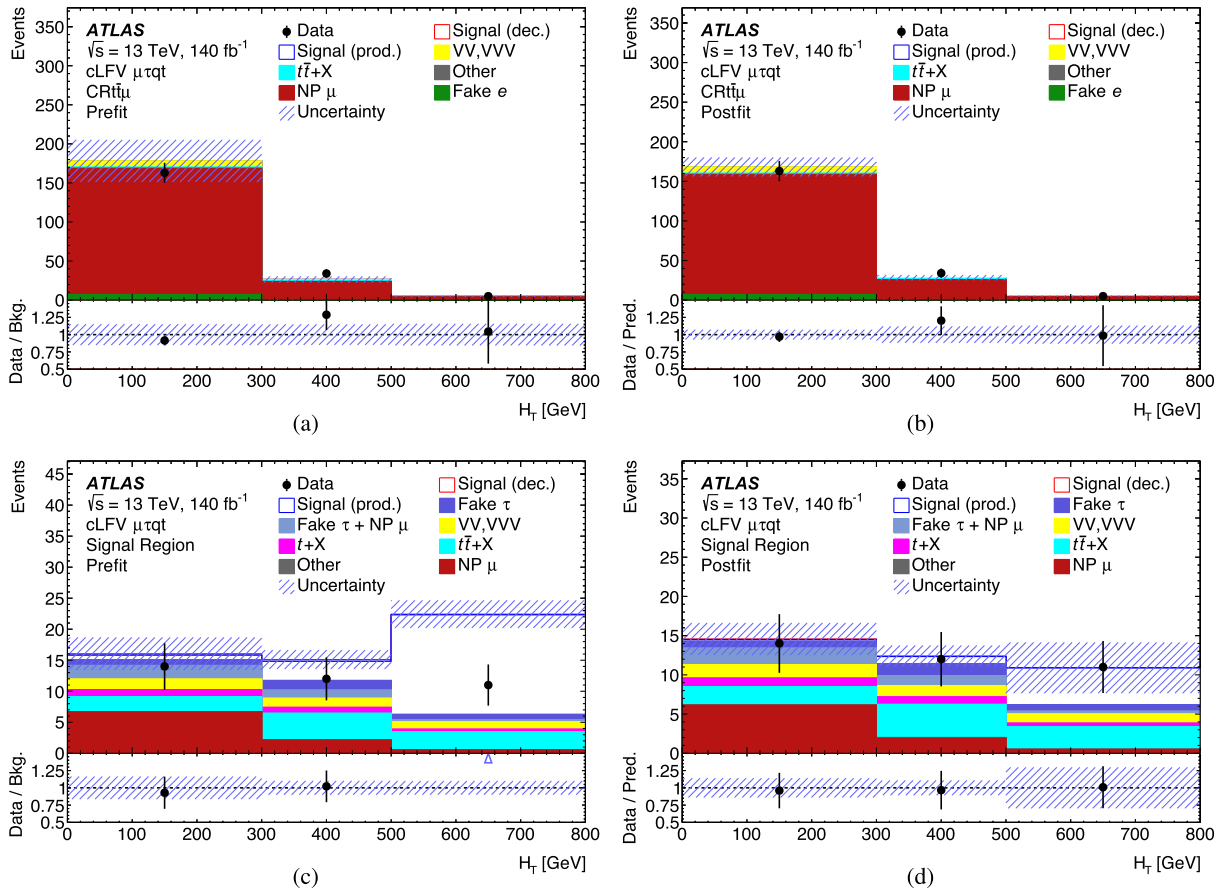

FIG. 4. Observed event yields in CR$t\bar{t}\mu$ and the SR compared with (a),(c) prefit and (b),(d) postfit expectations from Monte Carlo simulations respectively, as a function of the scalar sum of lepton and jet transverse momenta, H_{T}. The prefit signal yield represents all Wilson coefficients set to 0.1 simultaneously for a new physics scale of $\Lambda = 1$ TeV. "Signal (prod.)" and "Signal (dec.)" refer to the single-top-quark production and top-quark pair decay signal contributions, respectively, which are together stacked on the background distribution. The legend entry of $t\bar{t} + X$ is the sum of $t\bar{t}W$, $t\bar{t}Z$, and $t\bar{t}H$. The lower panels show the ratio of the data ("Data") to the background prediction ("Bkg.") for (a),(c) and to the background-plus-signal predictions ("Pred.") for (b),(d). The uncertainty band includes both the statistical and systematic uncertainties in the signal and background predictions. For the postfit plot, correlations among uncertainties were taken into account as determined in the fit under a signal + background hypothesis. An arrow on the lower panel indicates a point outside of the axis range. The last bin includes overflow events.

Observed event yields in the SR and CR$t\bar{t}\mu$, compared with prefit expectations from MC simulations, are shown in Figs. 4(a) and 4(c).

Figures 4(b) and 4(d) show the corresponding postfit distributions, with the postfit yields given in Table VI. The background contributions from NP muon production are scaled by a normalization factor estimated to be $k(\mathrm{NP}\mu) = 1.01 \pm 0.18$ determined by the profile-likelihood fit. The data and SM prediction agree within uncertainties, with the p-value = 0.053 for the background-only hypothesis. There is a small upward fluctuation in the data in the highest H_{T} bin, but no significant cLFV contributions are observed. Upper limits on the signal cross section are set at the 95% CL using the $\mathrm{CL_s}$ method [143]. The corresponding limits on the effective coupling parameters are also calculated [144].

The observed and expected 95% CL limits on the effective coupling strengths, which are set individually, are presented in Table VII. This table shows for comparison the existing limits of the relevant Wilson coefficients, which come from a reinterpretation of a previous ATLAS FCNC search in the tZq channel [40]. The calculation of these limits is performed in Ref. [34]. It can be seen from Table II that the signal cross section is dominated by the $gu \to t\ell^{\pm}\ell'^{\mp}$ process which leads to stronger exclusion limits on $\mu\tau ut$ interactions than $\mu\tau ct$. These Wilson coefficient limits are converted into limits on the top-decay branching ratios using Eq. (2) and presented in Table VIII. Finally, a fit using two inclusive MC samples with all EFT operators activated simultaneously is used to determine an inclusive branching-ratio limit given in Table IX. This complements searches for cLFV in $e\mu qt$

TABLE VI. Postfit event yields for each analysis region entering the fit, with correlations on the full systematic uncertainties taken into account as determined in the fit under a signal + background hypothesis. The "fake electron" category collects small contributions primarily from $t\bar{t}\gamma$ and $Z\gamma$ that enter the event selection due to photon conversions.

Process	SR	CR$t\bar{t}\mu$
$t\bar{t}$ + NP μ	7.9 ± 3.4	164 ± 14
$t\bar{t}W$	3.5 ± 1.8	1.2 ± 0.6
$t\bar{t}H$	3.1 ± 0.4	1.26 ± 0.14
$t\bar{t}Z$	2.9 ± 0.5	0.88 ± 0.33
t + X	2.48 ± 0.18	⋯
WZ	3.6 ± 1.3	7.3 ± 2.4
ZZ	0.59 ± 0.22	1.8 ± 0.6
VVV	0.01 ± 0.05	0.47 ± 0.24
Fake electron	⋯	7 ± 4
Fake τ	3.3 ± 0.4	⋯
Fake τ + NP μ	3.7 ± 2.7	⋯
t + X + NPμ	0.29 ± 0.31	15 ± 5
Z + NP μ	0.192 ± 0.010	1.8 ± 1.0
Other NP μ	0.051 ± 0.010	⋯
Other	0.23 ± 0.11	1.1 ± 0.6
Signal ($t\bar{t}$)	0.19 ± 0.14	0.025 ± 0.019
Signal (single top)	6 ± 4	0.022 ± 0.023
Total	38 ± 5	201 ± 14
Data	37	202

TABLE VII. Expected and observed 95% CL upper limits on Wilson coefficients corresponding to 2Q2L EFT operators that could introduce a cLFV top decay in the $\mu\tau$ channel, and existing limits from Ref. [34] (previous). The previous limits shown for $c_{\mathrm{lequ}}^{1(ijk3)}$ and $c_{\mathrm{lequ}}^{3(ijk3)}$ are tightened by a factor of $\sqrt{2}$ relative to the individual values given in Ref. [34], as that interpretation does not apply the assumption that these operators are Hermitian. The assumption of Hermitian operators results in a larger cross section for a Wilson coefficient of a given value, as its Hermitian conjugate is also considered. Consequently, an observed signal strength results in a tighter upper limit on a Wilson coefficient than if its Hermitian conjugate were considered separately. Results are shown separately for the $\mu\tau ut$ and $\mu\tau ct$ interactions. The lepton generations are denoted by i, $j = 2, 3$ for μ and τ (where $i \neq j$) and the quark generations are denoted by $k = 1, 2$ for u and c, respectively.

	95% CL upper limits on $\lvert c\rvert/\Lambda^2$ (TeV^{-2})					
	$c_{\mathrm{lq}}^{-(ijk3)}$	$c_{\mathrm{eq}}^{(ijk3)}$	$c_{\mathrm{lu}}^{(ijk3)}$	$c_{\mathrm{eu}}^{(ijk3)}$	$c_{\mathrm{lequ}}^{1(ijk3)}$	$c_{\mathrm{lequ}}^{3(ijk3)}$
Previous (u) [34]	12	12	12	12	18	2.4
Expected (u)	0.33	0.31	0.3	0.32	0.33	0.08
Observed (u)	0.43	0.41	0.4	0.42	0.44	0.10
Previous (c) [34]	14	14	14	14	21	2.6
Expected (c)	1.3	1.2	1.2	1.2	1.4	0.28
Observed (c)	1.6	1.6	1.6	1.6	1.8	0.36

TABLE VIII. Expected and observed 95% CL upper limits on the branching ratio ($\mathcal{B}$) corresponding to the decay of a top quark to a muon and a τ-lepton through a cLFV process using specific Wilson coefficients corresponding to 2Q2L EFT operators. Results are shown separately for $\mu\tau ut$ and $\mu\tau ct$ interactions. The lepton generations are denoted by i, $j = 2, 3$ for μ and τ (where $i \neq j$) and the quark generations are denoted by $k = 1, 2$ for u and c, respectively.

	95% CL upper limits on $\mathcal{B}(t \to \mu\tau q)(\times 10^{-7})$					
	$c_{\mathrm{lq}}^{-(ijk3)}$	$c_{\mathrm{eq}}^{(ijk3)}$	$c_{\mathrm{lu}}^{(ijk3)}$	$c_{\mathrm{eu}}^{(ijk3)}$	$c_{\mathrm{lequ}}^{1(ijk3)}$	$c_{\mathrm{lequ}}^{3(ijk3)}$
Expected (u)	2.3	2.0	1.9	2.2	1.2	3.0
Observed (u)	4.0	3.6	3.3	3.8	2.0	5.2
Expected (c)	33	32	32	33	20	41
Observed (c)	56	54	53	54	34	67

interactions by the CMS Collaboration [35] that set branching-ratio limits ranging from $\mathcal{B}(t \to e\mu u) < 0.12 \times 10^{-7}$ to $\mathcal{B}(t \to e\mu c) < 4.98 \times 10^{-7}$ for the scalar-structure up-quark coupling and tensor-structure charm-quark couplings, respectively, following the definitions in Table I.

It is also interesting to consider the case in which all vector operators contribute simultaneously with the same effective coupling strength. This assumes the new physics process couples equally to left- and right-handed fermions. Figure 5(a) shows the exclusion limits on the branching ratio $\mathcal{B}(t \to \mu\tau q)$ for $\mu\tau ut$ and $\mu\tau ct$ interactions when considering scalar, vector, and tensor couplings. Figure 5(b) shows the corresponding limits on the effective coupling strengths under this scenario.

The inclusive branching-ratio sensitivity is dominated by the cLFV single-top-quark production process, where the $t\bar{t}$ decay process improves the observed limits by 1%. The $t\bar{t}$ decay process has a more significant impact when considering the charm-quark EFT operators, for which it contributes up to 11% of the sensitivity.

In all of the limits extracted, the statistical uncertainty is dominant, while the largest sources of systematic uncertainty relate to the modeling of the $t\bar{t} + X$ and diboson processes. These processes populate the highest H_{T} bin of the SR, from which most of the sensitivity to the signal process derives. The $t\bar{t}W$ process utilizes a conservative

TABLE IX. Expected and observed 95% CL upper limits on the inclusive branching ratio ($\mathcal{B}$) corresponding to the decay of a top quark to a muon and a τ-lepton through a cLFV process. Limits are shown for the statistical uncertainty only and for the full set of statistical and systematic uncertainties.

	95% CL upper limits on $\mathcal{B}(t \to \mu\tau q)$	
	Stat. uncertainty	Stat. + syst. uncertainties
Expected	4.6×10^{-7}	5.0×10^{-7}
Observed	8.2×10^{-7}	8.7×10^{-7}

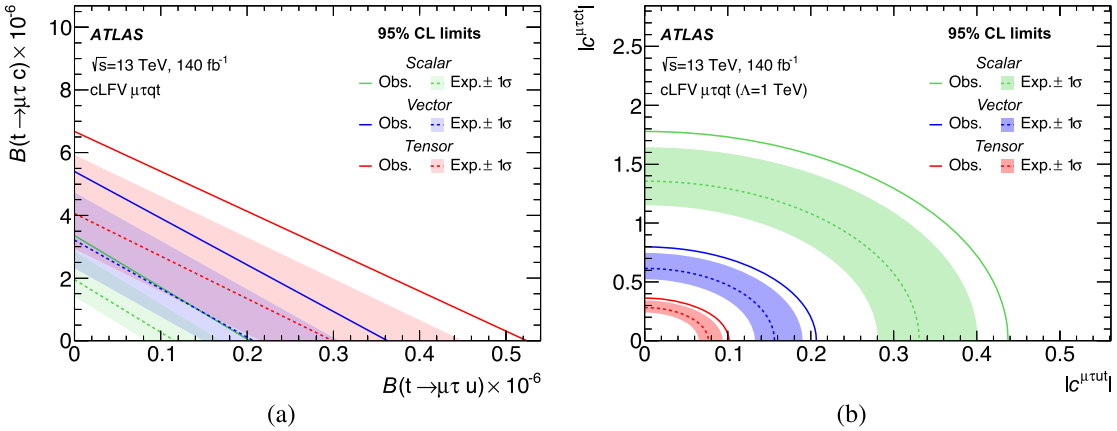

FIG. 5. Expected and observed 95% CL upper limits on the branching ratio corresponding to the decay of a top quark to a muon and a τ-lepton through a cLFV process (a) and on the relevant Wilson coefficients (b) for scalar, vector, and tensor couplings, as defined in Table I. In the vector case, all vector operators are assumed to contribute simultaneously with the same effective coupling strength. The shaded areas show the ± 1 standard deviation bands around the expected limits.

uncertainty in the cross section, which ranks highly. Additionally, as a nonzero EFT signal contribution is permitted by the fit, the associated signal parton-shower uncertainty also plays a leading role in the systematic uncertainty contributions.

B. Leptoquark interpretation

A search for the production of a scalar leptoquark S_1 was performed using the same analysis strategy as the EFT interpretation described in Sec. VIII A, based on the H_T distribution. As discussed in Sec. IV, MC samples are generated in which the S_1 leptoquark is produced in association with a charged lepton via quark-gluon fusion and subsequently decays into a top quark and a second charged lepton. The samples are simulated with masses in the range of $0.5 < m_{S_1} < 2.5$ TeV in steps of 250 GeV, and coupling values λ^{LQ} between 0.5 and 3.5 in steps of 0.5, using the generational hierarchy shown in Eq. (3). Observed and expected limits are set on the S_1 cross section using a profile-likelihood ratio in the asymptotic limit with nuisance parameters to account for systematic uncertainties. The limits on the cross section were extracted at the 95% CL. All experimental and modeling uncertainties that were considered for the EFT interpretation were also considered as nuisance parameters in the leptoquark fit, but with the free-floating parameters representing the Wilson coefficients replaced by a free-floating parameter for the cross section of S_1 production. The same

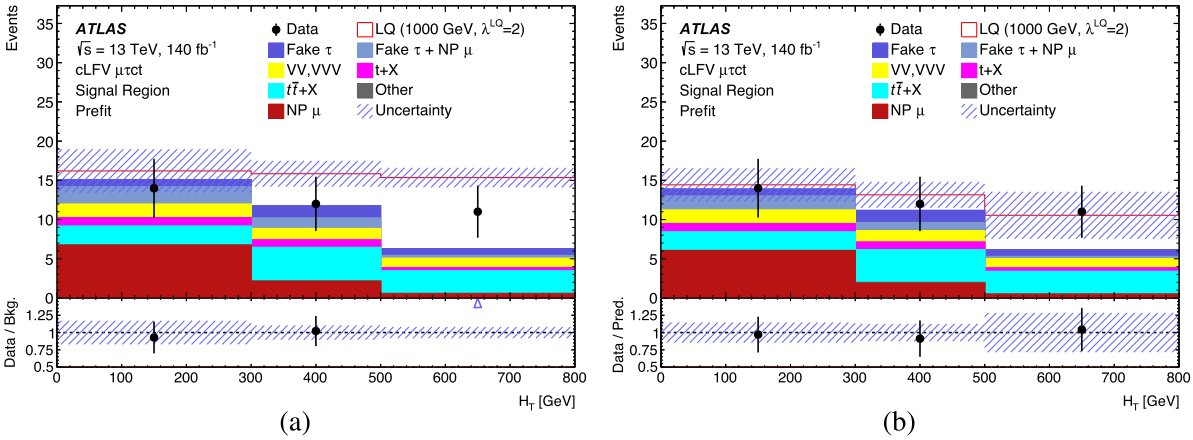

FIG. 6. Observed event yields in the SR compared with (a) prefit and (b) postfit expectations from Monte Carlo simulations. The signal yields represent a leptoquark mass of $m_{S_1} = 1$ TeV and a coupling strength of $\lambda^{LQ} = 2.0$. The uncertainty band includes both the statistical and systematic uncertainties in the signal and background predictions. The legend entry of $t\bar{t} + X$ is the sum of $t\bar{t}W$, $t\bar{t}Z$, and $t\bar{t}H$. The lower panels show the ratio of the data ("Data") to the background prediction ("Bkg.") for (a), and to the background-plus-signal predictions ("Pred.") for (b). An arrow on the lower panel indicates a point outside of the axis range. The last bin includes overflow events.

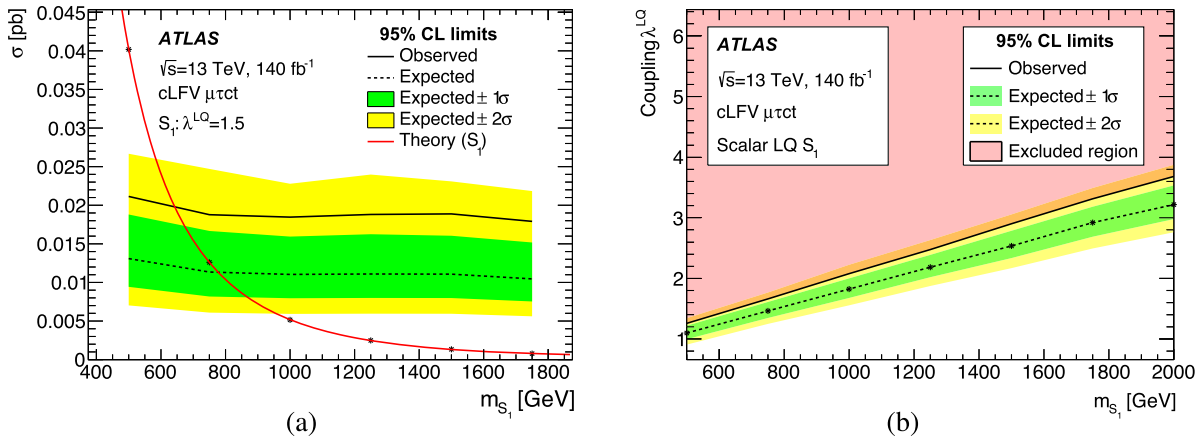

FIG. 7. (a) Expected and observed 95% CL upper limits on the production cross section of a scalar leptoquark with $\lambda^{\mathrm{LQ}} = 1.5$ and for a range of mass values. The overlaid theory line shows a polynominal fit to the theoretical cross-section values. (b) Expected and observed 95% CL upper limits as a function of the leptoquark mass m_{S_1} and the coupling strength λ^{LQ}. The solid line shows the observed limit while the dashed line shows the expected limit with the ± 1 and ± 2 standard deviation bands. The shaded area above the observed limit represents the excluded region.

background estimation techniques, event selection, and region definitions were used. The leptoquark fit was found to have comparable sensitivity to the background modeling as for the EFT interpretation, where the largest sources of systematic uncertainty were the $t\bar{t}W$ modeling and WZ normalization. The sensitivity is dominated by the statistical uncertainty.

Figure 6 shows the comparison between the data and both the prefit and postfit expectations for the H_{T} distribution in the SR, for the S_1 model at $m_{S_1} = 1$ TeV and $\lambda^{\mathrm{LQ}} = 2.0$. Example cross-section limits for different m_{S_1} samples are shown in Fig. 7(a) for $\lambda^{\mathrm{LQ}} = 1.5$. The experimentally observed (expected) cross-section limit is approximately 17–21 fb (10–13 fb) depending on the leptoquark mass.

Figure 7(b) shows the observed and expected limits as a function of both m_{S_1} and λ^{LQ}. Observed (expected) upper limits on leptoquark coupling strengths are set at the 95% CL, ranging from $\lambda^{\mathrm{LQ}} = 1.3(1.1)$ to $\lambda^{\mathrm{LQ}} = 3.7(3.2)$ for masses between 0.5 and 2.0 TeV. The sensitivity for $m_{S_1} > 2.0$ TeV was not high enough to set 95% CL limits for the generated values of λ^{LQ}.

IX. CONCLUSIONS

A search for charged-lepton-flavor violation in top-quark interactions is presented, using proton-proton collision data collected by the ATLAS experiment at the LHC at a center-of-mass energy of $\sqrt{s} = 13$ TeV, corresponding to an integrated luminosity of 140 fb^{-1}. The cLFV single-top-quark production and $t\bar{t}$ decay processes, $gq_k \to t\mu\tau$ and $t\bar{t} \to (\ell\ell' q)((W \to \ell\nu)b)$ respectively, are considered, whereby the SM top quark always produces a muon in the final state. The signal topology is thus characterized by the presence of two isolated muons, one hadronically decaying τ-lepton, at least one jet and exactly one b-tagged jet; to suppress backgrounds the muons are required to have the same electric charge.

The SM prediction is found to agree with the data to within 1.6σ. The limits obtained on the Wilson coefficients improve upon the previous results from a reinterpretation of an ATLAS FCNC tZq analysis, from a factor of 7.2 for $|c_{\mathrm{lequ}}^{3(2323)}|/\Lambda^2$ (for $\mu\tau ct$) to a factor of 41 for $|c_{\mathrm{lequ}}^{1(2313)}|/\Lambda^2$ (for $\mu\tau ut$). These Wilson coefficient limits are translated into an observed 95% confidence level upper limit on the $t \to \mu\tau q$ decay branching ratio of $\mathcal{B}(t \to \mu\tau q) < 8.7 \times 10^{-7}$.

A search for single scalar leptoquark S_1 production is also performed assuming fixed hierarchical couplings to multiple quark and lepton flavor generations. Limits are set on this model as a function of the leptoquark mass m_{S_1} and an overall coupling strength λ^{LQ}. Upper limits on leptoquark coupling strengths are set at the 95% CL, ranging from $\lambda^{\mathrm{LQ}} = 1.3$ to $\lambda^{\mathrm{LQ}} = 3.7$ for masses between 0.5 and 2.0 TeV.

ACKNOWLEDGMENTS

We thank CERN for the very successful operation of the LHC and its injectors, as well as the support staff at CERN and at our institutions worldwide without whom ATLAS could not be operated efficiently. The crucial computing support from all WLCG partners is acknowledged gratefully, in particular from CERN, the ATLAS Tier-1 facilities at TRIUMF/SFU (Canada), NDGF (Denmark, Norway, Sweden), CC-IN2P3 (France), KIT/GridKA (Germany), INFN-CNAF (Italy), NL-T1 (Netherlands), PIC (Spain), RAL (UK), and BNL (USA), the Tier-2 facilities worldwide, and large non-WLCG resource providers. Major contributors of computing resources are listed in

Ref. [145]. We gratefully acknowledge the support of ANPCyT, Argentina; YerPhI, Armenia; ARC, Australia; BMWFW and FWF, Austria; ANAS, Azerbaijan; CNPq and FAPESP, Brazil; NSERC, NRC, and CFI, Canada; CERN; ANID, Chile; CAS, MOST, and NSFC, China; Minciencias, Colombia; MEYS CR, Czech Republic; DNRF and DNSRC, Denmark; IN2P3-CNRS and CEA-DRF/IRFU, France; SRNSFG, Georgia; BMBF, HGF, and MPG, Germany; GSRI, Greece; RGC and Hong Kong SAR, China; ISF and Benoziyo Center, Israel; INFN, Italy; MEXT and JSPS, Japan; CNRST, Morocco; NWO, Netherlands; RCN, Norway; MEiN, Poland; FCT, Portugal; MNE/IFA, Romania; MESTD, Serbia; MSSR, Slovakia; ARRS and MIZŠ, Slovenia; DSI/NRF, South Africa; MICINN, Spain; SRC and Wallenberg Foundation, Sweden; SERI, SNSF, and Cantons of Bern and Geneva, Switzerland; MOST, Taipei; TENMAK, Türkiye; STFC, United Kingdom; DOE and NSF, USA. Individual groups and members have received support from BCKDF, CANARIE, CRC, and DRAC, Canada; PRIMUS 21/SCI/017 and UNCE SCI/013, Czech Republic; COST, ERC, ERDF, Horizon 2020, ICSC-NextGenerationEU, and Marie Skłodowska-Curie Actions, European Union; Investissements d'Avenir Labex, Investissements d'Avenir Idex, and ANR, France; DFG and AvH Foundation, Germany; Herakleitos, Thales, and Aristeia programs co-financed by EU-ESF and the Greek NSRF, Greece; BSF-NSF and MINERVA, Israel; Norwegian Financial Mechanism 2014–2021, Norway; NCN and NAWA, Poland; La Caixa Banking Foundation, CERCA Programme Generalitat de Catalunya and PROMETEO, and GenT Programmes Generalitat Valenciana, Spain; Göran Gustafssons Stiftelse, Sweden; The Royal Society and Leverhulme Trust, United Kingdom. In addition, individual members wish to acknowledge support from CERN: European Organization for Nuclear Research (CERN PJAS); Chile: Agencia Nacional de Investigación y Desarrollo (Grants No. FONDECYT 1190886, No. FONDECYT 1210400, and No. FONDECYT 1230987); China: National Natural Science Foundation of China (Grants No. NSFC—12175119 and No. NSFC 12275265); European Union: European Research Council (Grants No. ERC—948254 and No. ERC 101089007), Horizon 2020 Framework Programme (Grant No. MUCCA—CHIST-ERA-19-XAI-00), Italian Center for High Performance Computing, Big Data and Quantum Computing (ICSC, NextGenerationEU); France: Agence Nationale de la Recherche (Grants No. ANR-20-CE31-0013 and No. ANR-21-CE31-0022), Investissements d'Avenir Labex (Grant No. ANR-11-LABX-0012); Germany: Baden-Württemberg Stiftung (BW Stiftung-Postdoc Eliteprogramme), Deutsche Forschungsgemeinschaft (Grants No. DFG—469666862 and No. DFG—CR 312/5-2); Italy: Istituto Nazionale di Fisica Nucleare (ICSC, NextGenerationEU); Japan: Japan Society for the Promotion of Science (Grants No. JSPS KAKENHI 22H01227, No. JSPS KAKENHI 22KK0227, No. JSPS KAKENHI JP21H05085, and No. JSPS KAKENHI JP22H04944); Netherlands: Netherlands Organisation for Scientific Research (NWO Veni 2020—VI.Veni.202.179); Norway: Research Council of Norway (Grant No. RCN-314472); Poland: Polish National Agency for Academic Exchange (Grant No. PPN/PPO/2020/1/00002/U/00001), Polish National Science Centre (Grants No. NCN 2021/42/E/ST2/00350, No. NCN OPUS nr 2022/47/B/ST2/03059, No. NCN UMO-2019/34/E/ST2/00393, No. UMO-2020/37/B/ST2/01043, and No. UMO-2022/47/O/ST2/00148); Slovenia: Slovenian Research Agency (ARIS Grant No. J1-3010); Spain: BBVA Foundation (Grant No. LEO22-1-603), Generalitat Valenciana (Artemisa, FEDER, IDIFEDER/2018/048), Ministry of Science and Innovation (Grants No. RYC2019-028510-I and No. RYC2020-030254-I), PROMETEO and GenT Programmes Generalitat Valenciana (Grants No. CIDEGENT/2019/023 and No. CIDEGENT/2019/027); Sweden: Swedish Research Council (Grant No. VR 2022-03845), Knut and Alice Wallenberg Foundation (Grant No. KAW 2022.0358); Switzerland: Swiss National Science Foundation (Grant No. SNSF—PCEFP2_194658); United Kingdom: Leverhulme Trust (Leverhulme Trust Grant No. RPG-2020-004); USA: Neubauer Family Foundation.

[1] Z. Maki, M. Nakagawa, and S. Sakata, Remarks on the unified model of elementary particles, Prog. Theor. Phys. **28**, 870 (1962).

[2] B. Pontecorvo, Neutrino experiments and the problem of conservation of leptonic charge, Zh. Eksp. Teor. Fiz. **53**, 1717 (1967), http://jetp.ras.ru/cgi-bin/e/index/e/26/5/p984?a=list [Sov. Phys. JETP **26**, 984 (1968)].

[3] Super-Kamiokande Collaboration, Evidence for oscillation of atmospheric neutrinos, Phys. Rev. Lett. **81**, 1562 (1998).

[4] SNO Collaboration, Measurement of the rate of $\nu_e + d \rightarrow p + p + e^-$ interactions produced by ^{8}B solar neutrinos at the Sudbury Neutrino Observatory, Phys. Rev. Lett. **87**, 071301 (2001).

[5] SNO Collaboration, Direct evidence for neutrino flavor transformation from neutral-current interactions in the Sudbury Neutrino Observatory, Phys. Rev. Lett. **89**, 011301 (2002).

[6] L. Calibbi and G. Signorelli, Charged lepton flavour violation: An experimental and theoretical introduction, Riv. Nuovo Cimento **41**, 1 (2018).

[7] I. Doršner, S. Fajfer, A. Greljo, J. F. Kamenik, and N. Košnik, Physics of leptoquarks in precision experiments and at particle colliders, Phys. Rep. **641**, 1 (2016).

[8] T. J. Kim, P. Ko, J. Li, J. Park, and P. Wu, Correlation between $R_{D^{(*)}}$ and top quark FCNC decays in leptoquark models, J. High Energy Phys. 07 (2019) 025.

[9] H. Georgi and S. L. Glashow, Unity of all elementary-particle forces, Phys. Rev. Lett. **32**, 438 (1974).

[10] H. Georgi, The state of the art—gauge theories, AIP Conf. Proc. **23**, 575 (1975).

[11] H. Fritzsch and P. Minkowski, Unified interactions of leptons and hadrons, Ann. Phys. (N.Y.) **93**, 193 (1975).

[12] S. M. Barr, A new symmetry breaking pattern for SO(10) and proton decay, Phys. Lett. **112B**, 219 (1982).

[13] A. De Rújula, H. Georgi, and S. L. Glashow, Flavor goniometry by proton decay, Phys. Rev. Lett. **45**, 413 (1980).

[14] J.-P. Derendinger, J. E. Kim, and D. V. Nanopoulos, Anti-SU(5), Phys. Lett. **139B**, 170 (1984).

[15] I. Antoniadis, J. Ellis, J. S. Hagelin, and D. V. Nanopoulos, Supersymmetric flipped SU(5) revitalized, Phys. Lett. B **194**, 231 (1987).

[16] L. J. Hall and M. Suzuki, Explicit *R*-parity breaking in supersymmetric models, Nucl. Phys. **B231**, 419 (1984).

[17] S. Dawson, *R*-parity breaking in supersymmetric theories, Nucl. Phys. **B261**, 297 (1985).

[18] G. F. Giudice and R. Rattazzi, *R*-parity violation and unification, Phys. Lett. B **406**, 321 (1997).

[19] C. Csáki, Y. Grossman, and B. Heidenreich, Minimal flavor violation supersymmetry: A natural theory for *R*-parity violation, Phys. Rev. D **85**, 095009 (2012).

[20] B. Bajc and L. Di Luzio, *R*-parity violation in SU(5), J. High Energy Phys. 07 (2015) 123.

[21] E. Eichten, I. Hinchliffe, K. D. Lane, and C. Quigg, Signatures for technicolor, Phys. Rev. D **34**, 1547 (1986).

[22] E. Farhi and L. Susskind, Technicolour, Phys. Rep. **74**, 277 (1981).

[23] H. Georgi and S. L. Glashow, Unextended hypercolor and unification, Phys. Rev. Lett. **47**, 1511 (1981).

[24] *BABAR* Collaboration, Evidence for an excess of $\bar{B} \to D^{(*)}\tau^-\bar{\nu}_\tau$ decays, Phys. Rev. Lett. **109**, 101802 (2012).

[25] *BABAR* Collaboration, Measurement of an excess of $\bar{B} \to D^{(*)}\tau^-\bar{\nu}_\tau$ decays and implications for charged Higgs bosons, Phys. Rev. D **88**, 072012 (2013).

[26] Belle Collaboration, Measurement of the branching ratio of $\bar{B} \to D^{(*)}\tau^-\bar{\nu}_\tau$ relative to $\bar{B} \to D^{(*)}\ell^-\bar{\nu}_\ell$ decays with hadronic tagging at Belle, Phys. Rev. D **92**, 072014 (2015).

[27] Belle Collaboration, Measurement of the τ lepton polarization and $R(D^*)$ in the decay $\bar{B} \to D^*\tau^-\bar{\nu}_\tau$, Phys. Rev. Lett. **118**, 211801 (2017).

[28] Belle Collaboration, Measurement of the τ lepton polarization and $R(D^*)$ in the decay $\bar{B} \to D^*\tau^-\bar{\nu}_\tau$ with one-prong hadronic τ decays at Belle, Phys. Rev. D **97**, 012004 (2018).

[29] Belle Collaboration, Measurement of $\mathcal{R}(D)$ and $\mathcal{R}(D^*)$ with a semileptonic tagging method, Phys. Rev. Lett. **124**, 161803 (2020).

[30] LHCb Collaboration, Measurement of the ratios of branching fractions $\mathcal{R}(D^*)$ and $\mathcal{R}(D^0)$, Phys. Rev. Lett. **131**, 111802 (2023).

[31] LHCb Collaboration, Test of lepton flavor universality using $B^0 \to D^{*-}\tau^+\nu_\tau$ decays with hadronic τ channels, Phys. Rev. D **108**, 012018 (2023).

[32] Belle-II Collaboration, A test of lepton flavor universality with a measurement of $R(D^*)$ using hadronic B tagging at the Belle II experiment, arXiv:2401.02840.

[33] HFLAV Collaboration, Averages of b-hadron, c-hadron, and τ-lepton properties as of 2021, Phys. Rev. D **107**, 052008 (2023).

[34] M. Chala, J. Santiago, and M. Spannowsky, Constraining four-fermion operators using rare top decays, J. High Energy Phys. 04 (2019) 014.

[35] CMS Collaboration, Search for charged-lepton flavor violation in the production and decay of top quarks using trilepton final states in proton-proton collisions at $\sqrt{s} = 13$ TeV, arXiv:2312.03199.

[36] S. Davidson, M. L. Mangano, S. Perries, and V. Sordini, Lepton flavour violating top decays at the LHC, Eur. Phys. J. C **75**, 450 (2015).

[37] M. Schmaltz and Y.-M. Zhong, The leptoquark Hunter's guide: Large coupling, J. High Energy Phys. 01 (2019) 132.

[38] B. Grzadkowski, M. Iskrzyński, M. Misiak, and J. Rosiek, Dimension-six terms in the standard model Lagrangian, J. High Energy Phys. 10 (2010) 085.

[39] G. Durieux, F. Maltoni, and C. Zhang, Global approach to top-quark flavor-changing interactions, Phys. Rev. D **91**, 074017 (2015).

[40] ATLAS Collaboration, Search for flavour-changing neutral current top-quark decays $t \to qZ$ in proton-proton collisions at $\sqrt{s} = 13$ TeV with the ATLAS detector, J. High Energy Phys. 07 (2018) 176.

[41] ATLAS Collaboration, Search for leptoquarks decaying into the $b\tau$ final state in pp collisions at $\sqrt{s} = 13$ TeV with the ATLAS detector, J. High Energy Phys. 10 (2023) 001.

[42] CMS Collaboration, Search for a third-generation leptoquark coupled to a τ lepton and a b quark through single, pair, and nonresonant production in proton-proton collisions at $\sqrt{s} = 13$ TeV, J. High Energy Phys. 05 (2024) 311.

[43] E. Alvarez and M. Szewc, Nonresonant leptoquark with multigeneration couplings for $\mu\mu jj$ and $\mu\nu jj$ at the LHC, Phys. Rev. D **99**, 095004 (2019).

[44] L. Di Luzio, A. Greljo, and M. Nardecchia, Gauge leptoquark as the origin of B-physics anomalies, Phys. Rev. D **96**, 115011 (2017).

[45] I. de Medeiros Varzielas and J. Talbert, Simplified models of flavourful leptoquarks, Eur. Phys. J. C **79**, 536 (2019).

[46] W.-F. Chang, S.-C. Liou, C.-F. Wong, and F. Xu, Charged lepton flavor violating processes and scalar leptoquark

decay branching ratios in the colored Zee-Babu model, J. High Energy Phys. 10 (2016) 106.
[47] J. Aebischer, G. Isidori, M. Pesut, B. A. Stefanek, and F. Wilsch, Confronting the vector leptoquark hypothesis with new low- and high-energy data, Eur. Phys. J. C **83**, 153 (2023).
[48] ATLAS Collaboration, The ATLAS experiment at the CERN Large Hadron Collider, J. Instrum. **3**, S08003 (2008).
[49] ATLAS Collaboration, ATLAS insertable *B*-layer technical design report, Report No. ATLAS-TDR-19, 2010, https://cds.cern.ch/record/1291633; ATLAS insertable *B*-layer technical design report addendum, Report No. ATLAS-TDR-19-ADD-1, 2012, https://cds.cern.ch/record/1451888.
[50] B. Abbott *et al.*, Production and integration of the ATLAS insertable *B*-layer, J. Instrum. **13**, T05008 (2018).
[51] G. Avoni *et al.*, The new LUCID-2 detector for luminosity measurement and monitoring in ATLAS, J. Instrum. **13**, P07017 (2018).
[52] ATLAS Collaboration, Performance of the ATLAS trigger system in 2015, Eur. Phys. J. C **77**, 317 (2017).
[53] ATLAS Collaboration, The ATLAS Collaboration software and firmware, Report No. ATL-SOFT-PUB-2021-001, 2021, https://cds.cern.ch/record/2767187.
[54] ATLAS Collaboration, Performance of electron and photon triggers in ATLAS during LHC Run 2, Eur. Phys. J. C **80**, 47 (2020).
[55] ATLAS Collaboration, Performance of the ATLAS muon triggers in Run 2, J. Instrum. **15**, P09015 (2020).
[56] ATLAS Collaboration, ATLAS data quality operations and performance for 2015–2018 data-taking, J. Instrum. **15**, P04003 (2020).
[57] ATLAS Collaboration, Luminosity determination in pp collisions at $\sqrt{s} = 13$ TeV using the ATLAS detector at the LHC, Eur. Phys. J. C **83**, 982 (2023).
[58] T. Sjöstrand, S. Mrenna, and P. Skands, A brief introduction to PYTHIA8.1, Comput. Phys. Commun. **178**, 852 (2008).
[59] R. D. Ball *et al.* (NNPDF Collaboration), Parton distributions with LHC data, Nucl. Phys. **B867**, 244 (2013).
[60] ATLAS Collaboration, The PYTHIA8 A3 tune description of ATLAS minimum bias and inelastic measurements incorporating the Donnachie-Landshoff diffractive model, Report No. ATL-PHYS-PUB-2016-017, 2016, https://cds.cern.ch/record/2206965.
[61] ATLAS Collaboration, The ATLAS simulation infrastructure, Eur. Phys. J. C **70**, 823 (2010).
[62] S. Agostinelli *et al.*, GEANT4—A simulation toolkit, Nucl. Instrum. Methods Phys. Res., Sect. A **506**, 250 (2003).
[63] ATLAS Collaboration, The simulation principle and performance of the ATLAS fast calorimeter simulation FastCaloSim, Report No. ATL-PHYS-PUB-2010-013, 2010, https://cds.cern.ch/record/1300517.
[64] E. Bothmann *et al.*, Event generation with SHERPA2.2, SciPost Phys. **7**, 034 (2019).
[65] D. J. Lange, The EvtGen particle decay simulation package, Nucl. Instrum. Methods Phys. Res., Sect. A **462**, 152 (2001).
[66] C. Degrande, C. Duhr, B. Fuks, D. Grellscheid, O. Mattelaer, and T. Reiter, UFO—The universal FeynRules output, Comput. Phys. Commun. **183**, 1201 (2012).
[67] A. Alloul, N. D. Christensen, C. Degrande, C. Duhr, and B. Fuks, FeynRules 2.0—A complete toolbox for tree-level phenomenology, Comput. Phys. Commun. **185**, 2250 (2014).
[68] J. A. Aguilar-Saavedra *et al.*, Interpreting top-quark LHC measurements in the standard-model effective field theory, arXiv:1802.07237.
[69] J. Alwall, R. Frederix, S. Frixione, V. Hirschi, F. Maltoni, O. Mattelaer, H.-S. Shao, T. Stelzer, P. Torrielli, and M. Zaro, The automated computation of tree-level and next-to-leading order differential cross sections, and their matching to parton shower simulations, J. High Energy Phys. 07 (2014) 079.
[70] C. Bierlich *et al.*, A comprehensive guide to the physics and usage of PYTHIA8.3, SciPost Phys. Codebases **2022**, 8 (2022).
[71] NNPDF Collaboration, Parton distributions from high-precision collider data, Eur. Phys. J. C **77**, 663 (2017).
[72] ATLAS Collaboration, ATLAS PYTHIA8 tunes to 7 TeV data, Report No. ATL-PHYS-PUB-2014-021, 2014, https://cds.cern.ch/record/1966419.
[73] M. Czakon and A. Mitov, TOP++: A program for the calculation of the top-pair cross-section at hadron colliders, Comput. Phys. Commun. **185**, 2930 (2014).
[74] I. Brivio, Y. Jiang, and M. Trott, The SMEFTsim package, theory and tools, J. High Energy Phys. 12 (2017) 070.
[75] I. Brivio, SMEFTsim 3.0—A practical guide, J. High Energy Phys. 04 (2021) 073.
[76] M. Bähr *et al.*, HERWIG++ physics and manual, Eur. Phys. J. C **58**, 639 (2008).
[77] J. Bellm *et al.*, HERWIG7.0/HERWIG++ 3.0 release note, Eur. Phys. J. C **76**, 196 (2016).
[78] R. D. Ball *et al.* (NNPDF Collaboration), Parton distributions for the LHC run II, J. High Energy Phys. 04 (2015) 040.
[79] B. Diaz, M. Schmaltz, and Y.-M. Zhong, The leptoquark Hunter's guide: Pair production, J. High Energy Phys. 10 (2017) 097.
[80] S. Frixione, G. Ridolfi, and P. Nason, A positive-weight next-to-leading-order Monte Carlo for heavy flavour hadroproduction, J. High Energy Phys. 09 (2007) 126.
[81] P. Nason, A new method for combining NLO QCD with shower Monte Carlo algorithms, J. High Energy Phys. 11 (2004) 040.
[82] S. Frixione, P. Nason, and C. Oleari, Matching NLO QCD computations with parton shower simulations: The POWHEG method, J. High Energy Phys. 11 (2007) 070.
[83] S. Alioli, P. Nason, C. Oleari, and E. Re, A general framework for implementing NLO calculations in shower Monte Carlo programs: The POWHEG BOX, J. High Energy Phys. 06 (2010) 043.
[84] ATLAS Collaboration, Improvements in $t\bar{t}$ modelling using NLO + PS Monte Carlo generators for Run 2, Report No. ATL-PHYS-PUB-2018-009, 2018, https://cds.cern.ch/record/2630327.
[85] T. Sjöstrand, S. Ask, J. R. Christiansen, R. Corke, N. Desai, P. Ilten, S. Mrenna, S. Prestel, C. O. Rasmussen, and

P. Z. Skands, An introduction to PYTHIA8.2, Comput. Phys. Commun. **191**, 159 (2015).
[86] R. Frederix, E. Re, and P. Torrielli, Single-top t-channel hadroproduction in the four-flavour scheme with POWHEG and aMC@NLO, J. High Energy Phys. 09 (2012) 130.
[87] S. Alioli, P. Nason, C. Oleari, and E. Re, NLO single-top production matched with shower in POWHEG: s- and t-channel contributions, J. High Energy Phys. 09 (2009) 111.
[88] S. Frixione, E. Laenen, P. Motylinski, C. White, and B. R. Webber, Single-top hadroproduction in association with a W boson, J. High Energy Phys. 07 (2008) 029.
[89] S. Frixione, E. Laenen, P. Motylinski, and B. R. Webber, Angular correlations of lepton pairs from vector boson and top quark decays in Monte Carlo simulations, J. High Energy Phys. 04 (2007) 081.
[90] P. Artoisenet, R. Frederix, O. Mattelaer, and R. Rietkerk, Automatic spin-entangled decays of heavy resonances in Monte Carlo simulations, J. High Energy Phys. 03 (2013) 015.
[91] T. Gleisberg and S. Höche, COMIX, a new matrix element generator, J. High Energy Phys. 12 (2008) 039.
[92] S. Schumann and F. Krauss, A parton shower algorithm based on Catani-Seymour dipole factorisation, J. High Energy Phys. 03 (2008) 038.
[93] F. Buccioni, J.-N. Lang, J. M. Lindert, P. Maierhöfer, S. Pozzorini, H. Zhang, and M. F. Zoller, OpenLoops 2, Eur. Phys. J. C **79**, 866 (2019).
[94] F. Cascioli, P. Maierhöfer, and S. Pozzorini, Scattering amplitudes with open loops, Phys. Rev. Lett. **108**, 111601 (2012).
[95] A. Denner, S. Dittmaier, and L. Hofer, Collier: A FORTRAN-based complex one-loop library in extended regularizations, Comput. Phys. Commun. **212**, 220 (2017).
[96] S. Kallweit, J. M. Lindert, P. Maierhöfer, S. Pozzorini, and M. Schönherr, NLO QCD + EW predictions for V + jets including off-shell vector-boson decays and multijet merging, J. High Energy Phys. 04 (2016) 021.
[97] R. Frederix, D. Pagani, and M. Zaro, Large NLO corrections in $t\bar{t}W^{\pm}$ and $t\bar{t}t\bar{t}$ hadroproduction from supposedly subleading EW contributions, J. High Energy Phys. 02 (2018) 031.
[98] R. Frederix and I. Tsinikos, On improving NLO merging for ttW production, J. High Energy Phys. 11 (2021) 029.
[99] H. B. Hartanto, B. Jäger, L. Reina, and D. Wackeroth, Higgs boson production in association with top quarks in the POWHEG BOX, Phys. Rev. D **91**, 094003 (2015).
[100] D. de Florian *et al.*, Handbook of LHC Higgs cross sections: 4. Deciphering the nature of the Higgs sector, arXiv:1610.07922, 10.23731/CYRM-2017-002.
[101] S. Höche, F. Krauss, M. Schönherr, and F. Siegert, QCD matrix elements + parton showers. The NLO case, J. High Energy Phys. 04 (2013) 027.
[102] J.-C. Winter, F. Krauss, and G. Soff, A modified cluster-hadronisation model, Eur. Phys. J. C **36**, 381 (2004).
[103] S. Höche, F. Krauss, M. Schönherr, and F. Siegert, A critical appraisal of NLO + PS matching methods, J. High Energy Phys. 09 (2012) 049.
[104] S. Catani, F. Krauss, B. R. Webber, and R. Kuhn, QCD matrix elements + parton showers, J. High Energy Phys. 11 (2001) 063.
[105] S. Höche, F. Krauss, S. Schumann, and F. Siegert, QCD matrix elements and truncated showers, J. High Energy Phys. 05 (2009) 053.
[106] ATLAS Collaboration, Electron and photon performance measurements with the ATLAS detector using the 2015–2017 LHC proton–proton collision data, J. Instrum. **14**, P12006 (2019).
[107] ATLAS Collaboration, Muon reconstruction and identification efficiency in ATLAS using the full Run 2 pp collision data set at $\sqrt{s} = 13$ TeV, Eur. Phys. J. C **81**, 578 (2021).
[108] ATLAS Collaboration, Jet reconstruction and performance using particle flow with the ATLAS detector, Eur. Phys. J. C **77**, 466 (2017).
[109] M. Cacciari, G. P. Salam, and G. Soyez, The anti-k_t jet clustering algorithm, J. High Energy Phys. 04 (2008) 063.
[110] M. Cacciari, G. P. Salam, and G. Soyez, FastJet user manual, Eur. Phys. J. C **72**, 1896 (2012).
[111] ATLAS Collaboration, Jet energy scale and resolution measured in proton-proton collisions at $\sqrt{s} = 13$ TeV with the ATLAS detector, Eur. Phys. J. C **81**, 689 (2021).
[112] ATLAS Collaboration, Performance of pile-up mitigation techniques for jets in pp collisions at $\sqrt{s} = 8$ TeV using the ATLAS detector, Eur. Phys. J. C **76**, 581 (2016).
[113] ATLAS Collaboration, Selection of jets produced in 13 TeV proton-proton collisions with the ATLAS detector, Report No. ATLAS-CONF-2015-029, 2015, https://cds.cern.ch/record/2037702.
[114] ATLAS Collaboration, ATLAS flavour-tagging algorithms for the LHC Run 2 pp collision dataset, Eur. Phys. J. C **83**, 681 (2023).
[115] ATLAS Collaboration, Topological cell clustering in the ATLAS calorimeters and its performance in LHC Run 1, Eur. Phys. J. C **77**, 490 (2017).
[116] T. Barillari *et al.*, Local hadronic calibration, Report No. ATL-LARG-PUB-2009-001-2, 2008, https://cds.cern.ch/record/1112035.
[117] ATLAS Collaboration, Reconstruction, energy calibration, and identification of hadronically decaying tau leptons in the ATLAS experiment for Run-2 of the LHC, Report No. ATL-PHYS-PUB-2015-045, 2015, https://cds.cern.ch/record/2064383.
[118] ATLAS Collaboration, Measurement of the tau lepton reconstruction and identification performance in the ATLAS experiment using pp collisions at $\sqrt{s} = 13$ TeV, Report No. ATLAS-CONF-2017-029, 2017, https://cds.cern.ch/record/2261772.
[119] ATLAS Collaboration, Identification of hadronic tau lepton decays using neural networks in the ATLAS experiment, Report No. ATL-PHYS-PUB-2019-033, 2019, https://cds.cern.ch/record/2688062.
[120] ATLAS Collaboration, Electron and photon energy calibration with the ATLAS detector using 2015–2016 LHC proton–proton collision data, J. Instrum. **14**, P03017 (2019).
[121] ATLAS Collaboration, Studies of the muon momentum calibration and performance of the ATLAS detector with

pp collisions at $\sqrt{s} = 13$ TeV, Eur. Phys. J. C **83**, 686 (2023).
[122] ATLAS Collaboration, ATLAS b-jet identification performance and efficiency measurement with $t\bar{t}$ events in pp collisions at $\sqrt{s} = 13$ TeV, Eur. Phys. J. C **79**, 970 (2019).
[123] ATLAS Collaboration, Measurement of the c-jet mistagging efficiency in $t\bar{t}$ events using pp collision data at $\sqrt{s} = 13$ TeV collected with the ATLAS detector, Eur. Phys. J. C **82**, 95 (2022).
[124] ATLAS Collaboration, Calibration of the light-flavour jet mistagging efficiency of the b-tagging algorithms with $Z +$ jets events using 139 fb^{-1} of ATLAS proton-proton collision data at $\sqrt{s} = 13$ TeV, Eur. Phys. J. C **83**, 728 (2023).
[125] N. Kidonakis, Two-loop soft anomalous dimensions for single top quark associated production with a W^- or H^-, Phys. Rev. D **82**, 054018 (2010).
[126] N. Kidonakis, Top quark production, in *Proceedings of the Helmholtz International Summer School on Physics of Heavy Quarks and Hadrons (HQ 2013), JINR, Dubna, Russia, 2013*, p. 139, arXiv:1311.0283, 10.3204/DESY-PROC-2013-03/Kidonakis.
[127] ATLAS Collaboration, Observation of four-top-quark production in the multilepton final state with the ATLAS detector, Eur. Phys. J. C **83**, 496 (2023).
[128] CMS Collaboration, Measurement of the cross section of top quark-antiquark pair production in association with a W boson in proton-proton collisions at $\sqrt{s} = 13$ TeV, J. High Energy Phys. 07 (2023) 219.
[129] ATLAS Collaboration, Measurement of the total and differential cross-sections of $t\bar{t}W$ production in pp collisions at $\sqrt{s} = 13$ TeV with the ATLAS detector, J. High Energy Phys. 05 (2024) 131.
[130] ATLAS Collaboration, Search for flavor-changing neutral-current couplings between the top quark and the Z boson with proton-proton collisions at $\sqrt{s} = 13$ TeV with the ATLAS detector, Phys. Rev. D **108**, 032019 (2023).
[131] ATLAS Collaboration, Measurement of $W^{\pm}Z$ production cross sections and gauge boson polarisation in pp collisions at $\sqrt{s} = 13$ TeV with the ATLAS detector, Eur. Phys. J. C **79**, 535 (2019).
[132] ATLAS Collaboration, Evidence for the $H \to b\bar{b}$ decay with the ATLAS detector, J. High Energy Phys. 12 (2017) 024.
[133] ATLAS Collaboration, Measurement of the $t\bar{t}Z$ and $t\bar{t}W$ cross sections in proton-proton collisions at $\sqrt{s} = 13$ TeV with the ATLAS detector, Phys. Rev. D **99**, 072009 (2019).
[134] J. Butterworth *et al.*, PDF4LHC recommendations for LHC Run II, J. Phys. G **43**, 023001 (2016).
[135] J. Bellm *et al.*, HERWIG7.1 release note, arXiv:1705.06919.
[136] L. A. Harland-Lang, A. D. Martin, P. Motylinski, and R. S. Thorne, Parton distributions in the LHC era: MMHT 2014 PDFs, Eur. Phys. J. C **75**, 204 (2015).
[137] R. Frederix and S. Frixione, Merging meets matching in MC@NLO, J. High Energy Phys. 12 (2012) 061.
[138] K. Hamilton, P. Nason, and G. Zanderighi, MINLO: Multi-scale improved NLO, J. High Energy Phys. 10 (2012) 155.
[139] ATLAS Collaboration, A search for high-mass resonances decaying to $\tau^+\tau^-$ in pp collisions at $\sqrt{s} = 8$ TeV with the ATLAS detector, J. High Energy Phys. 07 (2015) 157.
[140] R. Barlow and C. Beeston, Fitting using finite Monte Carlo samples, Comput. Phys. Commun. **77**, 219 (1993).
[141] W. Verkerke and D. Kirkby, The RooFit toolkit for data modeling, arXiv:physics/0306116.
[142] W. Verkerke and D. Kirkby, RooFit users manual, http://roofit.sourceforge.net.
[143] A. L. Read, Presentation of search results: The CL_S technique, J. Phys. G **28**, 2693 (2002).
[144] G. Cowan, K. Cranmer, E. Gross, and O. Vitells, Asymptotic formulae for likelihood-based tests of new physics, Eur. Phys. J. C **71**, 1554 (2011).
[145] ATLAS Collaboration, ATLAS computing acknowledgements, Report No. ATL-SOFT-PUB-2023-001, 2023, https://cds.cern.ch/record/2869272.

G. Aad,[103] E. Aakvaag,[16] B. Abbott,[121] K. Abeling,[55] N. J. Abicht,[49] S. H. Abidi,[29] M. Aboelela,[44] A. Aboulhorma,[35e] H. Abramowicz,[152] H. Abreu,[151] Y. Abulaiti,[118] B. S. Acharya,[69a,69b,b] A. Ackermann,[63a] C. Adam Bourdarios,[4] L. Adamczyk,[86a] S. V. Addepalli,[26] M. J. Addison,[102] J. Adelman,[116] A. Adiguzel,[21c] T. Adye,[135] A. A. Affolder,[137] Y. Afik,[39] M. N. Agaras,[13] J. Agarwala,[73a,73b] A. Aggarwal,[101] C. Agheorghiesei,[27c] A. Ahmad,[36] F. Ahmadov,[38,c] W. S. Ahmed,[105] S. Ahuja,[96] X. Ai,[62e] G. Aielli,[76a,76b] A. Aikot,[164] M. Ait Tamlihat,[35e] B. Aitbenchikh,[35a] I. Aizenberg,[170] M. Akbiyik,[101] T. P. A. Åkesson,[99] A. V. Akimov,[37] D. Akiyama,[169] N. N. Akolkar,[24] S. Aktas,[21a] K. Al Khoury,[41] G. L. Alberghi,[23b] J. Albert,[166] P. Albicocco,[53] G. L. Albouy,[60] S. Alderweireldt,[52] Z. L. Alegria,[122] M. Aleksa,[36] I. N. Aleksandrov,[38] C. Alexa,[27b] T. Alexopoulos,[10] F. Alfonsi,[23b] M. Algren,[56] M. Alhroob,[142] B. Ali,[133] H. M. J. Ali,[92] S. Ali,[149] S. W. Alibocus,[93] M. Aliev,[33c] G. Alimonti,[71a] W. Alkakhi,[55] C. Allaire,[66] B. M. M. Allbrooke,[147] J. F. Allen,[52] C. A. Allendes Flores,[138f] P. P. Allport,[20] A. Aloisio,[72a,72b] F. Alonso,[91] C. Alpigiani,[139] M. Alvarez Estevez,[100] A. Alvarez Fernandez,[101] M. Alves Cardoso,[56] M. G. Alviggi,[72a,72b] M. Aly,[102] Y. Amaral Coutinho,[83b] A. Ambler,[105] C. Amelung,[36] M. Amerl,[102] C. G. Ames,[110] D. Amidei,[107] K. J. Amirie,[156] S. P. Amor Dos Santos,[131a] K. R. Amos,[164] S. An,[84] V. Ananiev,[126] C. Anastopoulos,[140] T. Andeen,[11]

J. K. Anders,[36] S. Y. Andrean,[47a,47b] A. Andreazza,[71a,71b] S. Angelidakis,[9] A. Angerami,[41,d] A. V. Anisenkov,[37] A. Annovi,[74a] C. Antel,[56] M. T. Anthony,[140] E. Antipov,[146] M. Antonelli,[53] F. Anulli,[75a] M. Aoki,[84] T. Aoki,[154] J. A. Aparisi Pozo,[164] M. A. Aparo,[147] L. Aperio Bella,[48] C. Appelt,[18] A. Apyan,[26] S. J. Arbiol Val,[87] C. Arcangeletti,[53] A. T. H. Arce,[51] E. Arena,[93] J-F. Arguin,[109] S. Argyropoulos,[54] J.-H. Arling,[48] O. Arnaez,[4] H. Arnold,[115] G. Artoni,[75a,75b] H. Asada,[112] K. Asai,[119] S. Asai,[154] N. A. Asbah,[36] K. Assamagan,[29] R. Astalos,[28a] K. S. V. Astrand,[99] S. Atashi,[160] R. J. Atkin,[33a] M. Atkinson,[163] H. Atmani,[35f] P. A. Atmasiddha,[129] K. Augsten,[133] S. Auricchio,[72a,72b] A. D. Auriol,[20] V. A. Austrup,[102] G. Avolio,[36] K. Axiotis,[56] G. Azuelos,[109,e] D. Babal,[28b] H. Bachacou,[136] K. Bachas,[153,f] A. Bachiu,[34] F. Backman,[47a,47b] A. Badea,[39] T. M. Baer,[107] P. Bagnaia,[75a,75b] M. Bahmani,[18] D. Bahner,[54] K. Bai,[124] J. T. Baines,[135] L. Baines,[95] O. K. Baker,[173] E. Bakos,[15] D. Bakshi Gupta,[8] V. Balakrishnan,[121] R. Balasubramanian,[115] E. M. Baldin,[37] P. Balek,[86a] E. Ballabene,[23b,23a] F. Balli,[136] L. M. Baltes,[63a] W. K. Balunas,[32] J. Balz,[101] E. Banas,[87] M. Bandieramonte,[130] A. Bandyopadhyay,[24] S. Bansal,[24] L. Barak,[152] M. Barakat,[48] E. L. Barberio,[106] D. Barberis,[57b,57a] M. Barbero,[103] M. Z. Barel,[115] K. N. Barends,[33a] T. Barillari,[111] M-S. Barisits,[36] T. Barklow,[144] P. Baron,[123] D. A. Baron Moreno,[102] A. Baroncelli,[62a] G. Barone,[29] A. J. Barr,[127] J. D. Barr,[97] F. Barreiro,[100] J. Barreiro Guimarães da Costa,[14a] U. Barron,[152] M. G. Barros Teixeira,[131a] S. Barsov,[37] F. Bartels,[63a] R. Bartoldus,[144] A. E. Barton,[92] P. Bartos,[28a] A. Basan,[101] M. Baselga,[49] A. Bassalat,[66,g] M. J. Basso,[157a] R. Bate,[165] R. L. Bates,[59] S. Batlamous,[100] B. Batool,[142] M. Battaglia,[137] D. Battulga,[18] M. Bauce,[75a,75b] M. Bauer,[36] P. Bauer,[24] L. T. Bazzano Hurrell,[30] J. B. Beacham,[51] T. Beau,[128] J. Y. Beaucamp,[91] P. H. Beauchemin,[159] P. Bechtle,[24] H. P. Beck,[19,h] K. Becker,[168] A. J. Beddall,[82] V. A. Bednyakov,[38] C. P. Bee,[146] L. J. Beemster,[15] T. A. Beermann,[36] M. Begalli,[83d] M. Begel,[29] A. Behera,[146] J. K. Behr,[48] J. F. Beirer,[36] F. Beisiegel,[24] M. Belfkir,[117b] G. Bella,[152] L. Bellagamba,[23b] A. Bellerive,[34] P. Bellos,[20] K. Beloborodov,[37] D. Benchekroun,[35a] F. Bendebba,[35a] Y. Benhammou,[152] K. C. Benkendorfer,[61] L. Beresford,[48] M. Beretta,[53] E. Bergeaas Kuutmann,[162] N. Berger,[4] B. Bergmann,[133] J. Beringer,[17a] G. Bernardi,[5] C. Bernius,[144] F. U. Bernlochner,[24] F. Bernon,[36,103] A. Berrocal Guardia,[13] T. Berry,[96] P. Berta,[134] A. Berthold,[50] S. Bethke,[111] A. Betti,[75a,75b] A. J. Bevan,[95] N. K. Bhalla,[54] M. Bhamjee,[33c] S. Bhatta,[146] D. S. Bhattacharya,[167] P. Bhattarai,[144] K. D. Bhide,[54] V. S. Bhopatkar,[122] R. M. Bianchi,[130] G. Bianco,[23b,23a] O. Biebel,[110] R. Bielski,[124] M. Biglietti,[77a] C. S. Billingsley,[44] M. Bindi,[55] A. Bingul,[21b] C. Bini,[75a,75b] A. Biondini,[93] C. J. Birch-sykes,[102] G. A. Bird,[32] M. Birman,[170] M. Biros,[134] S. Biryukov,[147] T. Bisanz,[49] E. Bisceglie,[43b,43a] J. P. Biswal,[135] D. Biswas,[142] I. Bloch,[48] A. Blue,[59] U. Blumenschein,[95] J. Blumenthal,[101] V. S. Bobrovnikov,[37] M. Boehler,[54] B. Boehm,[167] D. Bogavac,[36] A. G. Bogdanchikov,[37] C. Bohm,[47a] V. Boisvert,[96] P. Bokan,[36] T. Bold,[86a] M. Bomben,[5] M. Bona,[95] M. Boonekamp,[136] C. D. Booth,[96] A. G. Borbély,[59] I. S. Bordulev,[37] H. M. Borecka-Bielska,[109] G. Borissov,[92] D. Bortoletto,[127] D. Boscherini,[23b] M. Bosman,[13] J. D. Bossio Sola,[36] K. Bouaouda,[35a] N. Bouchhar,[164] J. Boudreau,[130] E. V. Bouhova-Thacker,[92] D. Boumediene,[40] R. Bouquet,[57b,57a] A. Boveia,[120] J. Boyd,[36] D. Boye,[29] I. R. Boyko,[38] J. Bracinik,[20] N. Brahimi,[4] G. Brandt,[172] O. Brandt,[32] F. Braren,[48] B. Brau,[104] J. E. Brau,[124] R. Brener,[170] L. Brenner,[115] R. Brenner,[162] S. Bressler,[170] D. Britton,[59] D. Britzger,[111] I. Brock,[24] G. Brooijmans,[41] E. Brost,[29] L. M. Brown,[166] L. E. Bruce,[61] T. L. Bruckler,[127] P. A. Bruckman de Renstrom,[87] B. Brüers,[48] A. Bruni,[23b] G. Bruni,[23b] M. Bruschi,[23b] N. Bruscino,[75a,75b] T. Buanes,[16] Q. Buat,[139] D. Buchin,[111] A. G. Buckley,[59] O. Bulekov,[37] B. A. Bullard,[144] S. Burdin,[93] C. D. Burgard,[49] A. M. Burger,[36] B. Burghgrave,[8] O. Burlayenko,[54] J. T. P. Burr,[32] C. D. Burton,[11] J. C. Burzynski,[143] E. L. Busch,[41] V. Büscher,[101] P. J. Bussey,[59] J. M. Butler,[25] C. M. Buttar,[59] J. M. Butterworth,[97] W. Buttinger,[135] C. J. Buxo Vazquez,[108] A. R. Buzykaev,[37] S. Cabrera Urbán,[164] L. Cadamuro,[66] D. Caforio,[58] H. Cai,[130] Y. Cai,[14a,14e] Y. Cai,[14c] V. M. M. Cairo,[36] O. Cakir,[3a] N. Calace,[36] P. Calafiura,[17a] G. Calderini,[128] P. Calfayan,[68] G. Callea,[59] L. P. Caloba,[83b] D. Calvet,[40] S. Calvet,[40] M. Calvetti,[74a,74b] R. Camacho Toro,[128] S. Camarda,[36] D. Camarero Munoz,[26] P. Camarri,[76a,76b] M. T. Camerlingo,[72a,72b] D. Cameron,[36] C. Camincher,[166] M. Campanelli,[97] A. Camplani,[42] V. Canale,[72a,72b] A. C. Canbay,[3a] E. Canonero,[96] J. Cantero,[164] Y. Cao,[163] F. Capocasa,[26] M. Capua,[43b,43a] A. Carbone,[71a,71b] R. Cardarelli,[76a] J. C. J. Cardenas,[8] F. Cardillo,[164] G. Carducci,[43b,43a] T. Carli,[36] G. Carlino,[72a] J. I. Carlotto,[13] B. T. Carlson,[130,i] E. M. Carlson,[166,157a] L. Carminati,[71a,71b] A. Carnelli,[136] M. Carnesale,[75a,75b] S. Caron,[114] E. Carquin,[138f] S. Carrá,[71a] G. Carratta,[23b,23a] A. M. Carroll,[124] T. M. Carter,[52] M. P. Casado,[13,j] M. Caspar,[48]

F. L. Castillo,[4] L. Castillo Garcia,[13] V. Castillo Gimenez,[164] N. F. Castro,[131a,131e] A. Catinaccio,[36] J. R. Catmore,[126] T. Cavaliere,[4] V. Cavaliere,[29] N. Cavalli,[23b,23a] Y. C. Cekmecelioglu,[48] E. Celebi,[21a] S. Cella,[36] F. Celli,[127] M. S. Centonze,[70a,70b] V. Cepaitis,[56] K. Cerny,[123] A. S. Cerqueira,[83a] A. Cerri,[147] L. Cerrito,[76a,76b] F. Cerutti,[17a] B. Cervato,[142] A. Cervelli,[23b] G. Cesarini,[53] S. A. Cetin,[82] D. Chakraborty,[116] J. Chan,[171] W. Y. Chan,[154] J. D. Chapman,[32] E. Chapon,[136] B. Chargeishvili,[150b] D. G. Charlton,[20] M. Chatterjee,[19] C. Chauhan,[134] Y. Che,[14c] S. Chekanov,[6] S. V. Chekulaev,[157a] G. A. Chelkov,[38,k] A. Chen,[107] B. Chen,[152] B. Chen,[166] H. Chen,[14c] H. Chen,[29] J. Chen,[62c] J. Chen,[143] M. Chen,[127] S. Chen,[154] S. J. Chen,[14c] X. Chen,[62c,136] X. Chen,[14b,l] Y. Chen,[62a] C. L. Cheng,[171] H. C. Cheng,[64a] S. Cheong,[144] A. Cheplakov,[38] E. Cheremushkina,[48] E. Cherepanova,[115] R. Cherkaoui El Moursli,[35e] E. Cheu,[7] K. Cheung,[65] L. Chevalier,[136] V. Chiarella,[53] G. Chiarelli,[74a] N. Chiedde,[103] G. Chiodini,[70a] A. S. Chisholm,[20] A. Chitan,[27b] M. Chitishvili,[164] M. V. Chizhov,[38] K. Choi,[11] Y. Chou,[139] E. Y. S. Chow,[114] K. L. Chu,[170] M. C. Chu,[64a] X. Chu,[14a,14e] J. Chudoba,[132] J. J. Chwastowski,[87] D. Cieri,[111] K. M. Ciesla,[86a] V. Cindro,[94] A. Ciocio,[17a] F. Cirotto,[72a,72b] Z. H. Citron,[170] M. Citterio,[71a] D. A. Ciubotaru,[27b] A. Clark,[56] P. J. Clark,[52] C. Clarry,[156] J. M. Clavijo Columbie,[48] S. E. Clawson,[48] C. Clement,[47a,47b] J. Clercx,[48] Y. Coadou,[103] M. Cobal,[69a,69c] A. Coccaro,[57b] R. F. Coelho Barrue,[131a] R. Coelho Lopes De Sa,[104] S. Coelli,[71a] B. Cole,[41] J. Collot,[60] P. Conde Muiño,[131a,131g] M. P. Connell,[33c] S. H. Connell,[33c] E. I. Conroy,[127] F. Conventi,[72a,m] H. G. Cooke,[20] A. M. Cooper-Sarkar,[127] F. A. Corchia,[23b,23a] A. Cordeiro Oudot Choi,[128] L. D. Corpe,[40] M. Corradi,[75a,75b] F. Corriveau,[105,n] A. Cortes-Gonzalez,[18] M. J. Costa,[164] F. Costanza,[4] D. Costanzo,[140] B. M. Cote,[120] G. Cowan,[96] K. Cranmer,[171] D. Cremonini,[23b,23a] S. Crépé-Renaudin,[60] F. Crescioli,[128] M. Cristinziani,[142] M. Cristoforetti,[78a,78b] V. Croft,[115] J. E. Crosby,[122] G. Crosetti,[43b,43a] A. Cueto,[100] H. Cui,[14a,14e] Z. Cui,[7] W. R. Cunningham,[59] F. Curcio,[164] J. R. Curran,[52] P. Czodrowski,[36] M. M. Czurylo,[36] M. J. Da Cunha Sargedas De Sousa,[57b,57a] J. V. Da Fonseca Pinto,[83b] C. Da Via,[102] W. Dabrowski,[86a] T. Dado,[49] S. Dahbi,[149] T. Dai,[107] D. Dal Santo,[19] C. Dallapiccola,[104] M. Dam,[42] G. D'amen,[29] V. D'Amico,[110] J. Damp,[101] J. R. Dandoy,[34] M. Danninger,[143] V. Dao,[36] G. Darbo,[57b] S. J. Das,[29,o] F. Dattola,[48] S. D'Auria,[71a,71b] A. D'avanzo,[72a,72b] C. David,[33a] T. Davidek,[134] B. Davis-Purcell,[34] I. Dawson,[95] H. A. Day-hall,[133] K. De,[8] R. De Asmundis,[72a] N. De Biase,[48] S. De Castro,[23b,23a] N. De Groot,[114] P. de Jong,[115] H. De la Torre,[116] A. De Maria,[14c] A. De Salvo,[75a] U. De Sanctis,[76a,76b] F. De Santis,[70a,70b] A. De Santo,[147] J. B. De Vivie De Regie,[60] D. V. Dedovich,[38] J. Degens,[93] A. M. Deiana,[44] F. Del Corso,[23b,23a] J. Del Peso,[100] F. Del Rio,[63a] L. Delagrange,[128] F. Deliot,[136] C. M. Delitzsch,[49] M. Della Pietra,[72a,72b] D. Della Volpe,[56] A. Dell'Acqua,[36] L. Dell'Asta,[71a,71b] M. Delmastro,[4] P. A. Delsart,[60] S. Demers,[173] M. Demichev,[38] S. P. Denisov,[37] L. D'Eramo,[40] D. Derendarz,[87] F. Derue,[128] P. Dervan,[93] K. Desch,[24] C. Deutsch,[24] F. A. Di Bello,[57b,57a] A. Di Ciaccio,[76a,76b] L. Di Ciaccio,[4] A. Di Domenico,[75a,75b] C. Di Donato,[72a,72b] A. Di Girolamo,[36] G. Di Gregorio,[36] A. Di Luca,[78a,78b] B. Di Micco,[77a,77b] R. Di Nardo,[77a,77b] M. Diamantopoulou,[34] F. A. Dias,[115] T. Dias Do Vale,[143] M. A. Diaz,[138a,138b] F. G. Diaz Capriles,[24] M. Didenko,[164] E. B. Diehl,[107] S. Díez Cornell,[48] C. Diez Pardos,[142] C. Dimitriadi,[162,24] A. Dimitrievska,[20] J. Dingfelder,[24] I-M. Dinu,[27b] S. J. Dittmeier,[63b] F. Dittus,[36] M. Divisek,[134] F. Djama,[103] T. Djobava,[150b] C. Doglioni,[102,99] A. Dohnalova,[28a] J. Dolejsi,[134] Z. Dolezal,[134] K. M. Dona,[39] M. Donadelli,[83c] B. Dong,[108] J. Donini,[40] A. D'Onofrio,[72a,72b] M. D'Onofrio,[93] J. Dopke,[135] A. Doria,[72a] N. Dos Santos Fernandes,[131a] P. Dougan,[102] M. T. Dova,[91] A. T. Doyle,[59] M. A. Draguet,[127] E. Dreyer,[170] I. Drivas-koulouris,[10] M. Drnevich,[118] M. Drozdova,[56] D. Du,[62a] T. A. du Pree,[115] F. Dubinin,[37] M. Dubovsky,[28a] E. Duchovni,[170] G. Duckeck,[110] O. A. Ducu,[27b] D. Duda,[52] A. Dudarev,[36] E. R. Duden,[26] M. D'uffizi,[102] L. Duflot,[66] M. Dührssen,[36] I. Duminica,[27g] A. E. Dumitriu,[27b] M. Dunford,[63a] S. Dungs,[49] K. Dunne,[47a,47b] A. Duperrin,[103] H. Duran Yildiz,[3a] M. Düren,[58] A. Durglishvili,[150b] B. L. Dwyer,[116] G. I. Dyckes,[17a] M. Dyndal,[86a] B. S. Dziedzic,[87] Z. O. Earnshaw,[147] G. H. Eberwein,[127] B. Eckerova,[28a] S. Eggebrecht,[55] E. Egidio Purcino De Souza,[128] L. F. Ehrke,[56] G. Eigen,[16] K. Einsweiler,[17a] T. Ekelof,[162] P. A. Ekman,[99] S. El Farkh,[35b] Y. El Ghazali,[35b] H. El Jarrari,[36] A. El Moussaouy,[109] V. Ellajosyula,[162] M. Ellert,[162] F. Ellinghaus,[172] N. Ellis,[36] J. Elmsheuser,[29] M. Elsawy,[117a] M. Elsing,[36] D. Emeliyanov,[135] Y. Enari,[154] I. Ene,[17a] S. Epari,[13] P. A. Erland,[87] M. Errenst,[172] M. Escalier,[66] C. Escobar,[164] E. Etzion,[152] G. Evans,[131a] H. Evans,[68] L. S. Evans,[96] A. Ezhilov,[37] S. Ezzarqtouni,[35a] F. Fabbri,[23b,23a] L. Fabbri,[23b,23a] G. Facini,[97]

V. Fadeyev,[137] R. M. Fakhrutdinov,[37] D. Fakoudis,[101] S. Falciano,[75a] L. F. Falda Ulhoa Coelho,[36] P. J. Falke,[24] F. Fallavollita,[111] J. Faltova,[134] C. Fan,[163] Y. Fan,[14a] Y. Fang,[14a,14e] M. Fanti,[71a,71b] M. Faraj,[69a,69b] Z. Farazpay,[98] A. Farbin,[8] A. Farilla,[77a] T. Farooque,[108] S. M. Farrington,[52] F. Fassi,[35e] D. Fassouliotis,[9] M. Faucci Giannelli,[76a,76b] W. J. Fawcett,[32] L. Fayard,[66] P. Federic,[134] P. Federicova,[132] O. L. Fedin,[37,k] M. Feickert,[171] L. Feligioni,[103] D. E. Fellers,[124] C. Feng,[62b] M. Feng,[14b] Z. Feng,[115] M. J. Fenton,[160] L. Ferencz,[48] R. A. M. Ferguson,[92] S. I. Fernandez Luengo,[138f] P. Fernandez Martinez,[13] M. J. V. Fernoux,[103] J. Ferrando,[92] A. Ferrari,[162] P. Ferrari,[115,114] R. Ferrari,[73a] D. Ferrere,[56] C. Ferretti,[107] F. Fiedler,[101] P. Fiedler,[133] A. Filipčič,[94] E. K. Filmer,[1] F. Filthaut,[114] M. C. N. Fiolhais,[131a,131c,p] L. Fiorini,[164] W. C. Fisher,[108] T. Fitschen,[102] P. M. Fitzhugh,[136] I. Fleck,[142] P. Fleischmann,[107] T. Flick,[172] M. Flores,[33d,q] L. R. Flores Castillo,[64a] L. Flores Sanz De Acedo,[36] F. M. Follega,[78a,78b] N. Fomin,[16] J. H. Foo,[156] A. Formica,[136] A. C. Forti,[102] E. Fortin,[36] A. W. Fortman,[17a] M. G. Foti,[17a] L. Fountas,[9,r] D. Fournier,[66] H. Fox,[92] P. Francavilla,[74a,74b] S. Francescato,[61] S. Franchellucci,[56] M. Franchini,[23b,23a] S. Franchino,[63a] D. Francis,[36] L. Franco,[114] V. Franco Lima,[36] L. Franconi,[48] M. Franklin,[61] G. Frattari,[26] W. S. Freund,[83b] Y. Y. Frid,[152] J. Friend,[59] N. Fritzsche,[50] A. Froch,[54] D. Froidevaux,[36] J. A. Frost,[127] Y. Fu,[62a] S. Fuenzalida Garrido,[138f] M. Fujimoto,[103] K. Y. Fung,[64a] E. Furtado De Simas Filho,[83e] M. Furukawa,[154] J. Fuster,[164] A. Gabrielli,[23b,23a] A. Gabrielli,[156] P. Gadow,[36] G. Gagliardi,[57b,57a] L. G. Gagnon,[17a] S. Gaid,[161] S. Galantzan,[152] E. J. Gallas,[127] B. J. Gallop,[135] K. K. Gan,[120] S. Ganguly,[154] Y. Gao,[52] F. M. Garay Walls,[138a,138b] B. Garcia,[29] C. García,[164] A. Garcia Alonso,[115] A. G. Garcia Caffaro,[173] J. E. García Navarro,[164] M. Garcia-Sciveres,[17a] G. L. Gardner,[129] R. W. Gardner,[39] N. Garelli,[159] D. Garg,[80] R. B. Garg,[144,s] J. M. Gargan,[52] C. A. Garner,[156] C. M. Garvey,[33a] P. Gaspar,[83b] V. K. Gassmann,[159] G. Gaudio,[73a] V. Gautam,[13] P. Gauzzi,[75a,75b] I. L. Gavrilenko,[37] A. Gavrilyuk,[37] C. Gay,[165] G. Gaycken,[48] E. N. Gazis,[10] A. A. Geanta,[27b] C. M. Gee,[137] A. Gekow,[120] C. Gemme,[57b] M. H. Genest,[60] A. D. Gentry,[113] S. George,[96] W. F. George,[20] T. Geralis,[46] P. Gessinger-Befurt,[36] M. E. Geyik,[172] M. Ghani,[168] K. Ghorbanian,[95] A. Ghosal,[142] A. Ghosh,[160] A. Ghosh,[7] B. Giacobbe,[23b] S. Giagu,[75a,75b] T. Giani,[115] P. Giannetti,[74a] A. Giannini,[62a] S. M. Gibson,[96] M. Gignac,[137] D. T. Gil,[86b] A. K. Gilbert,[86a] B. J. Gilbert,[41] D. Gillberg,[34] G. Gilles,[115] L. Ginabat,[128] D. M. Gingrich,[2,e] M. P. Giordani,[69a,69c] P. F. Giraud,[136] G. Giugliarelli,[69a,69c] D. Giugni,[71a] F. Giuli,[36] I. Gkialas,[9,r] L. K. Gladilin,[37] C. Glasman,[100] G. R. Gledhill,[124] G. Glemža,[48] M. Glisic,[124] I. Gnesi,[43b,t] Y. Go,[29] M. Goblirsch-Kolb,[36] B. Gocke,[49] D. Godin,[109] B. Gokturk,[21a] S. Goldfarb,[106] T. Golling,[56] M. G. D. Gololo,[33g] D. Golubkov,[37] J. P. Gombas,[108] A. Gomes,[131a,131b] G. Gomes Da Silva,[142] A. J. Gomez Delegido,[164] R. Gonçalo,[131a,131c] L. Gonella,[20] A. Gongadze,[150c] F. Gonnella,[20] J. L. Gonski,[144] R. Y. González Andana,[52] S. González de la Hoz,[164] R. Gonzalez Lopez,[93] C. Gonzalez Renteria,[17a] M. V. Gonzalez Rodrigues,[48] R. Gonzalez Suarez,[162] S. Gonzalez-Sevilla,[56] L. Goossens,[36] B. Gorini,[36] E. Gorini,[70a,70b] A. Gorišek,[94] T. C. Gosart,[129] A. T. Goshaw,[51] M. I. Gostkin,[38] S. Goswami,[122] C. A. Gottardo,[36] S. A. Gotz,[110] M. Gouighri,[35b] V. Goumarre,[48] A. G. Goussiou,[139] N. Govender,[33c] I. Grabowska-Bold,[86a] K. Graham,[34] E. Gramstad,[126] S. Grancagnolo,[70a,70b] C. M. Grant,[1,136] P. M. Gravila,[27f] F. G. Gravili,[70a,70b] H. M. Gray,[17a] M. Greco,[70a,70b] C. Grefe,[24] I. M. Gregor,[48] K. T. Greif,[160] P. Grenier,[144] S. G. Grewe,[111] A. A. Grillo,[137] K. Grimm,[31] S. Grinstein,[13,u] J.-F. Grivaz,[66] E. Gross,[170] J. Grosse-Knetter,[55] J. C. Grundy,[127] L. Guan,[107] C. Gubbels,[165] J. G. R. Guerrero Rojas,[164] G. Guerrieri,[69a,69c] F. Guescini,[111] R. Gugel,[101] J. A. M. Guhit,[107] A. Guida,[18] E. Guilloton,[168] S. Guindon,[36] F. Guo,[14a,14e] J. Guo,[62c] L. Guo,[48] Y. Guo,[107] R. Gupta,[48] R. Gupta,[130] S. Gurbuz,[24] S. S. Gurdasani,[54] G. Gustavino,[36] M. Guth,[56] P. Gutierrez,[121] L. F. Gutierrez Zagazeta,[129] M. Gutsche,[50] C. Gutschow,[97] C. Gwenlan,[127] C. B. Gwilliam,[93] E. S. Haaland,[126] A. Haas,[118] M. Habedank,[48] C. Haber,[17a] H. K. Hadavand,[8] A. Hadef,[50] S. Hadzic,[111] A. I. Hagan,[92] J. J. Hahn,[142] E. H. Haines,[97] M. Haleem,[167] J. Haley,[122] J. J. Hall,[140] G. D. Hallewell,[103] L. Halser,[19] K. Hamano,[166] M. Hamer,[24] G. N. Hamity,[52] E. J. Hampshire,[96] J. Han,[62b] K. Han,[62a] L. Han,[14c] L. Han,[62a] S. Han,[17a] Y. F. Han,[156] K. Hanagaki,[84] M. Hance,[137] D. A. Hangal,[41] H. Hanif,[143] M. D. Hank,[129] J. B. Hansen,[42] P. H. Hansen,[42] K. Hara,[158] D. Harada,[56] T. Harenberg,[172] S. Harkusha,[37] M. L. Harris,[104] Y. T. Harris,[127] J. Harrison,[13] N. M. Harrison,[120] P. F. Harrison,[168] N. M. Hartman,[111] N. M. Hartmann,[110] Y. Hasegawa,[141] S. Hassan,[16] R. Hauser,[108] C. M. Hawkes,[20] R. J. Hawkings,[36] Y. Hayashi,[154] S. Hayashida,[112] D. Hayden,[108] C. Hayes,[107] R. L. Hayes,[115] C. P. Hays,[127] J. M. Hays,[95] H. S. Hayward,[93] F. He,[62a]

M. He,[14a,14e] Y. He,[155] Y. He,[48] Y. He,[97] N. B. Heatley,[95] V. Hedberg,[99] A. L. Heggelund,[126] N. D. Hehir,[95,a] C. Heidegger,[54] K. K. Heidegger,[54] W. D. Heidorn,[81] J. Heilman,[34] S. Heim,[48] T. Heim,[17a] J. G. Heinlein,[129] J. J. Heinrich,[124] L. Heinrich,[111,v] J. Hejbal,[132] A. Held,[171] S. Hellesund,[16] C. M. Helling,[165] S. Hellman,[47a,47b] R. C. W. Henderson,[92] L. Henkelmann,[32] A. M. Henriques Correia,[36] H. Herde,[99] Y. Hernández Jiménez,[146] L. M. Herrmann,[24] T. Herrmann,[50] G. Herten,[54] R. Hertenberger,[110] L. Hervas,[36] M. E. Hesping,[101] N. P. Hessey,[157a] M. Hidaoui,[35b] E. Hill,[156] S. J. Hillier,[20] J. R. Hinds,[108] F. Hinterkeuser,[24] M. Hirose,[125] S. Hirose,[158] D. Hirschbuehl,[172] T. G. Hitchings,[102] B. Hiti,[94] J. Hobbs,[146] R. Hobincu,[27e] N. Hod,[170] M. C. Hodgkinson,[140] B. H. Hodkinson,[127] A. Hoecker,[36] D. D. Hofer,[107] J. Hofer,[48] T. Holm,[24] M. Holzbock,[111] L. B. A. H. Hommels,[32] B. P. Honan,[102] J. Hong,[62c] T. M. Hong,[130] B. H. Hooberman,[163] W. H. Hopkins,[6] Y. Horii,[112] S. Hou,[149] A. S. Howard,[94] J. Howarth,[59] J. Hoya,[6] M. Hrabovsky,[123] A. Hrynevich,[48] T. Hryn'ova,[4] P. J. Hsu,[65] S.-C. Hsu,[139] T. Hsu,[66] M. Hu,[17a] Q. Hu,[62a] S. Huang,[64b] X. Huang,[14a,14e] Y. Huang,[140] Y. Huang,[101] Y. Huang,[14a] Z. Huang,[102] Z. Hubacek,[133] M. Huebner,[24] F. Huegging,[24] T. B. Huffman,[127] C. A. Hugli,[48] M. Huhtinen,[36] S. K. Huiberts,[16] R. Hulsken,[105] N. Huseynov,[12] J. Huston,[108] J. Huth,[61] R. Hyneman,[144] G. Iacobucci,[56] G. Iakovidis,[29] I. Ibragimov,[142] L. Iconomidou-Fayard,[66] J. P. Iddon,[36] P. Iengo,[72a,72b] R. Iguchi,[154] T. Iizawa,[127] Y. Ikegami,[84] N. Ilic,[156] H. Imam,[35a] M. Ince Lezki,[56] T. Ingebretsen Carlson,[47a,47b] G. Introzzi,[73a,73b] M. Iodice,[77a] V. Ippolito,[75a,75b] R. K. Irwin,[93] M. Ishino,[154] W. Islam,[171] C. Issever,[18,48] S. Istin,[21a,w] H. Ito,[169] R. Iuppa,[78a,78b] A. Ivina,[170] J. M. Izen,[45] V. Izzo,[72a] P. Jacka,[132,133] P. Jackson,[1] B. P. Jaeger,[143] C. S. Jagfeld,[110] G. Jain,[157a] P. Jain,[54] K. Jakobs,[54] T. Jakoubek,[170] J. Jamieson,[59] K. W. Janas,[86a] M. Javurkova,[104] L. Jeanty,[124] J. Jejelava,[150a,x] P. Jenni,[54,y] C. E. Jessiman,[34] C. Jia,[62b] J. Jia,[146] X. Jia,[61] X. Jia,[14a,14e] Z. Jia,[14c] C. Jiang,[52] S. Jiggins,[48] J. Jimenez Pena,[13] S. Jin,[14c] A. Jinaru,[27b] O. Jinnouchi,[155] P. Johansson,[140] K. A. Johns,[7] J. W. Johnson,[137] D. M. Jones,[147] E. Jones,[48] P. Jones,[32] R. W. L. Jones,[92] T. J. Jones,[93] H. L. Joos,[55,36] R. Joshi,[120] J. Jovicevic,[15] X. Ju,[17a] J. J. Junggeburth,[104] T. Junkermann,[63a] A. Juste Rozas,[13,u] M. K. Juzek,[87] S. Kabana,[138e] A. Kaczmarska,[87] M. Kado,[111] H. Kagan,[120] M. Kagan,[144] A. Kahn,[41] A. Kahn,[129] C. Kahra,[101] T. Kaji,[154] E. Kajomovitz,[151] N. Kakati,[170] I. Kalaitzidou,[54] C. W. Kalderon,[29] N. J. Kang,[137] D. Kar,[33g] K. Karava,[127] M. J. Kareem,[157b] E. Karentzos,[54] I. Karkanias,[153] O. Karkout,[115] S. N. Karpov,[38] Z. M. Karpova,[38] V. Kartvelishvili,[92] A. N. Karyukhin,[37] E. Kasimi,[153] J. Katzy,[48] S. Kaur,[34] K. Kawade,[141] M. P. Kawale,[121] C. Kawamoto,[88] T. Kawamoto,[62a] E. F. Kay,[36] F. I. Kaya,[159] S. Kazakos,[108] V. F. Kazanin,[37] Y. Ke,[146] J. M. Keaveney,[33a] R. Keeler,[166] G. V. Kehris,[61] J. S. Keller,[34] A. S. Kelly,[97] J. J. Kempster,[147] P. D. Kennedy,[101] O. Kepka,[132] B. P. Kerridge,[135] S. Kersten,[172] B. P. Kerševan,[94] L. Keszeghova,[28a] S. Ketabchi Haghighat,[156] R. A. Khan,[130] A. Khanov,[122] A. G. Kharlamov,[37] T. Kharlamova,[37] E. E. Khoda,[139] M. Kholodenko,[37] T. J. Khoo,[18] G. Khoriauli,[167] J. Khubua,[150b] Y. A. R. Khwaira,[66] B. Kibirige,[33g] A. Kilgallon,[124] D. W. Kim,[47a,47b] Y. K. Kim,[39] N. Kimura,[97] M. K. Kingston,[55] A. Kirchhoff,[55] C. Kirfel,[24] F. Kirfel,[24] J. Kirk,[135] A. E. Kiryunin,[111] C. Kitsaki,[10] O. Kivernyk,[24] M. Klassen,[159] C. Klein,[34] L. Klein,[167] M. H. Klein,[44] S. B. Klein,[56] U. Klein,[93] P. Klimek,[36] A. Klimentov,[29] T. Klioutchnikova,[36] P. Kluit,[115] S. Kluth,[111] E. Kneringer,[79] T. M. Knight,[156] A. Knue,[49] R. Kobayashi,[88] D. Kobylianskii,[170] S. F. Koch,[127] M. Kocian,[144] P. Kodyš,[134] D. M. Koeck,[124] P. T. Koenig,[24] T. Koffas,[34] O. Kolay,[50] I. Koletsou,[4] T. Komarek,[123] K. Köneke,[54] A. X. Y. Kong,[1] T. Kono,[119] N. Konstantinidis,[97] P. Kontaxakis,[56] B. Konya,[99] R. Kopeliansky,[41] S. Koperny,[86a] K. Korcyl,[87] K. Kordas,[153,z] A. Korn,[97] S. Korn,[55] I. Korolkov,[13] N. Korotkova,[37] B. Kortman,[115] O. Kortner,[111] S. Kortner,[111] W. H. Kostecka,[116] V. V. Kostyukhin,[142] A. Kotsokechagia,[136] A. Kotwal,[51] A. Koulouris,[36] A. Kourkoumeli-Charalampidi,[73a,73b] C. Kourkoumelis,[9] E. Kourlitis,[111,v] O. Kovanda,[124] R. Kowalewski,[166] W. Kozanecki,[136] A. S. Kozhin,[37] V. A. Kramarenko,[37] G. Kramberger,[94] P. Kramer,[101] M. W. Krasny,[128] A. Krasznahorkay,[36] J. W. Kraus,[172] J. A. Kremer,[48] T. Kresse,[50] J. Kretzschmar,[93] K. Kreul,[18] P. Krieger,[156] S. Krishnamurthy,[104] M. Krivos,[134] K. Krizka,[20] K. Kroeninger,[49] H. Kroha,[111] J. Kroll,[132] J. Kroll,[129] K. S. Krowpman,[108] U. Kruchonak,[38] H. Krüger,[24] N. Krumnack,[81] M. C. Kruse,[51] O. Kuchinskaia,[37] S. Kuday,[3a] S. Kuehn,[36] R. Kuesters,[54] T. Kuhl,[48] V. Kukhtin,[38] Y. Kulchitsky,[37,k] S. Kuleshov,[138d,138b] M. Kumar,[33g] N. Kumari,[48] P. Kumari,[157b] A. Kupco,[132] T. Kupfer,[49] A. Kupich,[37] O. Kuprash,[54] H. Kurashige,[85] L. L. Kurchaninov,[157a] O. Kurdysh,[66] Y. A. Kurochkin,[37] A. Kurova,[37] M. Kuze,[155] A. K. Kvam,[104] J. Kvita,[123] T. Kwan,[105] N. G. Kyriacou,[107] L. A. O. Laatu,[103]

C. Lacasta,[164] F. Lacava,[75a,75b] H. Lacker,[18] D. Lacour,[128] N. N. Lad,[97] E. Ladygin,[38] A. Lafarge,[40] B. Laforge,[128] T. Lagouri,[173] F. Z. Lahbabi,[35a] S. Lai,[55] I. K. Lakomiec,[86a] J. E. Lambert,[166] S. Lammers,[68] W. Lampl,[7] C. Lampoudis,[153,z] G. Lamprinoudis,[101] A. N. Lancaster,[116] E. Lançon,[29] U. Landgraf,[54] M. P. J. Landon,[95] V. S. Lang,[54] O. K. B. Langrekken,[126] A. J. Lankford,[160] F. Lanni,[36] K. Lantzsch,[24] A. Lanza,[73a] A. Lapertosa,[57b,57a] J. F. Laporte,[136] T. Lari,[71a] F. Lasagni Manghi,[23b] M. Lassnig,[36] V. Latonova,[132] A. Laudrain,[101] A. Laurier,[151] S. D. Lawlor,[140] Z. Lawrence,[102] R. Lazaridou,[168] M. Lazzaroni,[71a,71b] B. Le,[102] E. M. Le Boulicaut,[51] L. T. Le Pottier,[17a] B. Leban,[23b,23a] A. Lebedev,[81] M. LeBlanc,[102] F. Ledroit-Guillon,[60] A. C. A. Lee,[97] S. C. Lee,[149] S. Lee,[47a,47b] T. F. Lee,[93] L. L. Leeuw,[33c] H. P. Lefebvre,[96] M. Lefebvre,[166] C. Leggett,[17a] G. Lehmann Miotto,[36] M. Leigh,[56] W. A. Leight,[104] W. Leinonen,[114] A. Leisos,[153,aa] M. A. L. Leite,[83c] C. E. Leitgeb,[18] R. Leitner,[134] K. J. C. Leney,[44] T. Lenz,[24] S. Leone,[74a] C. Leonidopoulos,[52] A. Leopold,[145] C. Leroy,[109] R. Les,[108] C. G. Lester,[32] M. Levchenko,[37] J. Levêque,[4] L. J. Levinson,[170] G. Levrini,[23b,23a] M. P. Lewicki,[87] C. Lewis,[139] D. J. Lewis,[4] A. Li,[5] B. Li,[62b] C. Li,[62a] C-Q. Li,[111] H. Li,[62a] H. Li,[62b] H. Li,[14c] H. Li,[14b] H. Li,[62b] J. Li,[62c] K. Li,[139] L. Li,[62c] M. Li,[14a,14e] Q. Y. Li,[62a] S. Li,[14a,14e] S. Li,[62d,62c,bb] T. Li,[5] X. Li,[105] Z. Li,[127] Z. Li,[105] Z. Li,[14a,14e] S. Liang,[14a,14e] Z. Liang,[14a] M. Liberatore,[136] B. Liberti,[76a] K. Lie,[64c] J. Lieber Marin,[83e] H. Lien,[68] K. Lin,[108] R. E. Lindley,[7] J. H. Lindon,[2] E. Lipeles,[129] A. Lipniacka,[16] A. Lister,[165] J. D. Little,[4] B. Liu,[14a] B. X. Liu,[143] D. Liu,[62d,62c] E. H. L. Liu,[20] J. B. Liu,[62a] J. K. K. Liu,[32] K. Liu,[62d] K. Liu,[62d,62c] M. Liu,[62a] M. Y. Liu,[62a] P. Liu,[14a] Q. Liu,[62d,139,62c] X. Liu,[62a] X. Liu,[62b] Y. Liu,[14d,14e] Y. L. Liu,[62b] Y. W. Liu,[62a] J. Llorente Merino,[143] S. L. Lloyd,[95] E. M. Lobodzinska,[48] P. Loch,[7] T. Lohse,[18] K. Lohwasser,[140] E. Loiacono,[48] M. Lokajicek,[132,a] J. D. Lomas,[20] J. D. Long,[163] I. Longarini,[160] L. Longo,[70a,70b] R. Longo,[163] I. Lopez Paz,[67] A. Lopez Solis,[48] N. Lorenzo Martinez,[4] A. M. Lory,[110] G. Löschcke Centeno,[147] O. Loseva,[37] X. Lou,[47a,47b] X. Lou,[14a,14e] A. Lounis,[66] P. A. Love,[92] G. Lu,[14a,14e] M. Lu,[66] S. Lu,[129] Y. J. Lu,[65] H. J. Lubatti,[139] C. Luci,[75a,75b] F. L. Lucio Alves,[14c] F. Luehring,[68] I. Luise,[146] O. Lukianchuk,[66] O. Lundberg,[145] B. Lund-Jensen,[145] N. A. Luongo,[6] M. S. Lutz,[36] A. B. Lux,[25] D. Lynn,[29] R. Lysak,[132] E. Lytken,[99] V. Lyubushkin,[38] T. Lyubushkina,[38] M. M. Lyukova,[146] M. Firdaus M. Soberi,[52] H. Ma,[29] K. Ma,[62a] L. L. Ma,[62b] W. Ma,[62a] Y. Ma,[122] D. M. Mac Donell,[166] G. Maccarrone,[53] J. C. MacDonald,[101] P. C. Machado De Abreu Farias,[83e] R. Madar,[40] T. Madula,[97] J. Maeda,[85] T. Maeno,[29] H. Maguire,[140] V. Maiboroda,[136] A. Maio,[131a,131b,131d] K. Maj,[86a] O. Majersky,[48] S. Majewski,[124] N. Makovec,[66] V. Maksimovic,[15] B. Malaescu,[128] Pa. Malecki,[87] V. P. Maleev,[37] F. Malek,[60,cc] M. Mali,[94] D. Malito,[96] U. Mallik,[80] S. Maltezos,[10] S. Malyukov,[38] J. Mamuzic,[13] G. Mancini,[53] M. N. Mancini,[26] G. Manco,[73a,73b] J. P. Mandalia,[95] I. Mandić,[94] L. Manhaes de Andrade Filho,[83a] I. M. Maniatis,[170] J. Manjarres Ramos,[90] D. C. Mankad,[170] A. Mann,[110] S. Manzoni,[36] L. Mao,[62c] X. Mapekula,[33c] A. Marantis,[153,aa] G. Marchiori,[5] M. Marcisovsky,[132] C. Marcon,[71a] M. Marinescu,[20] S. Marium,[48] M. Marjanovic,[121] A. Markhoos,[54] M. Markovitch,[66] E. J. Marshall,[92] Z. Marshall,[17a] S. Marti-Garcia,[164] T. A. Martin,[168] V. J. Martin,[52] B. Martin dit Latour,[16] L. Martinelli,[75a,75b] M. Martinez,[13,u] P. Martinez Agullo,[164] V. I. Martinez Outschoorn,[104] P. Martinez Suarez,[13] S. Martin-Haugh,[135] G. Martinovicova,[134] V. S. Martoiu,[27b] A. C. Martyniuk,[97] A. Marzin,[36] D. Mascione,[78a,78b] L. Masetti,[101] T. Mashimo,[154] J. Masik,[102] A. L. Maslennikov,[37] P. Massarotti,[72a,72b] P. Mastrandrea,[74a,74b] A. Mastroberardino,[43b,43a] T. Masubuchi,[154] T. Mathisen,[162] J. Matousek,[134] N. Matsuzawa,[154] J. Maurer,[27b] A. J. Maury,[66] B. Maček,[94] D. A. Maximov,[37] A. E. May,[102] R. Mazini,[149] I. Maznas,[116] M. Mazza,[108] S. M. Mazza,[137] E. Mazzeo,[71a,71b] C. Mc Ginn,[29] J. P. Mc Gowan,[166] S. P. Mc Kee,[107] C. C. McCracken,[165] E. F. McDonald,[106] A. E. McDougall,[115] J. A. Mcfayden,[147] R. P. McGovern,[129] G. Mchedlidze,[150b] R. P. Mckenzie,[33g] T. C. Mclachlan,[48] D. J. Mclaughlin,[97] S. J. McMahon,[135] C. M. Mcpartland,[93] R. A. McPherson,[166,n] S. Mehlhase,[110] A. Mehta,[93] D. Melini,[164] B. R. Mellado Garcia,[33g] A. H. Melo,[55] F. Meloni,[48] A. M. Mendes Jacques Da Costa,[102] H. Y. Meng,[156] L. Meng,[92] S. Menke,[111] M. Mentink,[36] E. Meoni,[43b,43a] G. Mercado,[116] C. Merlassino,[69a,69c] L. Merola,[72a,72b] C. Meroni,[71a,71b] J. Metcalfe,[6] A. S. Mete,[6] C. Meyer,[68] J-P. Meyer,[136] R. P. Middleton,[135] L. Mijović,[52] G. Mikenberg,[170] M. Mikestikova,[132] M. Mikuž,[94] H. Mildner,[101] A. Milic,[36] D. W. Miller,[39] E. H. Miller,[144] L. S. Miller,[34] A. Milov,[170] D. A. Milstead,[47a,47b] T. Min,[14c] A. A. Minaenko,[37] I. A. Minashvili,[150b] L. Mince,[59] A. I. Mincer,[118] B. Mindur,[86a] M. Mineev,[38] Y. Mino,[88] L. M. Mir,[13] M. Miralles Lopez,[59] M. Mironova,[17a] A. Mishima,[154] M. C. Missio,[114] A. Mitra,[168] V. A. Mitsou,[164] Y. Mitsumori,[112] O. Miu,[156] P. S. Miyagawa,[95]

T. Mkrtchyan,[63a] M. Mlinarevic,[97] T. Mlinarevic,[97] M. Mlynarikova,[36] S. Mobius,[19] P. Mogg,[110] M. H. Mohamed Farook,[113] A. F. Mohammed,[14a,14e] S. Mohapatra,[41] G. Mokgatitswane,[33g] L. Moleri,[170] B. Mondal,[142] S. Mondal,[133] K. Mönig,[48] E. Monnier,[103] L. Monsonis Romero,[164] J. Montejo Berlingen,[13] M. Montella,[120] F. Montereali,[77a,77b] F. Monticelli,[91] S. Monzani,[69a,69c] N. Morange,[66] A. L. Moreira De Carvalho,[48] M. Moreno Llácer,[164] C. Moreno Martinez,[56] P. Morettini,[57b] S. Morgenstern,[36] M. Morii,[61] M. Morinaga,[154] F. Morodei,[75a,75b] L. Morvaj,[36] P. Moschovakos,[36] B. Moser,[36] M. Mosidze,[150b] T. Moskalets,[54] P. Moskvitina,[114] J. Moss,[31,dd] A. Moussa,[35d] E. J. W. Moyse,[104] O. Mtintsilana,[33g] S. Muanza,[103] J. Mueller,[130] D. Muenstermann,[92] R. Müller,[19] G. A. Mullier,[162] A. J. Mullin,[32] J. J. Mullin,[129] D. P. Mungo,[156] D. Munoz Perez,[164] F. J. Munoz Sanchez,[102] M. Murin,[102] W. J. Murray,[168,135] M. Muškinja,[94] C. Mwewa,[29] A. G. Myagkov,[37,k] A. J. Myers,[8] G. Myers,[107] M. Myska,[133] B. P. Nachman,[17a] O. Nackenhorst,[49] K. Nagai,[127] K. Nagano,[84] J. L. Nagle,[29,o] E. Nagy,[103] A. M. Nairz,[36] Y. Nakahama,[84] K. Nakamura,[84] K. Nakkalil,[5] H. Nanjo,[125] R. Narayan,[44] E. A. Narayanan,[113] I. Naryshkin,[37] M. Naseri,[34] S. Nasri,[117b] C. Nass,[24] G. Navarro,[22a] J. Navarro-Gonzalez,[164] R. Nayak,[152] A. Nayaz,[18] P. Y. Nechaeva,[37] S. Nechaeva,[23b,23a] F. Nechansky,[48] L. Nedic,[127] T. J. Neep,[20] A. Negri,[73a,73b] M. Negrini,[23b] C. Nellist,[115] C. Nelson,[105] K. Nelson,[107] S. Nemecek,[132] M. Nessi,[36,ee] M. S. Neubauer,[163] F. Neuhaus,[101] J. Neundorf,[48] R. Newhouse,[165] P. R. Newman,[20] C. W. Ng,[130] Y. W. Y. Ng,[48] B. Ngair,[117a] H. D. N. Nguyen,[109] R. B. Nickerson,[127] R. Nicolaidou,[136] J. Nielsen,[137] M. Niemeyer,[55] J. Niermann,[55] N. Nikiforou,[36] V. Nikolaenko,[37,k] I. Nikolic-Audit,[128] K. Nikolopoulos,[20] P. Nilsson,[29] I. Ninca,[48] H. R. Nindhito,[56] G. Ninio,[152] A. Nisati,[75a] N. Nishu,[2] R. Nisius,[111] J-E. Nitschke,[50] E. K. Nkadimeng,[33g] T. Nobe,[154] D. L. Noel,[32] T. Nommensen,[148] M. B. Norfolk,[140] R. R. B. Norisam,[97] B. J. Norman,[34] M. Noury,[35a] J. Novak,[94] T. Novak,[48] L. Novotny,[133] R. Novotny,[113] L. Nozka,[123] K. Ntekas,[160] N. M. J. Nunes De Moura Junior,[83b] J. Ocariz,[128] A. Ochi,[85] I. Ochoa,[131a] S. Oerdek,[48,ff] J. T. Offermann,[39] A. Ogrodnik,[134] A. Oh,[102] C. C. Ohm,[145] H. Oide,[84] R. Oishi,[154] M. L. Ojeda,[48] Y. Okumura,[154] L. F. Oleiro Seabra,[131a] S. A. Olivares Pino,[138d] G. Oliveira Correa,[13] D. Oliveira Damazio,[29] D. Oliveira Goncalves,[83a] J. L. Oliver,[160] Ö. O. Öncel,[54] A. P. O'Neill,[19] A. Onofre,[131a,131e] P. U. E. Onyisi,[11] M. J. Oreglia,[39] G. E. Orellana,[91] D. Orestano,[77a,77b] N. Orlando,[13] R. S. Orr,[156] V. O'Shea,[59] L. M. Osojnak,[129] R. Ospanov,[62a] G. Otero y Garzon,[30] H. Otono,[89] P. S. Ott,[63a] G. J. Ottino,[17a] M. Ouchrif,[35d] F. Ould-Saada,[126] T. Ovsiannikova,[139] M. Owen,[59] R. E. Owen,[135] K. Y. Oyulmaz,[21a] V. E. Ozcan,[21a] F. Ozturk,[87] N. Ozturk,[8] S. Ozturk,[82] H. A. Pacey,[127] A. Pacheco Pages,[13] C. Padilla Aranda,[13] G. Padovano,[75a,75b] S. Pagan Griso,[17a] G. Palacino,[68] A. Palazzo,[70a,70b] J. Pampel,[24] J. Pan,[173] T. Pan,[64a] D. K. Panchal,[11] C. E. Pandini,[115] J. G. Panduro Vazquez,[96] H. D. Pandya,[1] H. Pang,[14b] P. Pani,[48] G. Panizzo,[69a,69c] L. Panwar,[128] L. Paolozzi,[56] S. Parajuli,[163] A. Paramonov,[6] C. Paraskevopoulos,[53] D. Paredes Hernandez,[64b] A. Pareti,[73a,73b] K. R. Park,[41] T. H. Park,[156] M. A. Parker,[32] F. Parodi,[57b,57a] E. W. Parrish,[116] V. A. Parrish,[52] J. A. Parsons,[41] U. Parzefall,[54] B. Pascual Dias,[109] L. Pascual Dominguez,[152] E. Pasqualucci,[75a] S. Passaggio,[57b] F. Pastore,[96] P. Patel,[87] U. M. Patel,[51] J. R. Pater,[102] T. Pauly,[36] C. I. Pazos,[159] J. Pearkes,[144] M. Pedersen,[126] R. Pedro,[131a] S. V. Peleganchuk,[37] O. Penc,[36] E. A. Pender,[52] G. D. Penn,[173] K. E. Penski,[110] M. Penzin,[37] B. S. Peralva,[83d] A. P. Pereira Peixoto,[139] L. Pereira Sanchez,[144] D. V. Perepelitsa,[29,o] E. Perez Codina,[157a] M. Perganti,[10] H. Pernegger,[36] O. Perrin,[40] K. Peters,[48] R. F. Y. Peters,[102] B. A. Petersen,[36] T. C. Petersen,[42] E. Petit,[103] V. Petousis,[133] C. Petridou,[153,z] T. Petru,[134] A. Petrukhin,[142] M. Pettee,[17a] N. E. Pettersson,[36] A. Petukhov,[37] K. Petukhova,[134] R. Pezoa,[138f] L. Pezzotti,[36] G. Pezzullo,[173] T. M. Pham,[171] T. Pham,[106] P. W. Phillips,[135] G. Piacquadio,[146] E. Pianori,[17a] F. Piazza,[124] R. Piegaia,[30] D. Pietreanu,[27b] A. D. Pilkington,[102] M. Pinamonti,[69a,69c] J. L. Pinfold,[2] B. C. Pinheiro Pereira,[131a] A. E. Pinto Pinoargote,[101,136] L. Pintucci,[69a,69c] K. M. Piper,[147] A. Pirttikoski,[56] D. A. Pizzi,[34] L. Pizzimento,[64b] A. Pizzini,[115] M.-A. Pleier,[29] V. Plesanovs,[54] V. Pleskot,[134] E. Plotnikova,[38] G. Poddar,[95] R. Poettgen,[99] L. Poggioli,[128] I. Pokharel,[55] S. Polacek,[134] G. Polesello,[73a] A. Poley,[143,157a] A. Polini,[23b] C. S. Pollard,[168] Z. B. Pollock,[120] E. Pompa Pacchi,[75a,75b] D. Ponomarenko,[114] L. Pontecorvo,[36] S. Popa,[27a] G. A. Popeneciu,[27d] A. Poreba,[36] D. M. Portillo Quintero,[157a] S. Pospisil,[133] M. A. Postill,[140] P. Postolache,[27c] K. Potamianos,[168] P. A. Potepa,[86a] I. N. Potrap,[38] C. J. Potter,[32] H. Potti,[1] J. Poveda,[164] M. E. Pozo Astigarraga,[36] A. Prades Ibanez,[164] J. Pretel,[54] D. Price,[102] M. Primavera,[70a] M. A. Principe Martin,[100] R. Privara,[123] T. Procter,[59] M. L. Proffitt,[139] N. Proklova,[129] K. Prokofiev,[64c]

G. Proto,[111] J. Proudfoot,[6] M. Przybycien,[86a] W. W. Przygoda,[86b] A. Psallidas,[46] J. E. Puddefoot,[140] D. Pudzha,[37] D. Pyatiizbyantseva,[37] J. Qian,[107] D. Qichen,[102] Y. Qin,[13] T. Qiu,[52] A. Quadt,[55] M. Queitsch-Maitland,[102] G. Quetant,[56] R. P. Quinn,[165] G. Rabanal Bolanos,[61] D. Rafanoharana,[54] F. Ragusa,[71a,71b] J. L. Rainbolt,[39] J. A. Raine,[56] S. Rajagopalan,[29] E. Ramakoti,[37] I. A. Ramirez-Berend,[34] K. Ran,[48,14e] N. P. Rapheeha,[33g] H. Rasheed,[27b] V. Raskina,[128] D. F. Rassloff,[63a] A. Rastogi,[17a] S. Rave,[101] B. Ravina,[55] I. Ravinovich,[170] M. Raymond,[36] A. L. Read,[126] N. P. Readioff,[140] D. M. Rebuzzi,[73a,73b] G. Redlinger,[29] A. S. Reed,[111] K. Reeves,[26] J. A. Reidelsturz,[172] D. Reikher,[152] A. Rej,[49] C. Rembser,[36] M. Renda,[27b] M. B. Rendel,[111] F. Renner,[48] A. G. Rennie,[160] A. L. Rescia,[48] S. Resconi,[71a] M. Ressegotti,[57b,57a] S. Rettie,[36] J. G. Reyes Rivera,[108] E. Reynolds,[17a] O. L. Rezanova,[37] P. Reznicek,[134] H. Riani,[35d] N. Ribaric,[92] E. Ricci,[78a,78b] R. Richter,[111] S. Richter,[47a,47b] E. Richter-Was,[86b] M. Ridel,[128] S. Ridouani,[35d] P. Rieck,[118] P. Riedler,[36] E. M. Riefel,[47a,47b] J. O. Rieger,[115] M. Rijssenbeek,[146] M. Rimoldi,[36] L. Rinaldi,[23b,23a] T. T. Rinn,[29] M. P. Rinnagel,[110] G. Ripellino,[162] I. Riu,[13] J. C. Rivera Vergara,[166] F. Rizatdinova,[122] E. Rizvi,[95] B. R. Roberts,[17a] S. H. Robertson,[105,n] D. Robinson,[32] C. M. Robles Gajardo,[138f] M. Robles Manzano,[101] A. Robson,[59] A. Rocchi,[76a,76b] C. Roda,[74a,74b] S. Rodriguez Bosca,[36] Y. Rodriguez Garcia,[22a] A. Rodriguez Rodriguez,[54] A. M. Rodríguez Vera,[116] S. Roe,[36] J. T. Roemer,[160] A. R. Roepe-Gier,[137] J. Roggel,[172] O. Røhne,[126] R. A. Rojas,[104] C. P. A. Roland,[128] J. Roloff,[29] A. Romaniouk,[37] E. Romano,[73a,73b] M. Romano,[23b] A. C. Romero Hernandez,[163] N. Rompotis,[93] L. Roos,[128] S. Rosati,[75a] B. J. Rosser,[39] E. Rossi,[127] E. Rossi,[72a,72b] L. P. Rossi,[61] L. Rossini,[54] R. Rosten,[120] M. Rotaru,[27b] B. Rottler,[54] C. Rougier,[90] D. Rousseau,[66] D. Rousso,[48] A. Roy,[163] S. Roy-Garand,[156] A. Rozanov,[103] Z. M. A. Rozario,[59] Y. Rozen,[151] A. Rubio Jimenez,[164] A. J. Ruby,[93] V. H. Ruelas Rivera,[18] T. A. Ruggeri,[1] A. Ruggiero,[127] A. Ruiz-Martinez,[164] A. Rummler,[36] Z. Rurikova,[54] N. A. Rusakovich,[38] H. L. Russell,[166] G. Russo,[75a,75b] J. P. Rutherfoord,[7] S. Rutherford Colmenares,[32] K. Rybacki,[92] M. Rybar,[134] E. B. Rye,[126] A. Ryzhov,[44] J. A. Sabater Iglesias,[56] P. Sabatini,[164] H. F-W. Sadrozinski,[137] F. Safai Tehrani,[75a] B. Safarzadeh Samani,[135] S. Saha,[1] M. Sahinsoy,[111] A. Saibel,[164] M. Saimpert,[136] M. Saito,[154] T. Saito,[154] A. Sala,[71a,71b] D. Salamani,[36] A. Salnikov,[144] J. Salt,[164] A. Salvador Salas,[152] D. Salvatore,[43b,43a] F. Salvatore,[147] A. Salzburger,[36] D. Sammel,[54] E. Sampson,[92] D. Sampsonidis,[153,z] D. Sampsonidou,[124] J. Sánchez,[164] V. Sanchez Sebastian,[164] H. Sandaker,[126] C. O. Sander,[48] J. A. Sandesara,[104] M. Sandhoff,[172] C. Sandoval,[22b] D. P. C. Sankey,[135] T. Sano,[88] A. Sansoni,[53] L. Santi,[75a,75b] C. Santoni,[40] H. Santos,[131a,131b] A. Santra,[170] E. Sanzani,[23b,23a] K. A. Saoucha,[161] J. G. Saraiva,[131a,131d] J. Sardain,[7] O. Sasaki,[84] K. Sato,[158] C. Sauer,[63b] F. Sauerburger,[54] E. Sauvan,[4] P. Savard,[156,e] R. Sawada,[154] C. Sawyer,[135] L. Sawyer,[98] I. Sayago Galvan,[164] C. Sbarra,[23b] A. Sbrizzi,[23b,23a] T. Scanlon,[97] J. Schaarschmidt,[139] U. Schäfer,[101] A. C. Schaffer,[66,44] D. Schaile,[110] R. D. Schamberger,[146] C. Scharf,[18] M. M. Schefer,[19] V. A. Schegelsky,[37] D. Scheirich,[134] F. Schenck,[18] M. Schernau,[160] C. Scheulen,[55] C. Schiavi,[57b,57a] M. Schioppa,[43b,43a] B. Schlag,[144,s] K. E. Schleicher,[54] S. Schlenker,[36] J. Schmeing,[172] M. A. Schmidt,[172] K. Schmieden,[101] C. Schmitt,[101] N. Schmitt,[101] S. Schmitt,[48] L. Schoeffel,[136] A. Schoening,[63b] P. G. Scholer,[34] E. Schopf,[127] M. Schott,[101] J. Schovancova,[36] S. Schramm,[56] T. Schroer,[56] H-C. Schultz-Coulon,[63a] M. Schumacher,[54] B. A. Schumm,[137] Ph. Schune,[136] A. J. Schuy,[139] H. R. Schwartz,[137] A. Schwartzman,[144] T. A. Schwarz,[107] Ph. Schwemling,[136] R. Schwienhorst,[108] A. Sciandra,[29] G. Sciolla,[26] F. Scuri,[74a] C. D. Sebastiani,[93] K. Sedlaczek,[116] P. Seema,[18] S. C. Seidel,[113] A. Seiden,[137] B. D. Seidlitz,[41] C. Seitz,[48] J. M. Seixas,[83b] G. Sekhniaidze,[72a] L. Selem,[60] N. Semprini-Cesari,[23b,23a] D. Sengupta,[56] V. Senthilkumar,[164] L. Serin,[66] L. Serkin,[69a,69b] M. Sessa,[76a,76b] H. Severini,[121] F. Sforza,[57b,57a] A. Sfyrla,[56] Q. Sha,[14a] E. Shabalina,[55] A. H. Shah,[32] R. Shaheen,[145] J. D. Shahinian,[129] D. Shaked Renous,[170] L. Y. Shan,[14a] M. Shapiro,[17a] A. Sharma,[36] A. S. Sharma,[165] P. Sharma,[80] P. B. Shatalov,[37] K. Shaw,[147] S. M. Shaw,[102] A. Shcherbakova,[37] Q. Shen,[62c,5] D. J. Sheppard,[143] P. Sherwood,[97] L. Shi,[97] X. Shi,[14a] C. O. Shimmin,[173] J. D. Shinner,[96] I. P. J. Shipsey,[127] S. Shirabe,[89] M. Shiyakova,[38,gg] J. Shlomi,[170] M. J. Shochet,[39] J. Shojaii,[106] D. R. Shope,[126] B. Shrestha,[121] S. Shrestha,[120,hh] E. M. Shrif,[33g] M. J. Shroff,[166] P. Sicho,[132] A. M. Sickles,[163] E. Sideras Haddad,[33g] A. C. Sidley,[115] A. Sidoti,[23b] F. Siegert,[50] Dj. Sijacki,[15] F. Sili,[91] J. M. Silva,[52] M. V. Silva Oliveira,[29] S. B. Silverstein,[47a] S. Simion,[66] R. Simoniello,[36] E. L. Simpson,[102] H. Simpson,[147] L. R. Simpson,[107] N. D. Simpson,[99] S. Simsek,[82] S. Sindhu,[55] P. Sinervo,[156] S. Singh,[156] S. Sinha,[48] S. Sinha,[102] M. Sioli,[23b,23a] I. Siral,[36] E. Sitnikova,[48] J. Sjölin,[47a,47b] A. Skaf,[55] E. Skorda,[20] P. Skubic,[121] M. Slawinska,[87]

V. Smakhtin,[170] B. H. Smart,[135] S. Yu. Smirnov,[37] Y. Smirnov,[37] L. N. Smirnova,[37,k] O. Smirnova,[99] A. C. Smith,[41] D. R. Smith,[160] E. A. Smith,[39] H. A. Smith,[127] J. L. Smith,[102] R. Smith,[144] M. Smizanska,[92] K. Smolek,[133] A. A. Snesarev,[37] S. R. Snider,[156] H. L. Snoek,[115] S. Snyder,[29] R. Sobie,[166,n] A. Soffer,[152] C. A. Solans Sanchez,[36] E. Yu. Soldatov,[37] U. Soldevila,[164] A. A. Solodkov,[37] S. Solomon,[26] A. Soloshenko,[38] K. Solovieva,[54] O. V. Solovyanov,[40] P. Sommer,[36] A. Sonay,[13] W. Y. Song,[157b] A. Sopczak,[133] A. L. Sopio,[97] F. Sopkova,[28b] J. D. Sorenson,[113] I. R. Sotarriva Alvarez,[155] V. Sothilingam,[63a] O. J. Soto Sandoval,[138c,138b] S. Sottocornola,[68] R. Soualah,[161] Z. Soumaimi,[35e] D. South,[48] N. Soybelman,[170] S. Spagnolo,[70a,70b] M. Spalla,[111] D. Sperlich,[54] G. Spigo,[36] S. Spinali,[92] D. P. Spiteri,[59] M. Spousta,[134] E. J. Staats,[34] R. Stamen,[63a] A. Stampekis,[20] M. Standke,[24] E. Stanecka,[87] W. Stanek-Maslouska,[48] M. V. Stange,[50] B. Stanislaus,[17a] M. M. Stanitzki,[48] B. Stapf,[48] E. A. Starchenko,[37] G. H. Stark,[137] J. Stark,[90] P. Staroba,[132] P. Starovoitov,[63a] S. Stärz,[105] R. Staszewski,[87] G. Stavropoulos,[46] J. Steentoft,[162] P. Steinberg,[29] B. Stelzer,[143,157a] H. J. Stelzer,[130] O. Stelzer-Chilton,[157a] H. Stenzel,[58] T. J. Stevenson,[147] G. A. Stewart,[36] J. R. Stewart,[122] M. C. Stockton,[36] G. Stoicea,[27b] M. Stolarski,[131a] S. Stonjek,[111] A. Straessner,[50] J. Strandberg,[145] S. Strandberg,[47a,47b] M. Stratmann,[172] M. Strauss,[121] T. Strebler,[103] P. Strizenec,[28b] R. Ströhmer,[167] D. M. Strom,[124] R. Stroynowski,[44] A. Strubig,[47a,47b] S. A. Stucci,[29] B. Stugu,[16] J. Stupak,[121] N. A. Styles,[48] D. Su,[144] S. Su,[62a] W. Su,[62d] X. Su,[62a] D. Suchy,[28a] K. Sugizaki,[154] V. V. Sulin,[37] M. J. Sullivan,[93] D. M. S. Sultan,[127] L. Sultanaliyeva,[37] S. Sultansoy,[3b] T. Sumida,[88] S. Sun,[107] S. Sun,[171] O. Sunneborn Gudnadottir,[162] N. Sur,[103] M. R. Sutton,[147] H. Suzuki,[158] M. Svatos,[132] M. Swiatlowski,[157a] T. Swirski,[167] I. Sykora,[28a] M. Sykora,[134] T. Sykora,[134] D. Ta,[101] K. Tackmann,[48,ff] A. Taffard,[160] R. Tafirout,[157a] J. S. Tafoya Vargas,[66] Y. Takubo,[84] M. Talby,[103] A. A. Talyshev,[37] K. C. Tam,[64b] N. M. Tamir,[152] A. Tanaka,[154] J. Tanaka,[154] R. Tanaka,[66] M. Tanasini,[57b,57a] Z. Tao,[165] S. Tapia Araya,[138f] S. Tapprogge,[101] A. Tarek Abouelfadl Mohamed,[108] S. Tarem,[151] K. Tariq,[14a] G. Tarna,[27b] G. F. Tartarelli,[71a] M. J. Tartarin,[90] P. Tas,[134] M. Tasevsky,[132] E. Tassi,[43b,43a] A. C. Tate,[163] G. Tateno,[154] Y. Tayalati,[35e,ii] G. N. Taylor,[106] W. Taylor,[157b] A. S. Tee,[171] R. Teixeira De Lima,[144] P. Teixeira-Dias,[96] J. J. Teoh,[156] K. Terashi,[154] J. Terron,[100] S. Terzo,[13] M. Testa,[53] R. J. Teuscher,[156,n] A. Thaler,[79] O. Theiner,[56] N. Themistokleous,[52] T. Theveneaux-Pelzer,[103] O. Thielmann,[172] D. W. Thomas,[96] J. P. Thomas,[20] E. A. Thompson,[17a] P. D. Thompson,[20] E. Thomson,[129] R. E. Thornberry,[44] Y. Tian,[55] V. Tikhomirov,[37,k] Yu. A. Tikhonov,[37] S. Timoshenko,[37] D. Timoshyn,[134] E. X. L. Ting,[1] P. Tipton,[173] S. H. Tlou,[33g] K. Todome,[155] S. Todorova-Nova,[134] S. Todt,[50] L. Toffolin,[69a,69c] M. Togawa,[84] J. Tojo,[89] S. Tokár,[28a] K. Tokushuku,[84] O. Toldaiev,[68] R. Tombs,[32] M. Tomoto,[84,112] L. Tompkins,[144,s] K. W. Topolnicki,[86b] E. Torrence,[124] H. Torres,[90] E. Torró Pastor,[164] M. Toscani,[30] C. Tosciri,[39] M. Tost,[11] D. R. Tovey,[140] A. Traeet,[16] I. S. Trandafir,[27b] T. Trefzger,[167] A. Tricoli,[29] I. M. Trigger,[157a] S. Trincaz-Duvoid,[128] D. A. Trischuk,[26] B. Trocmé,[60] L. Truong,[33c] M. Trzebinski,[87] A. Trzupek,[87] F. Tsai,[146] M. Tsai,[107] A. Tsiamis,[153,z] P. V. Tsiareshka,[37] S. Tsigaridas,[157a] A. Tsirigotis,[153,aa] V. Tsiskaridze,[156] E. G. Tskhadadze,[150a] M. Tsopoulou,[153] Y. Tsujikawa,[88] I. I. Tsukerman,[37] V. Tsulaia,[17a] S. Tsuno,[84] K. Tsuri,[119] D. Tsybychev,[146] Y. Tu,[64b] A. Tudorache,[27b] V. Tudorache,[27b] A. N. Tuna,[61] S. Turchikhin,[57b,57a] I. Turk Cakir,[3a] R. Turra,[71a] T. Turtuvshin,[38,jj] P. M. Tuts,[41] S. Tzamarias,[153,z] E. Tzovara,[101] F. Ukegawa,[158] P. A. Ulloa Poblete,[138c,138b] E. N. Umaka,[29] G. Unal,[36] A. Undrus,[29] G. Unel,[160] J. Urban,[28b] P. Urquijo,[106] P. Urrejola,[138a] G. Usai,[8] R. Ushioda,[155] M. Usman,[109] Z. Uysal,[82] V. Vacek,[133] B. Vachon,[105] T. Vafeiadis,[36] A. Vaitkus,[97] C. Valderanis,[110] E. Valdes Santurio,[47a,47b] M. Valente,[157a] S. Valentinetti,[23b,23a] A. Valero,[164] E. Valiente Moreno,[164] A. Vallier,[90] J. A. Valls Ferrer,[164] D. R. Van Arneman,[115] T. R. Van Daalen,[139] A. Van Der Graaf,[49] P. Van Gemmeren,[6] M. Van Rijnbach,[126] S. Van Stroud,[97] I. Van Vulpen,[115] P. Vana,[134] M. Vanadia,[76a,76b] W. Vandelli,[36] E. R. Vandewall,[122] D. Vannicola,[152] L. Vannoli,[53] R. Vari,[75a] E. W. Varnes,[7] C. Varni,[17b] T. Varol,[149] D. Varouchas,[66] L. Varriale,[164] K. E. Varvell,[148] M. E. Vasile,[27b] L. Vaslin,[84] G. A. Vasquez,[166] A. Vasyukov,[38] R. Vavricka,[101] F. Vazeille,[40] T. Vazquez Schroeder,[36] J. Veatch,[31] V. Vecchio,[102] M. J. Veen,[104] I. Veliscek,[29] L. M. Veloce,[156] F. Veloso,[131a,131c] S. Veneziano,[75a] A. Ventura,[70a,70b] S. Ventura Gonzalez,[136] A. Verbytskyi,[111] M. Verducci,[74a,74b] C. Vergis,[95] M. Verissimo De Araujo,[83b] W. Verkerke,[115] J. C. Vermeulen,[115] C. Vernieri,[144] M. Vessella,[104] M. C. Vetterli,[143,e] A. Vgenopoulos,[153,z] N. Viaux Maira,[138f] T. Vickey,[140] O. E. Vickey Boeriu,[140] G. H. A. Viehhauser,[127] L. Vigani,[63b] M. Villa,[23b,23a] M. Villaplana Perez,[164] E. M. Villhauer,[52] E. Vilucchi,[53]

M. G. Vincter,[34] G. S. Virdee,[20] A. Visibile,[115] C. Vittori,[36] I. Vivarelli,[23b,23a] E. Voevodina,[111] F. Vogel,[110] J. C. Voigt,[50] P. Vokac,[133] Yu. Volkotrub,[86b] J. Von Ahnen,[48] E. Von Toerne,[24] B. Vormwald,[36] V. Vorobel,[134] K. Vorobev,[37] M. Vos,[164] K. Voss,[142] M. Vozak,[115] L. Vozdecky,[121] N. Vranjes,[15] M. Vranjes Milosavljevic,[15] M. Vreeswijk,[115] N. K. Vu,[62d,62c] R. Vuillermet,[36] O. Vujinovic,[101] I. Vukotic,[39] S. Wada,[158] C. Wagner,[104] J. M. Wagner,[17a] W. Wagner,[172] S. Wahdan,[172] H. Wahlberg,[91] M. Wakida,[112] J. Walder,[135] R. Walker,[110] W. Walkowiak,[142] A. Wall,[129] E. J. Wallin,[99] T. Wamorkar,[6] A. Z. Wang,[137] C. Wang,[101] C. Wang,[11] H. Wang,[17a] J. Wang,[64c] R.-J. Wang,[101] R. Wang,[61] R. Wang,[6] S. M. Wang,[149] S. Wang,[62b] T. Wang,[62a] W. T. Wang,[80] W. Wang,[14a] X. Wang,[14c] X. Wang,[163] X. Wang,[62c] Y. Wang,[62d] Y. Wang,[14c] Z. Wang,[107] Z. Wang,[62d,51,62c] Z. Wang,[107] A. Warburton,[105] R. J. Ward,[20] N. Warrack,[59] S. Waterhouse,[96] A. T. Watson,[20] H. Watson,[59] M. F. Watson,[20] E. Watton,[59,135] G. Watts,[139] B. M. Waugh,[97] J. M. Webb,[54] C. Weber,[29] H. A. Weber,[18] M. S. Weber,[19] S. M. Weber,[63a] C. Wei,[62a] Y. Wei,[127] A. R. Weidberg,[127] E. J. Weik,[118] J. Weingarten,[49] M. Weirich,[101] C. Weiser,[54] C. J. Wells,[48] T. Wenaus,[29] B. Wendland,[49] T. Wengler,[36] N. S. Wenke,[111] N. Wermes,[24] M. Wessels,[63a] A. M. Wharton,[92] A. S. White,[61] A. White,[8] M. J. White,[1] D. Whiteson,[160] L. Wickremasinghe,[125] W. Wiedenmann,[171] M. Wielers,[135] C. Wiglesworth,[42] D. J. Wilbern,[121] H. G. Wilkens,[36] J. J. H. Wilkinson,[32] D. M. Williams,[41] H. H. Williams,[129] S. Williams,[32] S. Willocq,[104] B. J. Wilson,[102] P. J. Windischhofer,[39] F. I. Winkel,[30] F. Winklmeier,[124] B. T. Winter,[54] J. K. Winter,[102] M. Wittgen,[144] M. Wobisch,[98] T. Wojtkowski,[60] Z. Wolffs,[115] J. Wollrath,[160] M. W. Wolter,[87] H. Wolters,[131a,131c] M. C. Wong,[137] E. L. Woodward,[41] S. D. Worm,[48] B. K. Wosiek,[87] K. W. Woźniak,[87] S. Wozniewski,[55] K. Wraight,[59] C. Wu,[20] M. Wu,[14d] M. Wu,[114] S. L. Wu,[171] X. Wu,[56] Y. Wu,[62a] Z. Wu,[4] J. Wuerzinger,[111,v] T. R. Wyatt,[102] B. M. Wynne,[52] S. Xella,[42] L. Xia,[14c] M. Xia,[14b] J. Xiang,[64c] M. Xie,[62a] X. Xie,[62a] S. Xin,[14a,14e] A. Xiong,[124] J. Xiong,[17a] D. Xu,[14a] H. Xu,[62a] L. Xu,[62a] R. Xu,[129] T. Xu,[107] Y. Xu,[14b] Z. Xu,[52] Z. Xu,[14c] B. Yabsley,[148] S. Yacoob,[33a] Y. Yamaguchi,[155] E. Yamashita,[154] H. Yamauchi,[158] T. Yamazaki,[17a] Y. Yamazaki,[85] J. Yan,[62c] S. Yan,[59] Z. Yan,[104] H. J. Yang,[62c,62d] H. T. Yang,[62a] S. Yang,[62a] T. Yang,[64c] X. Yang,[36] X. Yang,[14a] Y. Yang,[44] Y. Yang,[62a] Z. Yang,[62a] W-M. Yao,[17a] H. Ye,[14c] H. Ye,[55] J. Ye,[14a] S. Ye,[29] X. Ye,[62a] Y. Yeh,[97] I. Yeletskikh,[38] B. K. Yeo,[17b] M. R. Yexley,[97] T. P. Yildirim,[127] P. Yin,[41] K. Yorita,[169] S. Younas,[27b] C. J. S. Young,[36] C. Young,[144] C. Yu,[14a,14e] Y. Yu,[62a] M. Yuan,[107] R. Yuan,[62d,62c] L. Yue,[97] M. Zaazoua,[62a] B. Zabinski,[87] E. Zaid,[52] Z. K. Zak,[87] T. Zakareishvili,[164] N. Zakharchuk,[34] S. Zambito,[56] J. A. Zamora Saa,[138d,138b] J. Zang,[154] D. Zanzi,[54] O. Zaplatilek,[133] C. Zeitnitz,[172] H. Zeng,[14a] J. C. Zeng,[163] D. T. Zenger Jr.,[26] O. Zenin,[37] T. Ženiš,[28a] S. Zenz,[95] S. Zerradi,[35a] D. Zerwas,[66] M. Zhai,[14a,14e] D. F. Zhang,[140] J. Zhang,[62b] J. Zhang,[6] K. Zhang,[14a,14e] L. Zhang,[62a] L. Zhang,[14c] P. Zhang,[14a,14e] R. Zhang,[171] S. Zhang,[107] S. Zhang,[44] T. Zhang,[154] X. Zhang,[62c] X. Zhang,[62b] Y. Zhang,[62c,5] Y. Zhang,[97] Y. Zhang,[14c] Z. Zhang,[17a] Z. Zhang,[66] H. Zhao,[139] T. Zhao,[62b] Y. Zhao,[137] Z. Zhao,[62a] Z. Zhao,[62a] A. Zhemchugov,[38] J. Zheng,[14c] K. Zheng,[163] X. Zheng,[62a] Z. Zheng,[144] D. Zhong,[163] B. Zhou,[107] H. Zhou,[7] N. Zhou,[62c] Y. Zhou,[14c] Y. Zhou,[7] C. G. Zhu,[62b] J. Zhu,[107] X. Zhu,[62d] Y. Zhu,[62c] Y. Zhu,[62a] X. Zhuang,[14a] K. Zhukov,[37] N. I. Zimine,[38] J. Zinsser,[63b] M. Ziolkowski,[142] L. Živković,[15] A. Zoccoli,[23b,23a] K. Zoch,[61] T. G. Zorbas,[140] O. Zormpa,[46] W. Zou,[41] and L. Zwalinski[36]

(ATLAS Collaboration)

[1]*Department of Physics, University of Adelaide, Adelaide, Australia*
[2]*Department of Physics, University of Alberta, Edmonton AB, Canada*
[3a]*Department of Physics, Ankara University, Ankara, Türkiye*
[3b]*Division of Physics, TOBB University of Economics and Technology, Ankara, Türkiye*
[4]*LAPP, Université Savoie Mont Blanc, CNRS/IN2P3, Annecy, France*
[5]*APC, Université Paris Cité, CNRS/IN2P3, Paris, France*
[6]*High Energy Physics Division, Argonne National Laboratory, Argonne, Illinois, USA*
[7]*Department of Physics, University of Arizona, Tucson, Arizona, USA*
[8]*Department of Physics, University of Texas at Arlington, Arlington, Texas, USA*
[9]*Physics Department, National and Kapodistrian University of Athens, Athens, Greece*
[10]*Physics Department, National Technical University of Athens, Zografou, Greece*
[11]*Department of Physics, University of Texas at Austin, Austin, Texas, USA*

[12]Institute of Physics, Azerbaijan Academy of Sciences, Baku, Azerbaijan
[13]Institut de Física d'Altes Energies (IFAE), Barcelona Institute of Science and Technology, Barcelona, Spain
[14a]Institute of High Energy Physics, Chinese Academy of Sciences, Beijing, China
[14b]Physics Department, Tsinghua University, Beijing, China
[14c]Department of Physics, Nanjing University, Nanjing, China
[14d]School of Science, Shenzhen Campus of Sun Yat-sen University, China
[14e]University of Chinese Academy of Science (UCAS), Beijing, China
[15]Institute of Physics, University of Belgrade, Belgrade, Serbia
[16]Department for Physics and Technology, University of Bergen, Bergen, Norway
[17a]Physics Division, Lawrence Berkeley National Laboratory, Berkeley, California, USA
[17b]University of California, Berkeley, California, USA
[18]Institut für Physik, Humboldt Universität zu Berlin, Berlin, Germany
[19]Albert Einstein Center for Fundamental Physics and Laboratory for High Energy Physics, University of Bern, Bern, Switzerland
[20]School of Physics and Astronomy, University of Birmingham, Birmingham, United Kingdom
[21a]Department of Physics, Bogazici University, Istanbul, Türkiye
[21b]Department of Physics Engineering, Gaziantep University, Gaziantep, Türkiye
[21c]Department of Physics, Istanbul University, Istanbul, Türkiye
[22a]Facultad de Ciencias y Centro de Investigaciónes, Universidad Antonio Nariño, Bogotá, Colombia
[22b]Departamento de Física, Universidad Nacional de Colombia, Bogotá, Colombia
[23a]Dipartimento di Fisica e Astronomia A. Righi, Università di Bologna, Bologna, Italy
[23b]INFN Sezione di Bologna, Italy
[24]Physikalisches Institut, Universität Bonn, Bonn, Germany
[25]Department of Physics, Boston University, Boston, Massachusetts, USA
[26]Department of Physics, Brandeis University, Waltham, Massachusetts, USA
[27a]Transilvania University of Brasov, Brasov, Romania
[27b]Horia Hulubei National Institute of Physics and Nuclear Engineering, Bucharest, Romania
[27c]Department of Physics, Alexandru Ioan Cuza University of Iasi, Iasi, Romania
[27d]National Institute for Research and Development of Isotopic and Molecular Technologies, Physics Department, Cluj-Napoca, Romania
[27e]National University of Science and Technology Politechnica, Bucharest, Romania
[27f]West University in Timisoara, Timisoara, Romania
[27g]Faculty of Physics, University of Bucharest, Bucharest, Romania
[28a]Faculty of Mathematics, Physics and Informatics, Comenius University, Bratislava, Slovak Republic
[28b]Department of Subnuclear Physics, Institute of Experimental Physics of the Slovak Academy of Sciences, Kosice, Slovak Republic
[29]Physics Department, Brookhaven National Laboratory, Upton, New York, USA
[30]Universidad de Buenos Aires, Facultad de Ciencias Exactas y Naturales, Departamento de Física, y CONICET, Instituto de Física de Buenos Aires (IFIBA), Buenos Aires, Argentina
[31]California State University, California, USA
[32]Cavendish Laboratory, University of Cambridge, Cambridge, United Kingdom
[33a]Department of Physics, University of Cape Town, Cape Town, South Africa
[33b]iThemba Labs, Western Cape, South Africa
[33c]Department of Mechanical Engineering Science, University of Johannesburg, Johannesburg, South Africa
[33d]National Institute of Physics, University of the Philippines Diliman (Philippines), Philippines
[33e]University of South Africa, Department of Physics, Pretoria, South Africa
[33f]University of Zululand, KwaDlangezwa, South Africa
[33g]School of Physics, University of the Witwatersrand, Johannesburg, South Africa
[34]Department of Physics, Carleton University, Ottawa ON, Canada
[35a]Faculté des Sciences Ain Chock, Réseau Universitaire de Physique des Hautes Energies—Université Hassan II, Casablanca, Morocco
[35b]Faculté des Sciences, Université Ibn-Tofail, Kénitra, Morocco
[35c]Faculté des Sciences Semlalia, Université Cadi Ayyad, LPHEA-Marrakech, Morocco
[35d]LPMR, Faculté des Sciences, Université Mohamed Premier, Oujda, Morocco
[35e]Faculté des sciences, Université Mohammed V, Rabat, Morocco
[35f]Institute of Applied Physics, Mohammed VI Polytechnic University, Ben Guerir, Morocco
[36]CERN, Geneva, Switzerland
[37]Affiliated with an institute covered by a cooperation agreement with CERN

[38]*Affiliated with an international laboratory covered by a cooperation agreement with CERN*
[39]*Enrico Fermi Institute, University of Chicago, Chicago, Illinois, USA*
[40]*LPC, Université Clermont Auvergne, CNRS/IN2P3, Clermont-Ferrand, France*
[41]*Nevis Laboratory, Columbia University, Irvington, New York, USA*
[42]*Niels Bohr Institute, University of Copenhagen, Copenhagen, Denmark*
[43a]*Dipartimento di Fisica, Università della Calabria, Rende, Italy*
[43b]*INFN Gruppo Collegato di Cosenza, Laboratori Nazionali di Frascati, Italy*
[44]*Physics Department, Southern Methodist University, Dallas, Texas, USA*
[45]*Physics Department, University of Texas at Dallas, Richardson, Texas, USA*
[46]*National Centre for Scientific Research "Demokritos", Agia Paraskevi, Greece*
[47a]*Department of Physics, Stockholm University, Sweden*
[47b]*Oskar Klein Centre, Stockholm, Sweden*
[48]*Deutsches Elektronen-Synchrotron DESY, Hamburg and Zeuthen, Germany*
[49]*Fakultät Physik, Technische Universität Dortmund, Dortmund, Germany*
[50]*Institut für Kern- und Teilchenphysik, Technische Universität Dresden, Dresden, Germany*
[51]*Department of Physics, Duke University, Durham, North Carolina, USA*
[52]*SUPA—School of Physics and Astronomy, University of Edinburgh, Edinburgh, United Kingdom*
[53]*INFN e Laboratori Nazionali di Frascati, Frascati, Italy*
[54]*Physikalisches Institut, Albert-Ludwigs-Universität Freiburg, Freiburg, Germany*
[55]*II. Physikalisches Institut, Georg-August-Universität Göttingen, Göttingen, Germany*
[56]*Département de Physique Nucléaire et Corpusculaire, Université de Genève, Genève, Switzerland*
[57a]*Dipartimento di Fisica, Università di Genova, Genova, Italy*
[57b]*INFN Sezione di Genova, Italy*
[58]*II. Physikalisches Institut, Justus-Liebig-Universität Giessen, Giessen, Germany*
[59]*SUPA—School of Physics and Astronomy, University of Glasgow, Glasgow, United Kingdom*
[60]*LPSC, Université Grenoble Alpes, CNRS/IN2P3, Grenoble INP, Grenoble, France*
[61]*Laboratory for Particle Physics and Cosmology, Harvard University, Cambridge, Massachusetts, USA*
[62a]*Department of Modern Physics and State Key Laboratory of Particle Detection and Electronics, University of Science and Technology of China, Hefei, China*
[62b]*Institute of Frontier and Interdisciplinary Science and Key Laboratory of Particle Physics and Particle Irradiation (MOE), Shandong University, Qingdao, China*
[62c]*School of Physics and Astronomy, Shanghai Jiao Tong University, Key Laboratory for Particle Astrophysics and Cosmology (MOE), SKLPPC, Shanghai, China*
[62d]*Tsung-Dao Lee Institute, Shanghai, China*
[62e]*School of Physics and Microelectronics, Zhengzhou University, China*
[63a]*Kirchhoff-Institut für Physik, Ruprecht-Karls-Universität Heidelberg, Heidelberg, Germany*
[63b]*Physikalisches Institut, Ruprecht-Karls-Universität Heidelberg, Heidelberg, Germany*
[64a]*Department of Physics, Chinese University of Hong Kong, Shatin, N.T., Hong Kong, China*
[64b]*Department of Physics, University of Hong Kong, Hong Kong, China*
[64c]*Department of Physics and Institute for Advanced Study, Hong Kong University of Science and Technology, Clear Water Bay, Kowloon, Hong Kong, China*
[65]*Department of Physics, National Tsing Hua University, Hsinchu, Taiwan*
[66]*IJCLab, Université Paris-Saclay, CNRS/IN2P3, 91405, Orsay, France*
[67]*Centro Nacional de Microelectrónica (IMB-CNM-CSIC), Barcelona, Spain*
[68]*Department of Physics, Indiana University, Bloomington, Indiana, USA*
[69a]*INFN Gruppo Collegato di Udine, Sezione di Trieste, Udine, Italy*
[69b]*ICTP, Trieste, Italy*
[69c]*Dipartimento Politecnico di Ingegneria e Architettura, Università di Udine, Udine, Italy*
[70a]*INFN Sezione di Lecce, Italy*
[70b]*Dipartimento di Matematica e Fisica, Università del Salento, Lecce, Italy*
[71a]*INFN Sezione di Milano, Italy*
[71b]*Dipartimento di Fisica, Università di Milano, Milano, Italy*
[72a]*INFN Sezione di Napoli, Italy*
[72b]*Dipartimento di Fisica, Università di Napoli, Napoli, Italy*
[73a]*INFN Sezione di Pavia, Italy*
[73b]*Dipartimento di Fisica, Università di Pavia, Pavia, Italy*
[74a]*INFN Sezione di Pisa, Italy*
[74b]*Dipartimento di Fisica E. Fermi, Università di Pisa, Pisa, Italy*
[75a]*INFN Sezione di Roma, Italy*
[75b]*Dipartimento di Fisica, Sapienza Università di Roma, Roma, Italy*

[76a]INFN Sezione di Roma Tor Vergata, Italy
[76b]Dipartimento di Fisica, Università di Roma Tor Vergata, Roma, Italy
[77a]INFN Sezione di Roma Tre, Italy
[77b]Dipartimento di Matematica e Fisica, Università Roma Tre, Roma, Italy
[78a]INFN-TIFPA, Italy
[78b]Università degli Studi di Trento, Trento, Italy
[79]Universität Innsbruck, Department of Astro and Particle Physics, Innsbruck, Austria
[80]University of Iowa, Iowa City, Iowa, USA
[81]Department of Physics and Astronomy, Iowa State University, Ames, Iowa, USA
[82]Istinye University, Sariyer, Istanbul, Türkiye
[83a]Departamento de Engenharia Elétrica, Universidade Federal de Juiz de Fora (UFJF), Juiz de Fora, Brazil
[83b]Universidade Federal do Rio De Janeiro COPPE/EE/IF, Rio de Janeiro, Brazil
[83c]Instituto de Física, Universidade de São Paulo, São Paulo, Brazil
[83d]Rio de Janeiro State University, Rio de Janeiro, Brazil
[83e]Federal University of Bahia, Bahia, Brazil
[84]KEK, High Energy Accelerator Research Organization, Tsukuba, Japan
[85]Graduate School of Science, Kobe University, Kobe, Japan
[86a]AGH University of Krakow, Faculty of Physics and Applied Computer Science, Krakow, Poland
[86b]Marian Smoluchowski Institute of Physics, Jagiellonian University, Krakow, Poland
[87]Institute of Nuclear Physics Polish Academy of Sciences, Krakow, Poland
[88]Faculty of Science, Kyoto University, Kyoto, Japan
[89]Research Center for Advanced Particle Physics and Department of Physics, Kyushu University, Fukuoka, Japan
[90]L2IT, Université de Toulouse, CNRS/IN2P3, UPS, Toulouse, France
[91]Instituto de Física La Plata, Universidad Nacional de La Plata and CONICET, La Plata, Argentina
[92]Physics Department, Lancaster University, Lancaster, United Kingdom
[93]Oliver Lodge Laboratory, University of Liverpool, Liverpool, United Kingdom
[94]Department of Experimental Particle Physics, Jožef Stefan Institute and Department of Physics, University of Ljubljana, Ljubljana, Slovenia
[95]School of Physics and Astronomy, Queen Mary University of London, London, United Kingdom
[96]Department of Physics, Royal Holloway University of London, Egham, United Kingdom
[97]Department of Physics and Astronomy, University College London, London, United Kingdom
[98]Louisiana Tech University, Ruston, Los Angeles, USA
[99]Fysiska institutionen, Lunds universitet, Lund, Sweden
[100]Departamento de Física Teorica C-15 and CIAFF, Universidad Autónoma de Madrid, Madrid, Spain
[101]Institut für Physik, Universität Mainz, Mainz, Germany
[102]School of Physics and Astronomy, University of Manchester, Manchester, United Kingdom
[103]CPPM, Aix-Marseille Université, CNRS/IN2P3, Marseille, France
[104]Department of Physics, University of Massachusetts, Amherst, Massachusetts, USA
[105]Department of Physics, McGill University, Montreal, Quebec, Canada
[106]School of Physics, University of Melbourne, Victoria, Australia
[107]Department of Physics, University of Michigan, Ann Arbor, Michigan, USA
[108]Department of Physics and Astronomy, Michigan State University, East Lansing, Michigan, USA
[109]Group of Particle Physics, University of Montreal, Montreal, Quebec, Canada
[110]Fakultät für Physik, Ludwig-Maximilians-Universität München, München, Germany
[111]Max-Planck-Institut für Physik (Werner-Heisenberg-Institut), München, Germany
[112]Graduate School of Science and Kobayashi-Maskawa Institute, Nagoya University, Nagoya, Japan
[113]Department of Physics and Astronomy, University of New Mexico, Albuquerque, New Mexico, USA
[114]Institute for Mathematics, Astrophysics and Particle Physics, Radboud University/Nikhef, Nijmegen, Netherlands
[115]Nikhef National Institute for Subatomic Physics and University of Amsterdam, Amsterdam, Netherlands
[116]Department of Physics, Northern Illinois University, DeKalb, Illinois, USA
[117a]New York University Abu Dhabi, Abu Dhabi, United Arab Emirates
[117b]United Arab Emirates University, Al Ain, United Arab Emirates
[118]Department of Physics, New York University, New York, New York, USA
[119]Ochanomizu University, Otsuka, Bunkyo-ku, Tokyo, Japan
[120]Ohio State University, Columbus, Ohio, USA
[121]Homer L. Dodge Department of Physics and Astronomy, University of Oklahoma, Norman, Oklahoma, USA

[122]*Department of Physics, Oklahoma State University, Stillwater, Oklahoma, USA*
[123]*Palacký University, Joint Laboratory of Optics, Olomouc, Czech Republic*
[124]*Institute for Fundamental Science, University of Oregon, Eugene, Oregon, USA*
[125]*Graduate School of Science, Osaka University, Osaka, Japan*
[126]*Department of Physics, University of Oslo, Oslo, Norway*
[127]*Department of Physics, Oxford University, Oxford, United Kingdom*
[128]*LPNHE, Sorbonne Université, Université Paris Cité, CNRS/IN2P3, Paris, France*
[129]*Department of Physics, University of Pennsylvania, Philadelphia, Pennsylvania, USA*
[130]*Department of Physics and Astronomy, University of Pittsburgh, Pittsburgh, Pennsylvania, USA*
[131a]*Laboratório de Instrumentação e Física Experimental de Partículas—LIP, Lisboa, Portugal*
[131b]*Departamento de Física, Faculdade de Ciências, Universidade de Lisboa, Lisboa, Portugal*
[131c]*Departamento de Física, Universidade de Coimbra, Coimbra, Portugal*
[131d]*Centro de Física Nuclear da Universidade de Lisboa, Lisboa, Portugal*
[131e]*Departamento de Física, Universidade do Minho, Braga, Portugal*
[131f]*Departamento de Física Teórica y del Cosmos, Universidad de Granada, Granada (Spain), Spain*
[131g]*Departamento de Física, Instituto Superior Técnico, Universidade de Lisboa, Lisboa, Portugal*
[132]*Institute of Physics of the Czech Academy of Sciences, Prague, Czech Republic*
[133]*Czech Technical University in Prague, Prague, Czech Republic*
[134]*Charles University, Faculty of Mathematics and Physics, Prague, Czech Republic*
[135]*Particle Physics Department, Rutherford Appleton Laboratory, Didcot, United Kingdom*
[136]*IRFU, CEA, Université Paris-Saclay, Gif-sur-Yvette, France*
[137]*Santa Cruz Institute for Particle Physics, University of California Santa Cruz, Santa Cruz, California, USA*
[138a]*Departamento de Física, Pontificia Universidad Católica de Chile, Santiago, Chile*
[138b]*Millennium Institute for Subatomic physics at high energy frontier (SAPHIR), Santiago, Chile*
[138c]*Instituto de Investigación Multidisciplinario en Ciencia y Tecnología, y Departamento de Física, Universidad de La Serena, Chile*
[138d]*Universidad Andres Bello, Department of Physics, Santiago, Chile*
[138e]*Instituto de Alta Investigación, Universidad de Tarapacá, Arica, Chile*
[138f]*Departamento de Física, Universidad Técnica Federico Santa María, Valparaíso, Chile*
[139]*Department of Physics, University of Washington, Seattle, Washington, USA*
[140]*Department of Physics and Astronomy, University of Sheffield, Sheffield, United Kingdom*
[141]*Department of Physics, Shinshu University, Nagano, Japan*
[142]*Department Physik, Universität Siegen, Siegen, Germany*
[143]*Department of Physics, Simon Fraser University, Burnaby BC, Canada*
[144]*SLAC National Accelerator Laboratory, Stanford, California, USA*
[145]*Department of Physics, Royal Institute of Technology, Stockholm, Sweden*
[146]*Departments of Physics and Astronomy, Stony Brook University, Stony Brook, New York, USA*
[147]*Department of Physics and Astronomy, University of Sussex, Brighton, United Kingdom*
[148]*School of Physics, University of Sydney, Sydney, Australia*
[149]*Institute of Physics, Academia Sinica, Taipei, Taiwan*
[150a]*E. Andronikashvili Institute of Physics, Iv. Javakhishvili Tbilisi State University, Tbilisi, Georgia*
[150b]*High Energy Physics Institute, Tbilisi State University, Tbilisi, Georgia*
[150c]*University of Georgia, Tbilisi, Georgia*
[151]*Department of Physics, Technion, Israel Institute of Technology, Haifa, Israel*
[152]*Raymond and Beverly Sackler School of Physics and Astronomy, Tel Aviv University, Tel Aviv, Israel*
[153]*Department of Physics, Aristotle University of Thessaloniki, Thessaloniki, Greece*
[154]*International Center for Elementary Particle Physics and Department of Physics, University of Tokyo, Tokyo, Japan*
[155]*Department of Physics, Tokyo Institute of Technology, Tokyo, Japan*
[156]*Department of Physics, University of Toronto, Toronto ON, Canada*
[157a]*TRIUMF, Vancouver BC, Canada*
[157b]*Department of Physics and Astronomy, York University, Toronto ON, Canada*
[158]*Division of Physics and Tomonaga Center for the History of the Universe, Faculty of Pure and Applied Sciences, University of Tsukuba, Tsukuba, Japan*
[159]*Department of Physics and Astronomy, Tufts University, Medford, Massachusetts, USA*
[160]*Department of Physics and Astronomy, University of California Irvine, Irvine, California, USA*
[161]*University of Sharjah, Sharjah, United Arab Emirates*
[162]*Department of Physics and Astronomy, University of Uppsala, Uppsala, Sweden*
[163]*Department of Physics, University of Illinois, Urbana, Illinois, USA*

[164]*Instituto de Física Corpuscular (IFIC), Centro Mixto Universidad de Valencia—CSIC, Valencia, Spain*
[165]*Department of Physics, University of British Columbia, Vancouver BC, Canada*
[166]*Department of Physics and Astronomy, University of Victoria, Victoria BC, Canada*
[167]*Fakultät für Physik und Astronomie, Julius-Maximilians-Universität Würzburg, Würzburg, Germany*
[168]*Department of Physics, University of Warwick, Coventry, United Kingdom*
[169]*Waseda University, Tokyo, Japan*
[170]*Department of Particle Physics and Astrophysics, Weizmann Institute of Science, Rehovot, Israel*
[171]*Department of Physics, University of Wisconsin, Madison, Wisconsin, USA*
[172]*Fakultät für Mathematik und Naturwissenschaften, Fachgruppe Physik, Bergische Universität Wuppertal, Wuppertal, Germany*
[173]*Department of Physics, Yale University, New Haven, Connecticut, USA*

[a]Deceased.
[b]Also at Department of Physics, King's College London, London, United Kingdom.
[c]Also at Institute of Physics, Azerbaijan Academy of Sciences, Baku, Azerbaijan.
[d]Also at Lawrence Livermore National Laboratory, Livermore, USA.
[e]Also at TRIUMF, Vancouver BC, Canada.
[f]Also at Department of Physics, University of Thessaly, Greece.
[g]Also at An-Najah National University, Nablus, Palestine.
[h]Also at Department of Physics, University of Fribourg, Fribourg, Switzerland.
[i]Also at Department of Physics, Westmont College, Santa Barbara, USA.
[j]Also at Departament de Fisica de la Universitat Autonoma de Barcelona, Barcelona, Spain.
[k]Also at Affiliated with an institute covered by a cooperation agreement with CERN.
[l]Also at The Collaborative Innovation Center of Quantum Matter (CICQM), Beijing, China.
[m]Also at Università di Napoli Parthenope, Napoli, Italy.
[n]Also at Institute of Particle Physics (IPP), Canada.
[o]Also at University of Colorado Boulder, Department of Physics, Colorado, USA.
[p]Also at Borough of Manhattan Community College, City University of New York, New York, New York, USA.
[q]Also at National Institute of Physics, University of the Philippines Diliman (Philippines), Philippines.
[r]Also at Department of Financial and Management Engineering, University of the Aegean, Chios, Greece.
[s]Also at Department of Physics, Stanford University, Stanford, California, USA.
[t]Also at Centro Studi e Ricerche Enrico Fermi, Italy.
[u]Also at Institucio Catalana de Recerca i Estudis Avancats, ICREA, Barcelona, Spain.
[v]Also at Technical University of Munich, Munich, Germany.
[w]Also at Yeditepe University, Physics Department, Istanbul, Türkiye.
[x]Also at Institute of Theoretical Physics, Ilia State University, Tbilisi, Georgia.
[y]Also at CERN, Geneva, Switzerland.
[z]Also at Center for Interdisciplinary Research and Innovation (CIRI-AUTH), Thessaloniki, Greece.
[aa]Also at Hellenic Open University, Patras, Greece.
[bb]Also at Center for High Energy Physics, Peking University, China.
[cc]Also at Department of Physics, Stellenbosch University, South Africa.
[dd]Also at Department of Physics, California State University, Sacramento, USA.
[ee]Also at Département de Physique Nucléaire et Corpusculaire, Université de Genève, Genève, Switzerland.
[ff]Also at Institut für Experimentalphysik, Universität Hamburg, Hamburg, Germany.
[gg]Also at Institute for Nuclear Research and Nuclear Energy (INRNE) of the Bulgarian Academy of Sciences, Sofia, Bulgaria.
[hh]Also at Washington College, Chestertown, Maryland, USA.
[ii]Also at Institute of Applied Physics, Mohammed VI Polytechnic University, Ben Guerir, Morocco.
[jj]Also at Institute of Physics and Technology, Mongolian Academy of Sciences, Ulaanbaatar, Mongolia.